

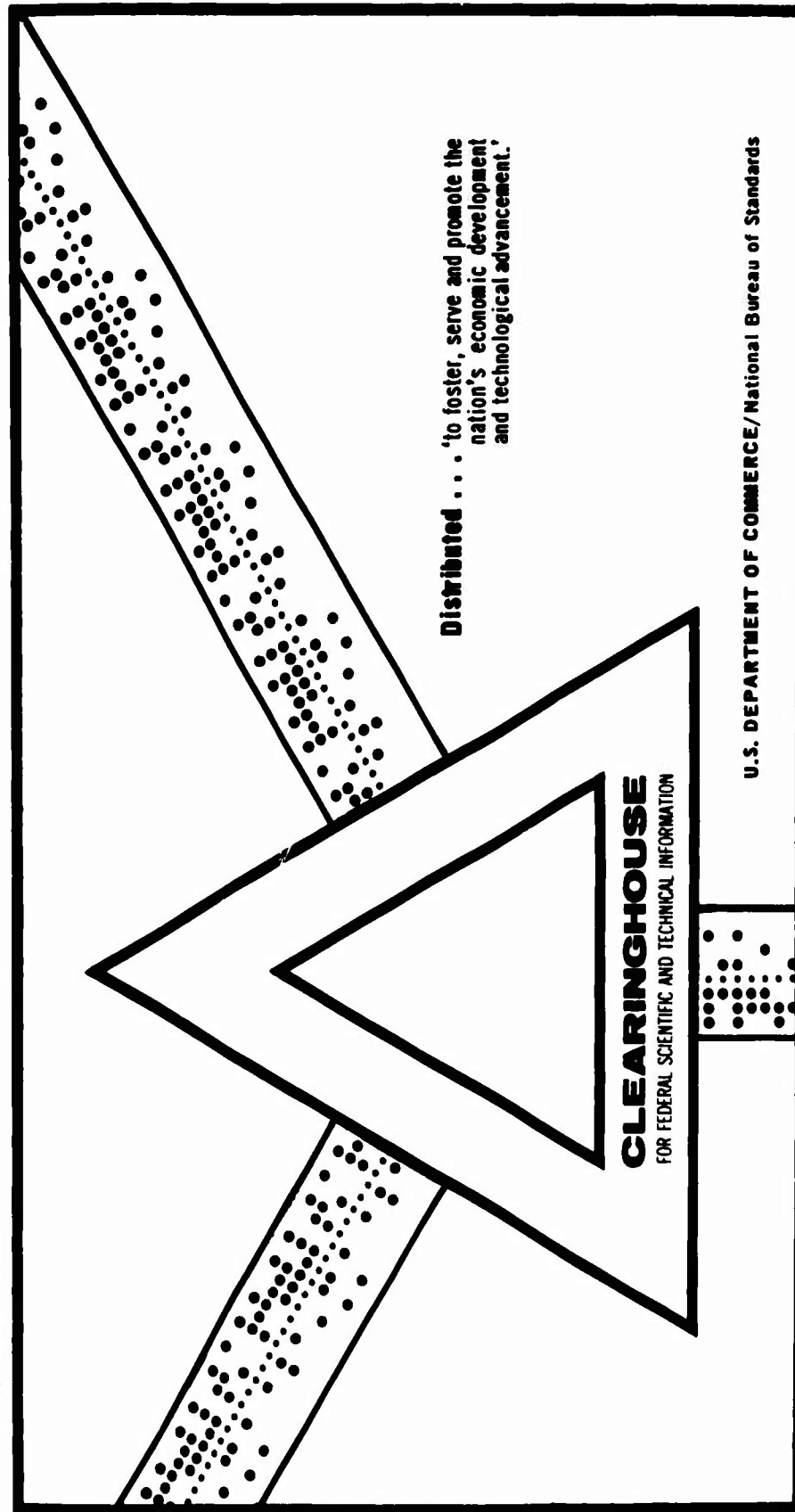
AD 700 918

EFFECTS OF NON-UNIFORM SAMPLING AND LIMITING ON CORRELATION
FUNCTIONS

C. L. Ackerman

Pennsylvania State University
University Park, Pennsylvania

13 August 1969



This document has been approved for public release and sale.

UNCLASSIFIED

AD700918

EFFECTS OF NON-UNIFORM SAMPLING AND
LIMITING ON CORRELATION FUNCTIONS

By C. L. Ackerman

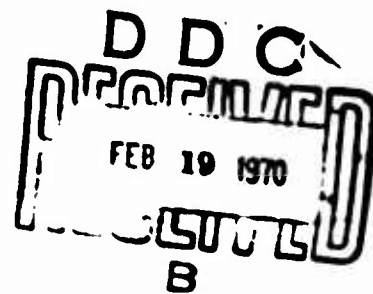
Technical Memorandum
File No. TM 676.2341-02
August 13, 1969
Contract NOw 65-0123-d
Copy No. 12

The Pennsylvania State University
Institute for Science and Engineering
ORDNANCE RESEARCH LABORATORY
University Park, Pennsylvania

DISTRIBUTION OF THIS
DOCUMENT IS UNLIMITED

NAVY DEPARTMENT · NAVAL ORDNANCE SYSTEMS COMMAND

Reproduced by the
CLEARINGHOUSE
for Federal Scientific & Technical
Information Springfield Va 22151



UNCLASSIFIED
209

ABSTRACT

The general topic of the research reported in this thesis is the study of nonuniform block sampling theory and its application to the study of correlation functions of sampled signals. The research evolved from the specific problem of trying to reduce the odd harmonic terms which appear in the correlation function of hard limited and uniformly sampled sinusoidal signals. These odd harmonic terms arise because of the synchronism between the periodicity of the uniform samples and the periodicity of the odd signal harmonics produced by hard limiting.

The general approach to the problem is to use nonuniform sampling to reduce the undesirable periodicity effects and thus to reduce the odd harmonic terms in the correlation function. A particularly useful class of nonuniform sampling functions for this application is shown to be "block sampling functions;" i.e., short sequences (or blocks) of nonuniform samples which are repeated periodically in time.

As a preliminary to a study of block sampling functions and their application to the odd harmonic problem, a detailed study of the general properties of correlation functions for large TV signals with uniform sampling is made. These results are then extended to the case of sinusoidal signals with uniform sampling to illustrate the role of both clipping and sampling in the generation of the undesirable odd harmonic terms in the correlation function. The uniform sampling correlation function results along with the results of the block

8
sampling spectrum analysis then form the basis for analysis of correlation functions of sinusoidal signals with nonuniform block sampling.

In the study of correlation functions of large TW signals, two alternative definitions of sampled correlation functions are compared: the regular correlation function, and a quadrature correlation function consisting of an average of a regular correlation function and the correlation function of the Hilbert transforms of the correlated signals. By eliminating the second harmonic sampling effects, the quadrature correlation function is shown to achieve more accurate correlation for deterministic signals and lower correlation variance for random signals. A comparison of the sampled quadrature correlation function variance for clipped and unclipped narrowband random processes shows that the variance for the clipped signals could be reduced by as much as 3 dB over the unclipped signal variance by sampling at a sufficiently high rate.

8
In extending the study of quadrature correlation function properties to sinusoidal signals, uniform sampling is shown to make the correlation function periodic (as a function of frequency) with a repetition period equal to the sampling rate, while clipping introduces extraneous correlations for input signal frequencies which are odd multiples of the reference signal frequency. When both clipping and uniform sampling are employed, each odd harmonic correlation function response is repeated at period frequency intervals which are related to the sampling rate, thus giving rise to the odd harmonic problem for correlation functions of sinusoidal signals.

After proposing nonuniform block sampling as a possible solution to the odd harmonic problem, the frequency spectrum properties of ideal block sampling are studied in detail. These properties include amplitude and phase characteristics of each spectral component, spectral periodicity conditions, conservation of spectral energy properties, and conditions for minimum variance of the sampling power spectrum. As an example of sampling spectrum amplitude shaping by choice of sample times, a block sampling function example is presented which uses a pseudo-random number generator for sampling time selection. This sampling technique achieves a unique spectrum shaping by suppressing the spectral amplitude for small values of frequency, a property that is shown to be important in the reduction of odd harmonic responses in correlation functions of clipped sinusoidal signals.

Considering the quadrature correlation function of two clipped sinusoidal signals with block sampling as a function of the two sinusoidal frequencies, it is shown that, although the odd harmonic effects are greatly reduced, certain "Worst Case" combinations of the two sinusoidal frequencies result in correlation functions whose average value is greater than those for all other frequency combinations. In addition to deriving the critical frequency relationships, an analytic expression is obtained relating the correlation function for these Worst Case frequencies to the coefficients of the block sampling frequency spectrum. Some experimental results, based on a digital computer simulation, are shown to verify the analytical model. It is concluded

UNCLASSIFIED

- 5 -

File No. 676.2341
13 August 1969
MTP:pml

that by proper choice of sampling parameters, block sampling can reduce the undesirable odd harmonic correlation function responses due to clipping and sampling by any desired degree.

UNCLASSIFIED

TABLE OF CONTENTS

	Page
Acknowledgements	ii
List of Figures	v
I. INTRODUCTION	
1.1 General Statement of the Problem	1
1.2 Importance of the Study	1
1.3 Previous Related Studies	3
1.4 Scope and Limitations of the Study	5
II. CORRELATION FUNCTION PROPERTIES OF SIGNALS WITH LARGE TW THAT ARE LIMITED TO A BAND OF FREQUENCIES	
2.1 Definition of Regular and Quadrature Correlation Functions	7
2.2 Comparison of Regular and Quadrature Sampled Correlation Functions	
A. Elimination of the Second Harmonic by Quadrature Correlation	13
B. Correlation Accuracy for Deterministic Signals	21
C. Correlation Variance for Narrowband Random Process Inputs	30
2.3 Comparison of Quadrature Correlation Functions for Clipped and Unclipped Signals	41
III. QUADRATURE CORRELATION FUNCTION PROPERTIES FOR SINUSOIDAL SIGNALS AND UNIFORM SAMPLING	
3.1 Quadrature Correlation Function for Sinusoidal Signals	53
3.2 Uniform Sampling Effects	57
3.3 Generation of Odd Harmonics by Clipping	61
3.4 Effect of Uniform Sampling of Clipped Sinusoids	70
3.5 Correlation Function Variance for Narrowband Random Process Input Functions	77
3.6 Use of Nonuniform Sampling to Eliminate Odd Harmonic Responses	80

TABLE OF CONTENTS

	Page
IV. SPECTRAL ANALYSIS OF NONUNIFORM BLOCK SAMPLING	
4.1 Introduction	81
4.2 Definition of Block Sampling	83
4.3 Sampling Spectrum Periodicity Properties	88
4.4 Spectrum Conservation Properties	95
4.5 Block Sampling Spectrum Examples	99
4.6 Minimizing the Spectrum Variance by Choice of Sampling Times	105
4.7 Sampling Time Selection Using Pseudo-Random Number Generators	114
V. APPLICATION OF BLOCK SAMPLING TO CORRELATION FUNCTIONS OF CLIPPED SINUSOIDAL SIGNALS	
5.1 Introduction	129
5.2 Qualitative Analysis of Correlation Functions with Block Sampling	130
5.3 Deterministic Analysis	144
5.4 Statistical Analysis	152
5.5 Example Using Pseudo-Random Block Sampling	166
VI. SUMMARY AND CONCLUSIONS	
6.1 Statement of the Problem	180
6.2 Approach	180
6.3 Discussion of Results	181
6.4 Suggestions for Further Research	187
APPENDIX: Correlation Function Variance for Random Process Input Signals with Rectangular Power Spectrum	189
BIBLIOGRAPHY	193

LIST OF FIGURES

<u>Figure</u>		<u>Page</u>
2.1	Analytic Model of Regular Correlation Function . . .	9
2.2	Analytic Model of Quadrature Correlation Function .	11
2.3	Typical Non-Zero Signal Spectrum Ranges	17
2.4	Non-Zero Spectral Range for Regular Correlation . .	17
2.5	Non-Zero Spectral Range for Quadrature Correlation .	17
2.6	Regular Correlation Function Variance Vs. Sampling Rate	39
2.7	Quadrature Correlation Function Variance Vs. Sampling Rate	40
2.8	Quadrature Correlation Function Model for Clipped Signals	43
2.9	Clipped Signal Quadrature Correlation Function Variance Vs. Sampling Rate	50
2.10	Clipped Signal Regular Correlation Function Variance Vs. Sampling Rate	52
3.1	Quadrature Correlation Function Model for Sinusoidal Signals	54
3.2	Frequency Selectivity of Quadrature Correlation Function	56
3.3	Quadrature Correlation Function Model for Sampled Sinusoidal Signals	58
3.4	Frequency Selectivity of Quadrature Correlation Function with Uniform Sampling	60
3.5	Quadrature Correlation Function Model for Clipped Sinusoidal Signals	62

LIST OF FIGURES

<u>Figure</u>		<u>Page</u>
3.6	Spectra of the Pre-Envelopes $p_x(t)$ and $p_y^*(t)$. . .	66
3.7	Frequency Selectivity of Correlation Function for Clipped Sinusoidal Signals	69
3.8	Quadrature Correlation Function Model for Clipped Sinusoidal Signals with Uniform Sampling	71
3.9	Fundamental, 3 rd , and 5 th Harmonic Correlation Response Frequencies for Clipped Sinusoids with Uniform Sampling	75
3.10	Location of Odd Harmonic Response Frequencies in Any f_s Interval	76
3.11	Clipped Sinusoidal Signal Quadrature Correlation Function Noise Variance Vs. Sampling Rate	79
4.1	Uniform Sample Train	82
4.2	Uniform Sampling Spectrum	82
4.3	Arbitrary Nonuniform Sampling Function with Period T_p	84
4.4	Decomposition of Nonuniform Sampling Function into Sum of N Uniform Sampling Functions	84
4.5	Typical Nonuniform Block Sampling Spectrum Illustrating Periodicity	87
4.6	Division of Block Interval T_p into K Possible Sampling Instants	94
4.7	Block Sampling Examples	100
4.8	Uniform Pairs Sampling Example	103
4.9	Examples of Variance Minimization Principles	113

LIST OF FIGURES

<u>Figures</u>		<u>Page</u>
4.10	Construction of Possible Sampling Times for Pseudo-Random Sampling	116
4.11	Sampling Time Generation Scheme Using a PRNG	117
4.12	Examples of Sampling Function Generated by 3 Stage PRNG	120
4.13	Sampling Spectrum for PRNG Sampling Function ($N = 96$)	126
5.1	Ideal Block Sampling Quadrature Correlation Function Model with Clipped Sinusoidal Inputs . . .	131
5.2	Typical Spectrum of Sampled Input Pre-Envelope . . .	134
5.3	Typical Spectrum of Sampled Reference Pre-Envelope .	134
5.4	Typical Input Pre-Envelope Spectrum When $4f_I = m_I f_p$	137
5.5	Typical Reference Pre-Envelope Spectrum When $4f_R = m_R f_p$	137
5.6	Non-Zero Reference Frequencies When $4f_I = m_I f_p$. .	140
5.7	Non-Zero Reference Frequencies When $4f_I \neq m_I f_p$. .	142
5.8	Quadrature Correlation Function Model with Block Sampling	145
5.9	Correlation Function Example Using Pseudo-Random Block Sampling ($N = 96$)	168
5.10	Correlation Function Examples Using Pseudo-Random Block Sampling ($N = 24$)	169

LIST OF FIGURES

<u>Figures</u>		<u>Page</u>
5.11	Comparisons of Typical Correlation Function with Output Approximations Using 1, 5, 10, and 55 Odd Harmonic Terms	171
5.12	Typical Experimental Plots of Peak Correlation Vs. Reference Frequency for Pseudo-Random Block Sampling ($N = 96$, $M = 3$)	173
5.13	Measured Correlation Histograms for Worst Case Frequencies in Large k Region - PRNG Sampling ($N = 96$)	176
5.14	Measured Correlation Histograms for Worst Case References in Small k Suppression Region - PRNG Sampling ($N = 96$)	178
5.15	Correlation Peak Histograms for Worst Case References in Small k Suppression Region	179

CHAPTER I

INTRODUCTION

1.1 General Statement of the Problem

The general topic of the research reported in this thesis is the application of nonuniform sampling theory to the study of correlation functions of sampled signals that are limited to a band of frequencies. In addition to nonuniform sampling, the research considers effects of uniform sampling and hard limiting on the correlation functions of signals with large TW products as well as sinusoids. The research evolved from the specific problem of trying to find a method to reduce the odd harmonic terms which appear in the correlation function of a sinusoidal signal which has been hard limited and uniformly sampled. These odd harmonic terms arise because of the synchronism between the periodicity of the uniform samples and the periodicity of the odd signal harmonics produced by hard limiting. This research considers the use of a special class of nonuniform sampling--"block sampling;" i.e., nonuniform samples with a periodically recurrent pattern--to eliminate this synchronism and reduce the odd harmonic correlation function terms.

1.2 Importance of the Study

The correlation function is an important analysis tool in a large number of applications [25, 26, 31, 32]. It is particularly

useful, for example, in the study of the response of linear systems to random inputs [33] where deterministic analysis methods do not apply and in determining the statistics of signals in the presence of noise [13]. Since the correlation function and the power spectrum are Fourier transforms of each other, it is also important in spectral analysis [13]. Other applications include Hilbert transform theory [14] and the correlation function method [14] for finding noise statistics at the output of certain nonlinear devices.

The operations of sampling and a hard limiting (clipping) have become common in many physical systems [29, 26, 14, 35]. These operations are often necessary because of physical limitations which make available only sampled information or signal polarity information. Sampling has become an important item in modern communication systems since the advent and wide spread use of digital techniques. Examples of the use of sampling include pulse code modulation (PCM) systems and pulsed radar. In most sampling applications in the literature, the concern is reconstruction of the original signal from its samples [14]. The basis for representing continuous signals by sampled values taken at discrete time instants lies in the well-known sampling theorems [4]. For signals limited to a frequency band, the sampling theorems are usually presented in terms of quadrature sampling [20]; i.e., taking samples of both the signal and its Hilbert transform at a rate determined by the signal bandwidth. In this thesis, we are not concerned with the reconstruction of the original signal from its sampled values, but in the effects of sampling on the auto-correlation

function of a signal or on its cross-correlation function with other signals.

A companion process to sampling in many digital applications is that of signal quantizing. Many communication systems require that signal samples be converted to digital numbers at some point within the system so they can be manipulated by digital computers or other digital devices. An important special case of quantizing is hard limiting [37, 23], or clipping, in which only two levels of quantization; i.e., signal polarities are employed. In this research, we will consider the implications of hard limiting on the correlation function of sampled signals that are limited to a band of frequencies [30, 38].

Although most of the sampling theory work in the literature is concerned with uniform sampling, many important applications [36, 28] either intentionally [1] or unintentionally [2, 9] make use of nonuniform sampling. For this reason, a good deal of research [41, 24, 5, 21, 40] has been done on the problem of signal reconstruction from nonuniformly spaced samples of a signal. The effect of nonuniform sampling on correlation function properties of sinusoidal signals is to be a major consideration in this thesis.

1.3 Previous Related Studies

The special class of nonuniform sampling functions--those with a periodically recurrent pattern--applied in this thesis to the problem of reduction of odd harmonics in correlation functions of clipped sinusoidal signals has been considered previously by several authors

[41, 24, 36, 7]. Yen [41], using the term "Recurrent Nonuniform Sampling," and Kohlenberg [24], using the term " p^{th} Order Sampling," both consider the problem of reconstruction (interpolation) of a continuous signal from its nonuniformly sampled values. Tou [36], using modified z-transform theory, analyzes the response of sampled-data systems using "Cyclic Variable-Rate Sampling," while Beutler and Leneman [7] consider "Periodically Recurrent" nonuniform sampling functions as a special class of processes in the general theory of stationary point processes.

More specifically, Yen [4] derived a reconstruction formula for low pass signals (bandlimited to W Hz) which were sampled by a recurrent nonuniform sampling function with N samples in each periodic sample "block". Kohlenberg [24] derives a more general method for obtaining reconstruction formulas for the same sampling function, requiring only that the sampled signal possess a Fourier Transform. While Kohlenberg's method applies in principle to signals for an arbitrary number N of samples per recurrent sample block, he applies it only for $N = 2$ obtaining a second-order sampling reconstruction formula. It is apparent that his method becomes very cumbersome for $N > 2$. Kohlenberg expresses recurrent nonuniform sampling with N samples per block as the sum of N uniform sampling functions with different time origins where the uniform sampling period of each function is equal to the block interval length in seconds. This representation proved useful in the study of "Block Sampling" in this thesis research.

Tou [36] models nonuniform block sampling in a slightly different way, shifting the continuous signal (in parallel) with N

different time advances (corresponding to the time of each sample instant in the block), sampling all N signals at the same instant, delaying each sampled signal by an amount equal to the time advance before sampling, and finally summing the N sampled signals to form the resultant sampled signal. A modified version of Tou's model was found useful in Chapter V for computing the correlation function of a clipped sinusoidal signal with nonuniform block sampling.

Block sampling is shown by Beutler and Leneman [7] to be a special example of a S.P.P (stationary point process) if the initial sampling instant is allowed to be a random variable. Studying the problem of analyzing stochastic sampling of wide-sense stationary random processes, Beutler, Leneman, and Lewis [6, 7, 27, 28] formulate a basic theory for S.P.P. deriving statistics on the number of points in intervals and on forward and backward recurrence times, and apply the theory to a number of problems including spectral analysis of randomly modulated processes and mean square error in the reconstruction of signals from randomly timed samples. In this thesis, block sampling will be treated as a deterministic process, making use of Fourier transform theory to derive and study its complex spectrum properties.

1.4 Scope and Limitations of the Study

The basic topic of this research--the study of nonuniform block sampling and its application in reducing the odd harmonic terms in correlation functions of clipped sinusoidal signals--is covered in Chapters IV and V. In Chapter IV, nonuniform "block sampling" is

defined and its spectral properties are derived. These results are then applied in Chapter V to the odd harmonic problem in correlation functions. Experimental results from a digital computer simulation are included to verify some of the theoretical results.

As a preliminary to the nonuniform sampling work of Chapters IV and V, a study of the general properties of correlation functions for large TW signals including the effects of uniform sampling and clipping is made in Chapter II. These results are then extended in Chapter III to quadrature correlation functions of sinusoidal signals illustrating the role of both clipping and uniform sampling in the generation of the odd harmonic correlation function terms.

CHAPTER II

CORRELATION FUNCTION PROPERTIES OF SIGNALS WITH LARGE TW THAT ARE LIMITED TO A BAND OF FREQUENCIES

2.1 Definition of Regular and Quadrature Correlation Functions

In this chapter, a study of the general properties of correlation functions of signals with large time-bandwidth (TW) products will be made. After comparing two alternative definitions for correlation functions of uniformly sampled signals, the effects of clipping will be considered.

The two alternative correlation function definitions to be compared are the regular, or standard, sampled correlation function [20] and the quadrature correlation function which makes use of Hilbert transform pairs of signal samples.

The regular correlation functions $\phi(MT_s)$ and $\hat{\phi}(MT_s)$ are defined by

$$\phi(MT_s) = \frac{1}{M} \sum_{m=1}^M x(mT_s) y(mT_s) \quad (2.1)$$

and

$$\hat{\phi}(MT_s) = \frac{1}{M} \sum_{m=1}^M x(mT_s) \hat{y}(mT_s), \quad (2.2)$$

where T_s is a uniform sampling period, M is the number of samples

in a signal duration T , $x(t)$ and $y(t)$ are real-valued signals which can be either deterministic or random, and $\hat{y}(t)$ is the Hilbert transform of $y(t)$. The usual correlation function dependence on time shift τ can be found by setting $x(t)$ in Equations (2.1) and (2.2) equal the time shifted version of itself; i.e., by setting $x(t) = x(t - \tau)$. The envelope of the regular correlation function can be written as

$$\xi(MT_s) = \sqrt{\phi^2(MT_s) + \hat{\phi}^2(MT_s)} . \quad (2.3)$$

An analytical model for the regular correlation function is shown in Figure 2.1 using complex signal representation [15]. In this model, the sampled pre-envelope $p_y(mT_s)$ of the reference signal $y(t)$, defined by

$$p_y(mT_s) = y(mT_s) + j \hat{y}(mT_s) ,$$

is correlated with the sampled input signal $x(mT_s)$ giving the following complex correlation function:

$$\begin{aligned} z(MT_s) &= \frac{1}{M} \sum_{m=1}^M x(mT_s) p_y(mT_s) \\ &= \frac{1}{M} \sum_{m=1}^M x(mT_s) y(mT_s) + j \frac{1}{M} \sum_{m=1}^M x(mT_s) \hat{y}(mT_s) \\ &= \phi(MT_s) + j \hat{\phi}(MT_s) . \end{aligned}$$

NOTE . H INDICATES THE OPERATION OF TAKING THE HILBERT TRANSFORM.

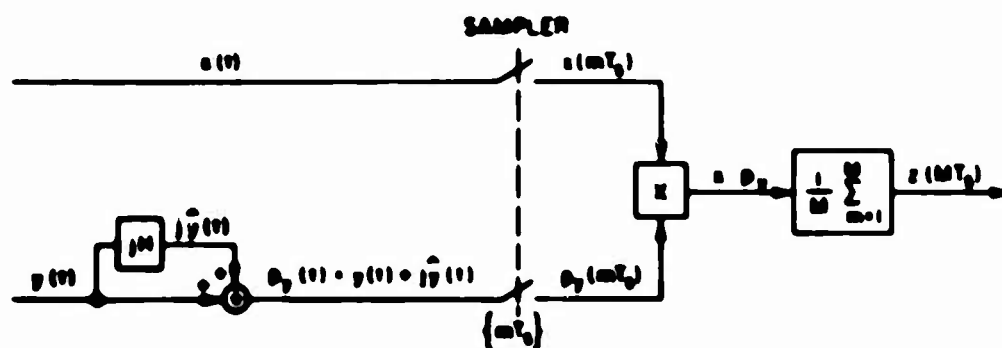


Figure 2.1 Analytic Model of Regular Correlation Function

Thus, the complex correlation function $z(MT_s)$ contains both quadrature components, $\phi(MT_s)$ and $\hat{\phi}(MT_s)$, and the envelope, $\xi(MT_s)$; i.e.,

$$\operatorname{Re}[z(MT_s)] = \phi(MT_s) = \text{"in-phase" component of the regular correlation function,}$$

$$\operatorname{Im}[z(MT_s)] = \hat{\phi}(MT_s) = \text{"quadrature phase" component,}$$

and

$$|z(MT_s)| = \xi(MT_s) = \text{regular correlation function envelope.}$$

We will next consider a modified version of the regular correlation function model of Figure 2.1. The "Quadrature Correlation Function" model of Figure 2.2 differs from the "Regular Correlation Function" model of Figure 2.1 in that, for the quadrature version, Hilbert transforms are taken of both the input and reference signals rather than just the reference signal. Instead of sampling the signal $x(t)$ every T_s seconds as shown in Figure 2.1, the quadrature correlation requires pairs of samples, $x(2mT_s)$ and $\hat{x}(2mT_s)$, every $2T_s$ seconds, giving the same total number M of samples during the finite signal duration, where M is assumed to be an even integer. The resulting equations for the in-phase component $\phi_Q(MT_s)$, the quadrature-phase component $\hat{\phi}_Q(MT_s)$, and the envelope $\xi_Q(MT_s)$ of the quadrature correlation function are

NOTE: H INDICATES THE OPERATION OF TAKING THE HILBERT TRANSFORM.

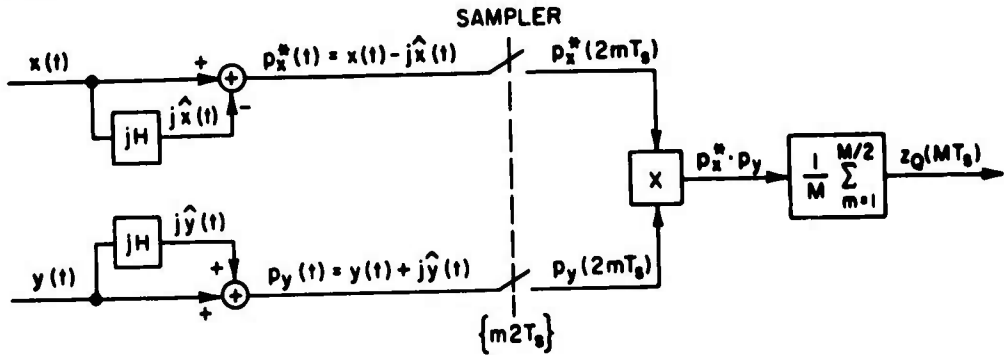


Figure 2.2 Analytic Model of Quadrature Correlation Function

$$\phi_Q(MT_s) = \frac{1}{M} \sum_{m=1}^{M/2} [x(2mT_s) y(2mT_s) + \hat{x}(2mT_s) \hat{y}(2mT_s)], \quad (2.4)$$

$$\hat{\phi}_Q(MT_s) = \frac{1}{M} \sum_{m=1}^{M/2} [x(2mT_s) \hat{y}(2mT_s) - \hat{x}(2mT_s) y(2mT_s)], \quad (2.5)$$

$$\xi_Q(MT_s) = \sqrt{\phi_Q^2(MT_s) + \hat{\phi}_Q^2(MT_s)}. \quad (2.6)$$

A comparison of Equations (2.4) and (2.1) show that both types of correlation function definitions require the same number of numerical computations (products and sums) per second to compute one value of the correlation function. However, successive values of the quadrature correlation function can only be computed at $2T_s$ second intervals instead of at T_s second intervals if the time delay τ is performed after sampling.

In the analytic quadrature correlation function model shown in Figure 2.2, the pre-envelope of the reference signal $y(t)$ is correlated with the complex conjugate of the pre-envelope of the input signal $x(t)$ giving the following equation for the complex quadrature correlation function, $z_Q(MT_s)$:

$$z_Q(MT_s) = \frac{1}{M} \sum_{m=1}^{M/2} p_x^*(2mT_s) p_y(2mT_s)$$

$$\begin{aligned}
&= \frac{1}{M} \sum_{m=1}^{M/2} [x(2mT_s) - j\hat{x}(2mT_s)][y(2mT_s) + j\hat{y}(2mT_s)] \\
&= \frac{1}{M} \sum_{m=1}^{M/2} [x(2mT_s) y(2mT_s) + \hat{x}(2mT_s) \hat{y}(2mT_s)] \\
&\quad + j \frac{1}{M} \sum_{m=1}^{M/2} [x(2mT_s) \hat{y}(2mT_s) - \hat{x}(2mT_s) y(2mT_s)] \\
&= \phi_Q(MT_s) + j \hat{\phi}_Q(MT_s).
\end{aligned}$$

Taking the real and imaginary parts and the absolute value of $z_Q(MT_s)$ gives:

$$\text{Re} [z_Q(MT_s)] = \phi_Q(MT_s), \text{ the in-phase component,}$$

$$\text{Im} [z_Q(MT_s)] = \hat{\phi}_Q(MT_s), \text{ the quadrature-phase component,}$$

$$|z_Q(MT_s)| = \xi_Q(MT_s), \text{ the correlation envelope.}$$

2.2 Comparison of Regular and Quadrature Sampled Correlation Functions

A. Elimination of the Second Harmonic by Quadrature Correlation.

Consider the equations for the two basic correlation techniques being compared, regular correlation and quadrature correlation. From Equation (2.1), the regular correlation function "in-phase" component is:

$$\phi(MT_s) = \frac{1}{M} \sum_{m=1}^M x(mT_s) y(mT_s) \quad (2.7)$$

and, from Equation (2.4), the quadrature correlation function "in-phase" component is:

$$\phi_Q(MT_s) = \frac{1}{M} \sum_{m=1}^{M/2} [x(2mT_s) y(2mT_s) + \hat{x}(2mT_s) \hat{y}(2mT_s)]. \quad (2.8)$$

Equations (2.7) and (2.8) are both sampled approximations to the desired analog correlation function given by

$$\phi(T) = \frac{1}{T} \int_0^T x(t) y(t) dt, \quad (2.9)$$

where $x(t)$ and $y(t)$ are continuous real-valued functions that are approximately limited in time T and bandwidth W such that $TW \gg 1$. The basic question that we now wish to examine is how accurately the sampled correlation functions of Equations (2.7) and (2.8) approximate the desired continuous correlation function of Equation(2.9) for two specific cases. The two cases considered here are: (1) $x(t)$ and $y(t)$ are both deterministic functions for which Fourier transforms can be written [as a special case, $y(t)$ could be a delayed version of $x(t)$], and (2) both $x(t)$ and $y(t)$ (either deterministic or random) can be represented by narrow-band representations of the form [37]

$$s(t) = a(t) \cos \omega_0 t - b(t) \sin \omega_0 t,$$

where $a(t)$ and $b(t)$ are low-pass functions and ω_0 is the center frequency of the signal $s(t)$. Case 1 thus considers the sampling errors in obtaining the correlation function between two deterministic signals, and Case 2 considers the effects of sampling on the correlation function variance when a reference signal is correlated with a narrow band random process. In both cases, it will be found that the sampled quadrature correlation function represents a more accurate approximation to Equation (2.9) if the sampling rate is sufficiently high and that the sampling errors associated with the regular correlation function are a function of a signal bandwidth, center frequency, and sampling rate.

The basic phenomenon that makes quadrature correlation more accurate than regular correlation in both cases is that quadrature correlation eliminates the second harmonic in the frequency spectrum of the unsampled product of $x(t)$ and $y(t)$. This will be shown by obtaining expressions for the Fourier transforms of the products $[x(t) \cdot y(t)]$ for regular correlation and $\frac{1}{2} [x(t) y(t) + \hat{x}(t) \hat{y}(t)]$ for quadrature correlation.

Considering Case 1, let $X(\omega)$ and $Y(\omega)$ represent the Fourier transforms of $x(t)$ and $y(t)$, and let $\hat{X}(\omega)$ and $\hat{Y}(\omega)$ represent the Fourier transforms of $\hat{x}(t)$ and $\hat{y}(t)$. Assume $x(t)$ and $y(t)$ are deterministic signals whose non-negligible positive spectrums, as

illustrated in Figure 2.3, are confined to the frequency interval $(\omega_0 - \frac{\Delta}{2}) < \omega < (\omega_0 + \frac{\Delta}{2})$, where ω_0 is the center of the frequency band, $\Delta = 2\pi W$, and W is the signal bandwidth in Hertz. According to [15], $\hat{X}(\omega)$ and $\hat{Y}(\omega)$ can be expressed in terms of $X(\omega)$ and $Y(\omega)$ as

$$\hat{X}(\omega) = \begin{cases} -jX(\omega) & \text{for } \omega > 0 \\ jX(\omega) & \text{for } \omega < 0 \end{cases}, \quad (2.10)$$

and

$$\hat{Y}(\omega) = \begin{cases} -jY(\omega) & \text{for } \omega > 0 \\ jY(\omega) & \text{for } \omega < 0 \end{cases}. \quad (2.11)$$

The Fourier transform $F_R(\omega)$ of the regular correlation product $x(t) y(t)$ is:

$$F_R(\omega) = \mathcal{F}[x(t) y(t)] = \int_{-\infty}^{\infty} x(t) y(t) e^{-j\omega t} dt. \quad (2.12)$$

Substituting the expressions for the inverse transforms of $x(t)$ and $y(t)$ into Equation (2.12) gives $F_R(\omega)$ as the convolution of $X(\omega)$ and $Y(\omega)$:

$$F_R(\omega) = \frac{1}{2\pi} \int_{-\infty}^{\infty} X(\beta) Y(\omega - \beta) d\beta. \quad (2.13)$$

Likewise, for the product $\hat{x}(t) \cdot \hat{y}(t)$, if

$$F_2(\omega) = \mathcal{F}[\hat{x}(t) \hat{y}(t)] = \int_{-\infty}^{\infty} \hat{x}(t) \hat{y}(t) e^{-j\omega t} dt,$$

then

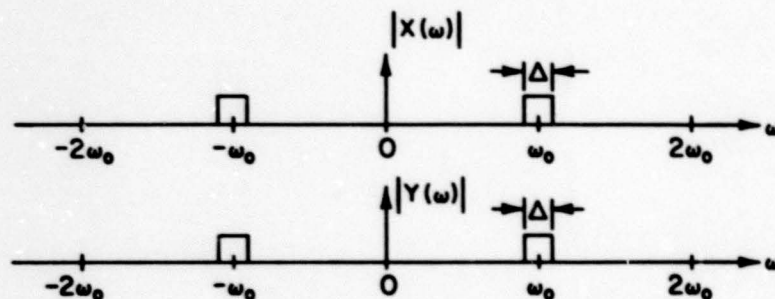


Figure 2.3 Typical Non-Zero Signal Spectrum Ranges

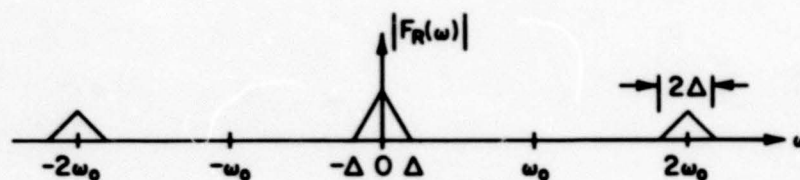


Figure 2.4 Non-Zero Spectral Range for Regular Correlation

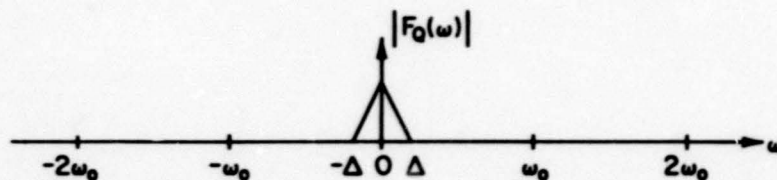


Figure 2.5 Non-Zero Spectral Range for Quadrature Correlation

$$F_2(\omega) = \frac{1}{2\pi} \int_{-\infty}^{\infty} \hat{X}(\beta) \hat{Y}(\omega-\beta) d\beta. \quad (2.14)$$

The spectrum of the quadrature correlation product

$\frac{1}{2} [x(t) y(t) + \hat{x}(t) \hat{y}(t)]$ in terms of $F_R(\omega)$ and $F_2(\omega)$ is:

$$\begin{aligned} F_Q(\omega) &= \mathcal{F} \left\{ \frac{1}{2} [x(t) y(t) + \hat{x}(t) \hat{y}(t)] \right\} \\ &= \frac{1}{2} [F_R(\omega) + F_2(\omega)]. \end{aligned} \quad (2.15)$$

An examination of the frequencies at which $F_R(\omega)$ and $F_Q(\omega)$ are non-negligible will show that, for $F_Q(\omega)$, the second harmonic terms around $\omega = 2\omega_0$ cancel when the sum of $F_R(\omega)$ and $F_2(\omega)$ is taken in Equation (2.15). Consider first the non-negligible regions of the regular correlation spectrum $F_R(\omega)$. The graphical convolution shown in Figure 2.4 of $X(\omega)$ and $Y(\omega)$ from Figure 2.3 shows that the non-negligible portions of $F_R(\omega)$ are given by

$$F_R(\omega) \neq 0 \text{ for } \begin{cases} -\Delta < \omega < \Delta, & (\text{modulation term}) \\ (2\omega_0 - \Delta) < \omega < (2\omega_0 + \Delta), & (\text{positive second harmonic}) \\ (-2\omega_0 - \Delta) < \omega < (-2\omega_0 + \Delta), & (\text{negative second harmonic}). \end{cases} \quad (2.16)$$

The corresponding expressions for $F_R(\omega)$ obtained from Equation (2.13) are:

$$\begin{aligned}
F_R(\omega) &= \frac{1}{2\pi} \int_{-\omega_0 - \Delta/2}^{-\omega_0 + \Delta/2} X(\beta) Y(\omega - \beta) d\beta \\
&\quad + \frac{1}{2\pi} \int_{\omega_0 - \Delta/2}^{\omega_0 + \Delta/2} X(\beta) Y(\omega - \beta) d\beta, \\
&\quad \text{for } -\Delta < \omega < \Delta, \\
&= \frac{1}{2\pi} \int_{\omega_0 - \Delta/2}^{\omega_0 + \Delta/2} X(\beta) Y(\omega - \beta) d\beta, \\
&\quad \text{for } (2\omega_0 - \Delta) < \omega < (2\omega_0 + \Delta), \\
&= \frac{1}{2\pi} \int_{-\omega_0 - \Delta/2}^{-\omega_0 + \Delta/2} X(\beta) Y(\omega - \beta) d\beta, \\
&\quad \text{for } (-2\omega_0 - \Delta) < \omega < (-2\omega_0 + \Delta).
\end{aligned}
\tag{2.17}$$

An examination of $F_2(\omega) = \mathcal{F}[\hat{x}(t) \hat{y}(t)]$ from Equation (2.14) shows the same non-negligible spectral regions given by Equation (2.16), where $F_2(\omega)$ can be derived using the Hilbert transform spectral properties of Equations (2.10) and (2.11) as:

$$\begin{aligned}
F_2(\omega) &= \frac{1}{2\pi} \int_{-\omega_0 - \Delta/2}^{-\omega_0 + \Delta/2} [jX(\beta)] [-jY(\omega - \beta)] d\beta \\
&\quad + \frac{1}{2\pi} \int_{\omega_0 - \Delta/2}^{\omega_0 + \Delta/2} [-jX(\beta)] [jY(\beta)] d\beta, \\
&\quad \text{for } -\Delta < \omega < \Delta,
\end{aligned}$$

$$= \frac{1}{2\pi} \int_{\omega_0 - \Delta/2}^{\omega_0 + \Delta/2} [-jX(\beta)] [-jY(\omega-\beta)] d\beta,$$

$$\text{for } (2\omega_0 - \Delta) < \omega < (2\omega_0 + \Delta),$$

$$= \frac{1}{2\pi} \int_{-\omega_0 - \Delta/2}^{-\omega_0 + \Delta/2} [jX(\beta)] [jY(\omega-\beta)] d\beta,$$

$$\text{for } (-2\omega_0 - \Delta) < \omega < (-2\omega_0 + \Delta).$$

(2.18)

Combining $F_R(\omega)$ and $F_2(\omega)$ from Equations (2.17) and (2.18) to give $F_Q(\omega) = \frac{1}{2} [F_R(\omega) + F_2(\omega)]$ for quadrature correlation yields:

$$F_Q(\omega) = F_R(\omega) = \frac{1}{2\pi} \int_{-\omega_0 - \Delta/2}^{-\omega_0 + \Delta/2} X(\beta) Y(\omega-\beta) d\beta$$

$$+ \frac{1}{2\pi} \int_{\omega_0 - \Delta/2}^{\omega_0 + \Delta/2} X(\beta) Y(\omega-\beta) d\beta,$$

$$\text{for } -\Delta < \omega < \Delta,$$

$$= 0,$$

$$\text{for } (2\omega_0 - \Delta) < \omega < (2\omega_0 + \Delta),$$

$$= 0,$$

$$\text{for } (-2\omega_0 - \Delta) < \omega < (-2\omega_0 + \Delta).$$

(2.19)

Thus, from Equations (2.17) and (2.19), $F_Q(\omega)$ and $F_R(\omega)$ are identical for $-\Delta < \omega < \Delta$ and $F_Q(\omega)$ is zero elsewhere, while $F_R(\omega)$ contains second harmonic terms around $\omega = \pm 2\omega_0$ as

illustrated in Figures 2.4 and 2.5. It will now be shown that these second harmonic terms in the regular correlation product spectrum produce sampling errors which are not present in the quadrature correlation function.

B. Correlation Accuracy for Deterministic Signals. In order to evaluate the correlation function sampling errors when both the input and references are deterministic signals (or time-delayed versions of the same deterministic signal), consider first the problem of representing the integral of an arbitrary Fourier transformable function $f(t)$ by the sum of uniformly spaced samples $f(mT_s)$ of the function.

Let $f(t)$ be any Fourier transformable deterministic real-valued signal defined for $0 \leq t \leq T$ and essentially zero elsewhere. We can represent $f(t)$ in the time interval $[0, T]$ by the complex Fourier series:

$$f(t) = \frac{1}{T} \sum_{n=-\infty}^{\infty} c_n e^{j \frac{2\pi n t}{T}} \quad (2.20)$$

where

$$c_n = \int_0^T f(t) e^{-j \frac{2\pi n}{T} t} dt. \quad (2.21)$$

Next, consider sampling $f(t)$ at a uniform sampling rate $f_s = \frac{1}{T_s}$, where T_s = time between samples in seconds, and averaging the resulting $N = \frac{T}{T_s}$ samples; i.e.,

$$\frac{1}{N} \sum_{m=1}^N f(mT_s) = \frac{1}{NT} \sum_{m=1}^N \sum_{n=-\infty}^{\infty} c_n e^{j \frac{2\pi n m}{N}} \quad (2.22)$$

Since the Fourier series for $f(t)$ in Equation (2.20) is periodic with period T and since $e^{-j \frac{2\pi n}{T} (t \pm T)} = e^{-j \frac{2\pi n}{T} t}$, the integral of Equation (2.21) for the coefficient c_n can be rewritten as:

$$c_n = \int_{-T/2}^{T/2} f(t) e^{-j \frac{2\pi n}{T} t} dt,$$

and Equation (2.22) as

$$\frac{1}{N} \sum_{m=1}^N f(mT_s) = \frac{1}{NT} \sum_{n=-\infty}^{\infty} \left[\int_{-T/2}^{T/2} f(t) e^{-j \frac{2\pi n}{T} t} dt \right] \sum_{m=1}^N e^{j \frac{2\pi n m}{N}}.$$

$$\text{Substituting } \sum_{m=1}^N e^{j \frac{2\pi n}{N} m} = \frac{(1 - e^{j 2\pi n})}{(e^{-j \frac{2\pi n}{N}} - 1)} = \begin{cases} 0 & \text{for } n \neq kN \\ N & \text{for } n = kN \end{cases}$$

where k is any integer, gives

$$\frac{1}{N} \sum_{m=1}^N f(mT_s) = \frac{1}{T} \sum_{k=-\infty}^{\infty} \int_{-T/2}^{T/2} f(t) e^{-j \frac{2\pi k N}{T} t} dt. \quad (2.23)$$

Moving the $k = 0$ term from the right-hand side of Equation (2.23) to the left-hand side and noting $\frac{N}{T} = f_s$ gives:

$$\begin{aligned}
 E_T &= \left[\frac{1}{N} \sum_{m=1}^N f(mT_s) - \frac{1}{T} \int_0^T f(t) dt \right] \\
 &= \frac{1}{T} \sum_{\substack{k=-\infty \\ k \neq 0}}^{\infty} \int_{-T/2}^{T/2} f(t) e^{-j2\pi k f_s t} dt, \quad (2.24)
 \end{aligned}$$

where E_T is the error in representing the integral $\frac{1}{T} \int_0^T f(t) dt$ by the discrete sum $\frac{1}{N} \sum_{m=1}^N f(mT_s)$. If the inverse Fourier

Transform $f(t) = \int_{-\infty}^{\infty} F(2\pi f) e^{j2\pi f t} df$ is substituted into the

right-hand side of Equation (2.24), E_T becomes:

$$\begin{aligned}
 E_T &= \frac{1}{T} \sum_{\substack{k=-\infty \\ k \neq 0}}^{\infty} \int_{-T/2}^{T/2} \int_{-\infty}^{\infty} F(2\pi f) e^{j2\pi f t} df e^{-j2\pi k f_s t} dt \\
 &= \sum_{\substack{k=-\infty \\ k \neq 0}}^{\infty} \int_{-\infty}^{\infty} F(2\pi f) \frac{1}{T} \left[\int_{-T/2}^{T/2} e^{j2\pi t(f - k f_s)} dt \right] df \\
 &= \sum_{\substack{k=-\infty \\ k \neq 0}}^{\infty} \int_{-\infty}^{\infty} F(2\pi f) \frac{\sin \pi T(f - k f_s)}{\pi T(f - k f_s)} df. \quad (2.25)
 \end{aligned}$$

Equation (2.25) can be simplified further by writing $F(2\pi f)$ in terms of its real and imaginary parts $F(2\pi f) = {}_r F(2\pi f) + j {}_i F(2\pi f)$

to give

$$E_T = \int_{-\infty}^{\infty} F(2\pi f) \frac{\sin \pi T(f - kf_s)}{\pi T(f - kf_s)} df \\ + \int_{-\infty}^{\infty} F(2\pi f) \frac{\sin \pi T(f - kf_s)}{\pi T(f - kf_s)} df.$$

The second integral is zero because the integrand is an odd function of frequency. The first integral can be reduced to the integral over positive frequency since the integrand is an even function of frequency. Thus, E_T becomes

$$E_T = 2 \int_{k=0}^{\infty} F(2\pi f) \frac{\sin \pi T(f - kf_s)}{\pi T(f - kf_s)} df. \quad (2.26)$$

For a given $F(2\pi f)$, T , and f_s , Equation (2.26) could be used to compute the error E_T .

Further simplification of Equation (2.26) results in many cases for signals with large TW products. If $\frac{1}{T} \ll W$ and $F(2\pi f)$ is approximately constant for $(f_s - \frac{1}{T}) < f < (f_s + \frac{1}{T})$, Equation (2.26) approximately reduces to

$$E_T \approx 2 \int_{k=-\infty}^{\infty} F(2\pi kf_s) \frac{\sin \pi T(f - kf_s)}{\pi T(f - kf_s)} df.$$

If $f_s \gg \frac{1}{T}$, the above integral is approximately equal to $\frac{1}{T}$

for all $k \geq 0$. Let E represent the approximation to the error E_k under these assumptions. Then,

$$E = \sum_{k=1}^{\infty} \frac{1}{k!} \int_{-\infty}^{\infty} x(t) y(t) e^{-j\omega t} dt. \quad (2.27)$$

These results can now be used to compare the accuracy of regular and quadrature correlation by letting $f(t)$ of Equation (2.2) be equal to the product $x(t)y(t)$ for regular correlation and $\frac{1}{2}[x(t)y(t) + \hat{x}(t)\hat{y}(t)]$ for quadrature correlation.

From Equation (2.12), the Fourier transform, $F_R(\omega)$, of the regular correlation product $x(t)y(t)$ is

$$F_R(\omega) = \int_{-\infty}^{\infty} x(t)y(t) e^{-j\omega t} dt = \text{Re } F_R(\omega) + j \text{Im } F_R(\omega),$$

where $\text{Re } F_R(\omega)$ and $\text{Im } F_R(\omega)$ are the real and imaginary parts of $F_R(\omega)$ which can be computed from Equation (2.17). Figure 2.4 shows the range of non-negligible values of $F_R(\omega)$ for the case where both $x(t)$ and $y(t)$ are approximately band-limited to $(\omega_0 - \Delta/2) < \omega < (\omega_0 + \Delta/2)$. The corresponding plot for the quadrature correlation spectrum is shown in Figure 2.5 where

$$F_Q(\omega) = \int_{-\infty}^{\infty} \frac{1}{2} [x(t)y(t) + \hat{x}(t)\hat{y}(t)] e^{-j\omega t} dt \\ = \text{Re } F_Q(\omega) + j \text{Im } F_Q(\omega),$$

can be computed from Equation (2.19).

For the quadrature correlation function, Equation (2.27) and Figure 2.5 show that the correlation error $E = \sum_{k=1}^{\infty} \frac{1}{k} J_0(2\pi k f_s)$ is essentially zero for the quadrature pair sampling rate \hat{f}_s such that

$$\hat{f}_s \geq \frac{1}{2T} \quad (2.26)$$

because $J_0(2\pi f) \approx 0$ for all $f > \frac{1}{2T}$. The sampling rate \hat{f}_s represents the uniform rate at which quadrature pair samples are taken. Thus, $\hat{f}_s = \frac{1}{2T} = \frac{1}{2} f_s$, where f_s is the regular correlation uniform sampling rate.

For the regular correlation function, Equation (2.17) and Figure 2.4 show that second harmonic spectral components of $J_0(2\pi f)$ exist in the range

$$2\omega_0 - 1 \leq \omega \leq 2\omega_0 + 1.$$

If any multiple of the sampling rate f_s falls in this frequency range, a non-negligible sampling error E given by Equation (2.27) will result. Whether or not some multiple $K2\pi f_s$ falls in the interval $(2\omega_0 - 1) \leq \omega \leq (2\omega_0 + 1)$ depends upon the relationship between ω_0 and f_s . For example, if $f_s = \frac{1}{T}$ (Shannon rate), the error will be negligible if

$$\left| \frac{\omega_0}{f_s} - \frac{1}{2} \right| = N \text{ (any integer),}$$

which is the condition for multiples of $2\pi f_s$ to occur at $(2\omega_0 - 1)$

Thus, the real part of $F_p(\omega)$ is:

$$F_p(\omega) = \frac{1}{\pi} \int_{-\infty}^{\infty} f(t) \cos(\omega t) dt = \frac{1}{\pi} \int_{-\infty}^{\infty} f(t) \cos(\omega t) dt$$

and Equation 2.29 becomes:

$$E = \frac{1}{\pi} \int_{-\infty}^{\infty} F_p(\omega) \cos(\omega t) d\omega = \frac{1}{\pi} \int_{-\infty}^{\infty} F_p(\omega) \cos(\omega t) d\omega \quad (2.30)$$

For the special case of $x(t) = y(t)$, Equation (2.30) becomes:

$$E = \frac{1}{\pi} \int_{-\infty}^{\infty} F_p(\omega) \cos(\omega t) d\omega = \frac{1}{\pi} \int_{-\infty}^{\infty} F_p(\omega) \cos(\omega t) d\omega \quad (2.31)$$

Equation 2.31 gives the correlation error E in terms of the complex spectrum of $x(t)$ for the special case $x(t) = y(t)$, $f_p = \frac{1}{\pi}$, and $\frac{1}{\pi}$ is an integer. An expression for E in terms of the time function $x(t)$ for the same case can be obtained from Equation 2.29 using the same assumptions used in deriving Equation 2.17 as

$$E = \frac{1}{\pi} \int_{-\infty}^{\infty} F_p(\omega) \cos(\omega t) d\omega = \frac{1}{\pi} \int_{-\infty}^{\infty} F_p(\omega) \cos(\omega t) d\omega$$

using the expressions for $F_p(\omega)$ and $F_p(\omega)$ from Equation (2.17),

It becomes:

$$E = \frac{1}{T} \sum_{n=0}^{T-1} \left[\frac{1}{2} \left(1 + \cos \frac{2\pi n}{T} \right) + \frac{1}{2} \left(1 - \cos \frac{2\pi n}{T} \right) \right] \quad (2.11)$$

$$= \frac{1}{T} \sum_{n=0}^{T-1} 1 = 1 \quad (2.12)$$

Letting $\lambda = \frac{2\pi}{T}$, Equation 2.11 can be shown to be equal to:

$$E = \frac{1}{T} \sum_{n=0}^{T-1} \left[\frac{1}{2} \left(1 + \cos \frac{2\pi n}{T} \right) + \frac{1}{2} \left(1 - \cos \frac{2\pi n}{T} \right) \right] \quad (2.13)$$

or

$$E = \frac{1}{T} \sum_{n=0}^{T-1} \cos \frac{2\pi n}{T} \quad (2.14)$$

where $\cos \frac{2\pi n}{T}$ is non-negligible for $0 \leq n \leq T$.

In summary, the quadrature correlation function sampling error E was shown to be essentially zero for a quadrature pair sampling rate f_s greater than the Shannon rate, $1/T$. However, the regular correlation function sampling error was shown to be dependent upon the values of f_s , f_m , and f_c . For sampling rates f_s greater than the Shannon rate $1/T$, the regular correlation sampling error is essentially zero for $\frac{f_s}{f_m} = \frac{1}{M}$ an integer and non-negligible for any other combinations of f_s and f_m .

3. Correlation Variance for Narrowband Random Process Inputs.

The second harmonic in the regular correlation product spectrum also has an important effect on the correlation function variance for the case where the function $x(t)$ is assumed to be a member of a wide-sense stationary random process which can be represented by

$$x(t) = n(t) = \tilde{x}_1(t) \cos \omega_0 t + \tilde{x}_2(t) \sin \omega_0 t,$$

where ω_0 is the center frequency, $\tilde{x}_1(t)$ and $\tilde{x}_2(t)$ are low pass random functions whose auto- and cross-correlation functions are known.

Assume that the function $y(t)$ can also be represented by the narrow band approximation

$$y(t) = \tilde{L}_1(t) \cos \omega_0 t + \tilde{L}_2(t) \sin \omega_0 t, \quad (2.34)$$

where $\tilde{L}_1(t)$ and $\tilde{L}_2(t)$ can either be deterministic or random low pass functions. For the purpose of this analysis, the only properties of $\tilde{L}_1(t)$ and $\tilde{L}_2(t)$ that will be assumed known are the correlation functions

$$\overline{\tilde{L}_1(t) \tilde{L}_1(t+\tau)} = \overline{\tilde{L}_1^2(t)} \rho_1(\tau), \text{ and } \overline{\tilde{L}_1(t) \tilde{L}_2(t+\tau)} = \overline{\tilde{L}_2^2(t)} \rho_2(\tau)$$

Assume also that the $n(t)$ and $y(t)$ are uncorrelated; i.e., that

$$\overline{\tilde{L}_i(t) \tilde{x}_j(t+\tau)} = 0 \quad \text{for } i, j = 1, 2. \quad (2.35)$$

Under these assumptions, the in-phase regular correlation function from Equation (2.1) is given by:

$$\begin{aligned} \phi(\mathbf{u}^T_0) &= \frac{1}{N} \sum_{n=1}^N n(\mathbf{u}^T_0) y(\mathbf{u}^T_0) \\ &= \frac{1}{N} \sum_{n=1}^N \lambda_1 \mathbf{u}^T_0 \cos \omega_0 \mathbf{u}^T_0 + \lambda_2 \mathbf{u}^T_0 \sin \omega_0 \mathbf{u}^T_0 \\ &= E_1 \mathbf{u}^T_0 \cos \omega_0 \mathbf{u}^T_0 + E_2 \mathbf{u}^T_0 \sin \omega_0 \mathbf{u}^T_0. \end{aligned}$$

The mean value of ϕ is zero by Equation (2.56). The variance, σ_ϕ^2 , of ϕ is

$$\sigma_\phi^2 = \overline{\phi^2} = \frac{1}{N^2} \sum_{n=1}^N \sum_{m=1}^N \overline{n(\mathbf{u}^T_0) y(\mathbf{u}^T_0) n(\mathbf{u}^T_m) y(\mathbf{u}^T_m)}. \quad (2.56)$$

If $n(t)$ and $y(t)$ are assumed to be independent so that the probability density function $p(n(\mathbf{u}^T_0), y(\mathbf{u}^T_0), n(\mathbf{u}^T_m), y(\mathbf{u}^T_m)) = p(n(\mathbf{u}^T_0), n(\mathbf{u}^T_m)) p(y(\mathbf{u}^T_0), y(\mathbf{u}^T_m))$, the four-fold expectation of Equation (2.56) can be reduced to:

$$\overline{n(\mathbf{u}^T_0) y(\mathbf{u}^T_0) n(\mathbf{u}^T_m) y(\mathbf{u}^T_m)} = \overline{n(\mathbf{u}^T_0) n(\mathbf{u}^T_m)} \cdot \overline{y(\mathbf{u}^T_0) y(\mathbf{u}^T_m)}.$$

σ_ϕ^2 of Equation (2.56) then reduces to:

$$\sigma_\phi^2 = \frac{1}{N^2} \sum_{n=1}^N \sum_{m=1}^N \overline{n(\mathbf{u}^T_0) n(\mathbf{u}^T_m)} \cdot \overline{y(\mathbf{u}^T_0) y(\mathbf{u}^T_m)}. \quad (2.57)$$

where

$$\begin{aligned} \overline{n(kT_s) n(mT_s)} &= \overline{N_1(kT_s) N_1(mT_s) \cos \omega_0 kT_s \cos \omega_0 mT_s} \\ &\quad + \overline{N_1(kT_s) N_2(mT_s) \cos \omega_0 kT_s \sin \omega_0 mT_s} \\ &\quad + \overline{N_2(kT_s) N_2(mT_s) \sin \omega_0 kT_s \sin \omega_0 mT_s} \\ &\quad + \overline{N_2(kT_s) N_1(mT_s) \sin \omega_0 kT_s \cos \omega_0 mT_s} \end{aligned}$$

and the expression for $y(kT_s) y(mT_s)$ is identical with each N_1 replaced by E_1 . Define the correlation functions

$$\overline{n(kT_s) n(mT_s)} = r_{nn}[(k-m)T_s],$$

$$\begin{aligned} \overline{N_1(kT_s) N_1(mT_s)} &= r_{N_1 N_1}[(k-m)T_s] = r_{N_1 N_1}[(m-k)T_s] \\ &= r_{N_2 N_2}[(m-k)T_s], \end{aligned}$$

$$\overline{N_1(kT_s) N_2(mT_s)} = r_{N_1 N_2}[(k-m)T_s] = -r_{N_1 N_2}[(m-k)T_s],$$

where for $k = m$,

$$r_{N_1 N_1}(0) = r_{N_2 N_2}(0) = \overline{n^2(mT_s)} = \sigma_n^2,$$

and

$$r_{N_1 N_2}(0) = 0.$$

Substituting Equations (2.38) and (2.39) into Equation (2.40) gives

$$\begin{aligned}
 \sigma_R^2 = & \frac{\sigma_n^2 \sigma_y^2}{M} + \frac{1}{M} \sum_{m=1}^M \left(1 - \frac{m}{M}\right) \left\{ \left[\phi_{N_1 N_1}(mT_s) \phi_{E_1 E_1}(mT_s) \right. \right. \\
 & + \phi_{N_1 N_2}(mT_s) \phi_{E_1 E_2}(mT_s) \left. \right] + \cos 2\omega_0 mT_s [\phi_{N_1 N_1}(mT_s) \phi_{E_1 E_1}(mT_s) \\
 & - \phi_{N_1 N_2}(mT_s) \phi_{E_1 E_2}(mT_s) \\
 & + \sin 2\omega_0 mT_s [\phi_{N_1 N_1}(mT_s) \phi_{E_1 E_2}(mT_s) \\
 & + \phi_{N_1 N_2}(mT_s) \phi_{E_1 E_1}(mT_s)] \left. \right\} \quad (2.41)
 \end{aligned}$$

The in-phase quadrature correlation function for these same conditions is, from Equation (2.4):

$$\rho_Q = \frac{1}{M} \sum_{m=1}^M [n(2mT_s) y(2mT_s) + \hat{n}(2mT_s) \hat{y}(2mT_s)].$$

From the above equations, $\phi_{nn}[(k-m)T_s]$ and $\phi_{yy}[(k-m)T_s]$ can be written as

$$\begin{aligned}\phi_{nn}[(k-m)T_s] &= \phi_{N_1 N_1}[(k-m)T_s] \cos \omega_0(k-m)T_s \\ &\quad + \phi_{N_1 N_2}[(k-m)T_s] \sin \omega_0(k-m)T_s,\end{aligned}\quad (2.38)$$

and

$$\begin{aligned}\phi_{yy}[(k-m)T_s] &= \phi_{E_1 E_1}[(k-m)T_s] \cos \omega_0(k-m)T_s \\ &\quad + \phi_{E_1 E_2}[(k-m)T_s] \sin \omega_0(k-m)T_s.\end{aligned}\quad (2.39)$$

σ_R^2 from Equation (2.37) now becomes:

$$\begin{aligned}\sigma_R^2 &= \frac{1}{M^2} \sum_{k=1}^M \sum_{m=1}^M \phi_{nn}[(k-m)T_s] \phi_{yy}[(k-m)T_s] \\ &= \frac{1}{M^2} \sum_{m=1}^M \phi_{nn}(0) \phi_{yy}(0) \\ &\quad + 2 \sum_{\substack{k=1 \\ k > m}}^M \sum_{m=1}^M \phi_{nn}[(k-m)T_s] \phi_{yy}[(k-m)T_s] \\ &= \frac{\sigma_n^2 \sigma_y^2}{M} + \frac{2}{M} \sum_{m=1}^M \left(1 - \frac{m}{M}\right) \phi_{nn}(mT_s) \phi_{yy}(mT_s).\end{aligned}\quad (2.40)$$

The mean value of ϕ_Q is zero and the variance is

$$\begin{aligned}
 \sigma_Q^2 &= \overline{\phi_Q^2} = \frac{1}{M^2} \sum_{k=1}^{M/2} \sum_{m=1}^{M/2} \overline{[n(2kT_s) y(2kT_s) + \hat{n}(2kT_s) \hat{y}(2kT_s)]} \\
 &\quad \overline{[n(2mT_s) y(2mT_s) + \hat{n}(2mT_s) \hat{y}(2mT_s)]} \\
 &= \frac{1}{M^2} \sum_{k=1}^{M/2} \sum_{m=1}^{M/2} \overline{[n(2kT_s) y(2kT_s) n(2mT_s) y(2mT_s) \\
 &\quad + n(2kT_s) y(2kT_s) \hat{n}(2mT_s) \hat{y}(2mT_s) \\
 &\quad + \hat{n}(2kT_s) \hat{y}(2kT_s) n(2mT_s) y(2mT_s) \\
 &\quad + \hat{n}(2kT_s) \hat{y}(2kT_s) \hat{n}(2mT_s) \hat{y}(2mT_s)]}. \tag{2.42}
 \end{aligned}$$

The first expectation in Equation (2.42) is given by the regular correlation function result of Equations (2.38) - (2.40) as

$$\begin{aligned}
 \overline{n(2kT_s) y(2kT_s) n(2mT_s) y(2mT_s)} &= \left\{ \begin{aligned} &\phi_{N_1 N_1} [2(k-m)T_s] \cos 2\omega_0(k-m)T_s \\ &+ \phi_{N_1 N_2} [2(k-m)T_s] \sin 2\omega_0(k-m)T_s \end{aligned} \right\} \\
 &\quad \cdot \left\{ \begin{aligned} &\phi_{E_1 E_1} [2(k-m)T_s] \cos 2\omega_0(k-m)T_s \\ &+ \phi_{E_1 E_2} [2(k-m)T_s] \sin 2\omega_0(k-m)T_s \end{aligned} \right\}. \tag{2.43}
 \end{aligned}$$

The fourth expectation $\overline{\hat{n}(2kT_s) \hat{y}(2kT_s) \hat{n}(2mT_s) \hat{y}(2mT_s)}$ can also be shown to be given by Equation (2.43). Similarly, the second expectation in Equation (2.42) is:

$$\begin{aligned}
 \overline{n(kT_s) y(2kT_s) \hat{n}(2mT_s) \hat{y}(2mT_s)} &= \overline{[n(2kT_s) \hat{n}(2mT_s)]} \cdot \\
 &\quad \overline{[y(2kT_s) \hat{y}(2mT_s)]} \\
 &= \left\{ -\phi_{N_1 N_1} [2(k-m)T_s] \sin 2\omega_0(k-m)T_s \right. \\
 &\quad \left. + \phi_{N_1 N_2} [2(k-m)T_s] \cos 2\omega_0(k-m)T_s \right\} \\
 &\quad \cdot \left\{ -\phi_{E_1 E_1} [2(k-m)T_s] \sin 2\omega_0(k-m)T_s \right. \\
 &\quad \left. + \phi_{E_1 E_2} [2(k-m)T_s] \cos 2\omega_0(k-m)T_s \right\}, \\
 &\quad (2.44)
 \end{aligned}$$

and the third expectation becomes:

$$\begin{aligned}
 \overline{\hat{n}(2kT_s) \hat{y}(2kT_s) n(2mT_s) y(2mT_s)} &= \overline{[\hat{n}(2kT_s) n(2mT_s)]} \cdot \\
 &\quad \overline{[\hat{y}(2kT_s) y(2mT_s)]} \\
 &= \left\{ \begin{aligned} &\phi_{N_1 N_1} [2(k-m)T_s] \sin 2\omega_o(k-m)T_s \\ &- \phi_{N_1 N_2} [2(k-m)T_s] \cos 2\omega_o(k-m)T_s \end{aligned} \right\} \\
 &\quad \cdot \left\{ \begin{aligned} &\phi_{E_1 E_1} [2(k-m)T_s] \sin 2\omega_o(k-m)T_s \\ &- \phi_{E_1 E_2} [2(k-m)T_s] \cos 2\omega_o(k-m)T_s \end{aligned} \right\} .
 \end{aligned}
 \tag{2.45}$$

σ_Q^2 can now be obtained from Equations (2.42) - (2.45),

$$\begin{aligned} \sigma_Q^2 = & \frac{2}{M^2} \sum_{k=1}^{M/2} \sum_{m=1}^{M/2} \left\{ \phi_{N_1 N_1} [2(k-m)T_s] \phi_{E_1 E_1} [2(k-m)T_s] \right. \\ & \left. + \phi_{N_1 N_2} [2(k-m)T_s] \phi_{E_1 E_2} [2(k-m)T_s] \right\} \\ & + \frac{c_n^2 \sigma_y^2}{M} + \frac{2}{M} \sum_{m=1}^{M/2} [\phi_{N_1 N_1} (2mT_s) \phi_{E_1 E_2} (2mT_s) \\ & + \phi_{N_1 N_2} (2mT_s) \phi_{E_1 E_2} (2mT_s)] (1 - \frac{2m}{M}). \end{aligned} \quad (2.46)$$

A comparison of σ_R^2 from Equation (2.41) for the regular correlation function and σ_Q^2 from Equation (2.46) for the quadrature correlation function shows the presence of second harmonic terms in σ_R^2 which do not appear in σ_Q^2 . Thus, while σ_Q^2 depends only upon the relation between the sampling period T_s and the signal bandwidth W , σ_R^2 also depends upon the center frequency ω_0 of the signal spectrum. This is illustrated in the example derived in the Appendix for the case where $n(t)$ is bandlimited white noise with a flat power spectrum for $(f_0 - \frac{W}{2}) < f < (f_0 + \frac{W}{2})$. For this example, σ_R^2 from Equation (2.41) and σ_Q^2 from Equation (2.46) are plotted in Figures 2.6 and 2.7, respectively, for $\frac{f_0}{W} = 9$ and

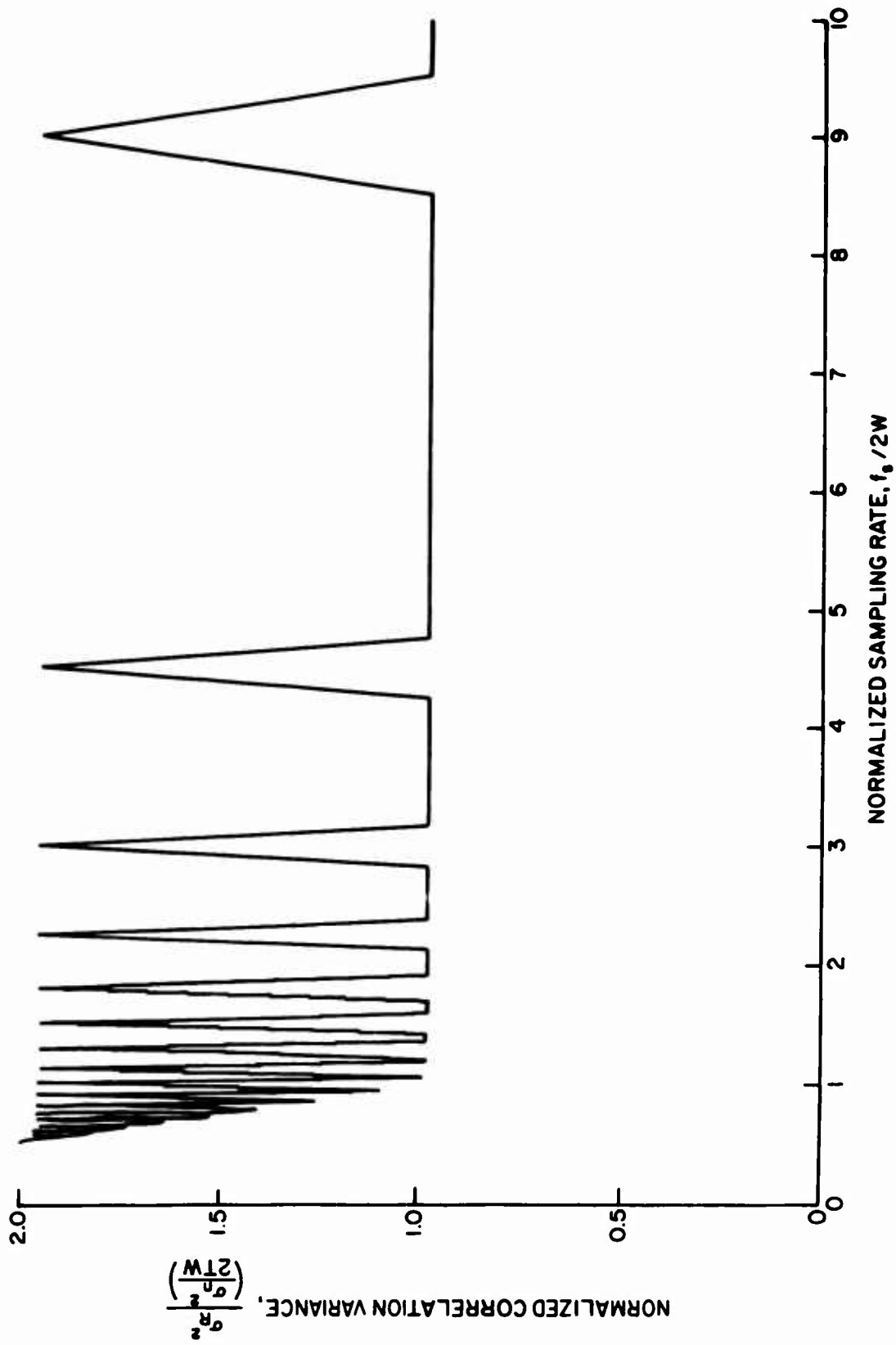


Figure 2.6 Regular Correlation Function Variance Vs. Sampling Rate

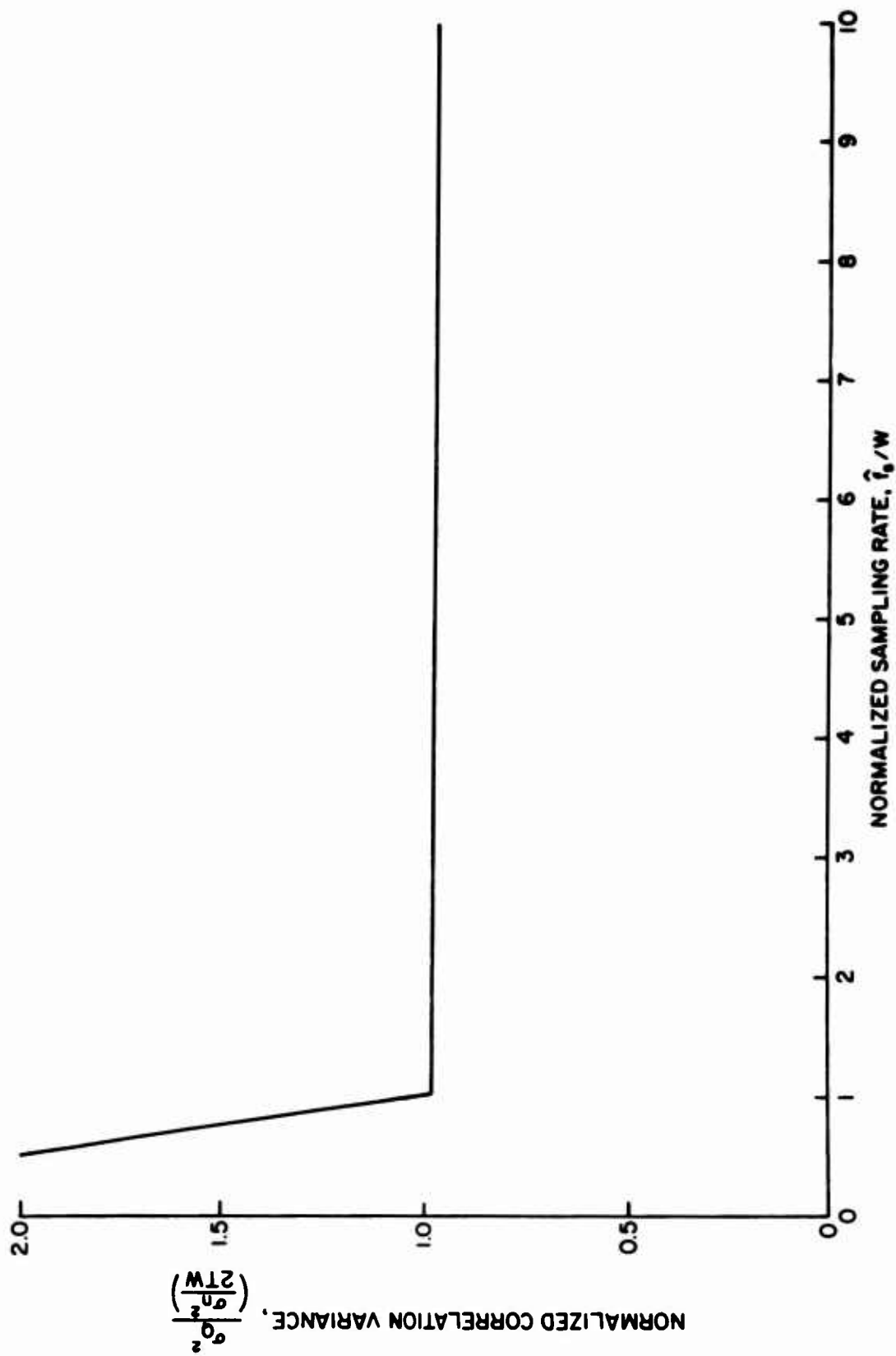


Figure 2.7 Quadrature Correlation Function Variance Vs. Sampling Rate

a $2TW$ product of 50. Figure 2.6 shows that the regular correlation variance can be as much as 0 to 3 dB higher than the quadrature correlation variance of Figure 2.7 depending upon the relationship of the sampling rate to f_0 and W . For this example, not only is the effect of the second harmonic missing in Figure 3.7, but the quadrature correlation function variance is seen to be constant at about

$$\sigma_Q^2 = \frac{\sigma_n^2}{2TW}, \quad (2.47)$$

for all $\hat{f}_s \geq W$.

To summarize, for the quadrature correlation function, the sampling error E was found to be zero and the correlation variance σ_Q^2 was found to be a constant independent of \hat{f}_s for $\hat{f}_s \geq \Delta/2\pi$. However, for the regular correlation function, both the sampling error and the correlation variance were found to have undesirable second harmonic terms at some values of f_s .

2.3 Comparison of Quadrature Correlation Functions for Clipped and Unclipped Signals

In this section, we wish to consider the properties of the quadrature correlation function for a special class of functions—clipped narrowband signals. The relationship between a real-valued function $x(t)$ before clipping and its value $u(t)$ after clipping is given by

$$u(t) = \text{sgn } x(t) = \begin{cases} 1 & \text{for } x(t) \geq 0 \\ -1 & \text{for } x(t) < 0. \end{cases}$$

Hard limiting thus destroys all "amplitude" information in $x(t)$ and retains the "phase" information in the sense that only the zero axis crossings of $x(t)$ are preserved in $u(t)$.

The analytic model for the quadrature correlation function for clipped signals shown in Figure 2.8 differs from the quadrature correlation function model for unclipped signals of Figure 2.2 only by the fact that $u(t)$ and $v(t)$ are hard limited versions of the signals $x(t)$ and $y(t)$. The quadrature correlation function, Equations (2.4) - (2.5), can thus be used to describe the clipped correlation functions of Figure 2.8 by replacing $x(t)$ by $\text{sgn } x(t)$ and $y(t)$ by $\text{sgn } y(t)$.

We wish to compare the clipped and unclipped quadrature correlation functions of $x(t)$ and $y(t)$ for two cases:

[1] $x(t) = \sigma_s s(t)$ and $y(t) = s(t - \tau)$ are both equal to the same narrowband gaussian signal $s(t)$ but with different relative amplitude σ_s , and [2] $y(t) = s(t)$ and $x(t) = \sigma_n n(t)$, a member of a wide-sense stationary gaussian random process. Let

$$n(t) = N_1(t) \cos \omega_0 t - N_2(t) \sin \omega_0 t$$

and

$$s(t) = E_1(t) \cos \omega_0 t - E_2(t) \sin \omega_0 t,$$

where

$$\overline{N_1^2(t)} = \overline{N_2^2(t)} = 1$$

$$\overline{E_1^2(t)} = \overline{E_2^2(t)} = 1$$

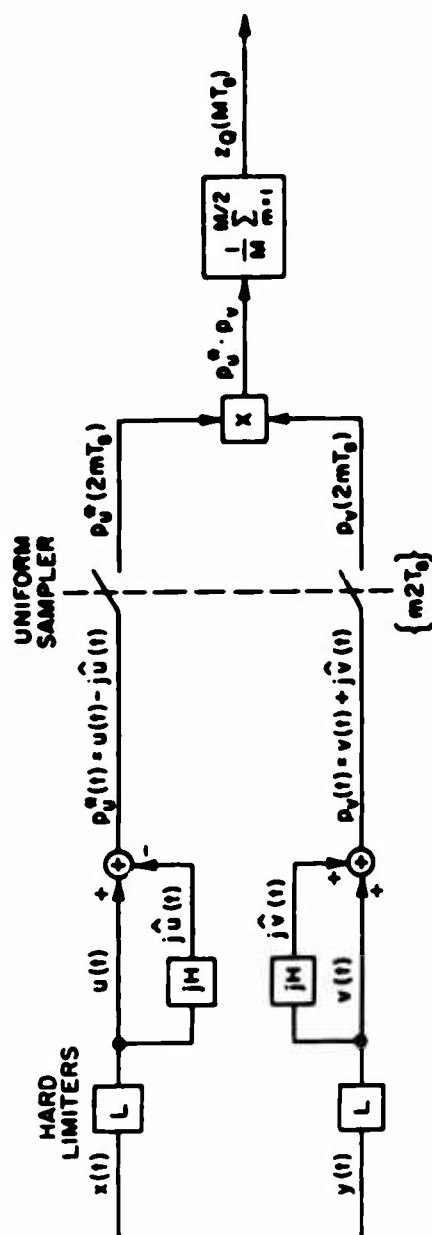


Figure 2.8 Quadrature Correlation Function Model for Clipped Signals

and

$$\overline{E_i(t) N_j(t - \tau)} = 0 \text{ for } i, j = 1, 2.$$

The values c_s and c_n account for differences in relative amplitude between $x(t)$ and $y(t)$.

Let the quadrature sampling rate be at the Shannon rate of $\hat{f}_s = \frac{1}{2T_s} = W$ sample pairs, $[x(2nT_s), \hat{x}(2nT_s)]$, per second. The Hilbert transform of $s(t)$ is given by

$$s(t) = E_1(t) \sin \omega_0 t + E_2(t) \cos \omega_0 t$$

and the pre-envelope of $s(t)$ by

$$s(t) + j\hat{s}(t) = [E_1(t) + jE_2(t)][\cos \omega_0 t + j \sin \omega_0 t] = f(t) e^{j\omega_0 t},$$

where $f(t)$ is the low pass modulation function whose spectrum is equal to the positive spectrum of $s(t)$ translated down to zero frequency and

$$\begin{aligned} z_{ff}(\tau) &= \overline{f^*(t) f(t - \tau)} = \overline{2[E_1(t) E_1(t - \tau)] + j2[E_1(t) E_2(t - \tau)]} \\ &= 2 \overline{E_1 E_1}(\tau) + j 2 \overline{E_1 E_2}(\tau). \end{aligned}$$

Consider first the quadrature correlation function for the unclipped case defined by

$$\phi_Q(MT_s) = \frac{1}{M} \sum_{m=1}^{M/2} [x(2mT_s) y(2mT_s) + \hat{x}(2mT_s) \hat{y}(2mT_s)],$$

$$\hat{\phi}_Q(MT_s) = \frac{1}{M} \sum_{m=1}^{M/2} [x(2mT_s) \hat{y}(2mT_s) - \hat{x}(2mT_s) y(2mT_s)],$$

and

$$z_Q(MT_s) = \phi_Q(MT_s) + j \hat{\phi}_Q(MT_s).$$

Considering Case 1, if we let $x(t) = \sigma_s s(t)$ and $y(t) = s(t - \tau)$,

$z_Q(\tau)$ will be the auto-correlation function of $s(t)$. Computing

$z_Q(\tau)$ at increments of τ equal to the spacing between samples,

$2T_s$, gives

$$\begin{aligned} z_Q(2nT_s) &= \frac{1}{M} \sum_{m=1}^{M/2} [x(2mT_s) - j\hat{x}(2mT_s)][y(2mT_s) + j\hat{y}(2mT_s)] \\ &= \frac{\sigma_s}{M} \sum_{m=1}^{M/2} [s(2mT_s) - j\hat{s}(2mT_s)][s(2mT_s - 2nT_s) \\ &\quad + j\hat{s}(2mT_s - 2nT_s)] \\ &= \frac{1}{2} \sigma_s e^{j2\omega_0 nT_s} \frac{1}{M/2} \sum_{m=1}^{M/2} f^*(2mT_s) f(2mT_s - 2nT_s) \\ &= \frac{\sigma_s}{2} e^{j2\omega_0 nT_s} z_{ff}(2nT_s), \end{aligned} \tag{2.48}$$

where, by Equations (2.27) and (2.28), $z_{ff}(2nT_s)$ is equal to

$\frac{1}{T} \int_0^T f^*(t) \cdot f(t - \tau) dt$ for $f_s \geq W$ and $\tau = 2nT_s$. Taking the real and imaginary parts of Equation (2.48):

$$z_Q(2nT_s) = \sigma_s [z_{E_1 F_1}(2nT_s) \cos 2\omega_0 nT_s - z_{E_1 E_2}(2nT_s) \sin 2\omega_0 nT_s], \quad (2.49)$$

and

$$\hat{z}_Q(2nT_s) = \sigma_s [z_{E_1 E_1}(2nT_s) \sin 2\omega_0 nT_s + z_{E_1 E_2}(2nT_s) \cos 2\omega_0 nT_s]. \quad (2.50)$$

The correlation function envelope is given by:

$$\begin{aligned} \xi_Q(2nT_s) &= \sqrt{z_Q^2(2nT_s) + \hat{z}_Q^2(2nT_s)} = |z_Q(2nT_s)| \\ &= \sigma_s \sqrt{z_{E_1 E_1}^2(2nT_s) + z_{E_1 E_2}^2(2nT_s)}. \end{aligned} \quad (2.51)$$

The maximum value of $\xi_Q(2nT_s)$ occurs at $n = 0$ and is given by:

$$(\xi_Q)_{\max} = \xi_Q(0) = \sigma_s. \quad (2.52)$$

For the clipped case, the auto-correlation function of $s(t)$ can be found by using the relationship [37] between the cross-correlation function of two Gaussian signals before and after clipping:

$$\rho_{ab}^{\text{clipped}}(\tau) = \frac{2}{\pi} \sin^{-1} \rho_{ab}(-) \quad (2.53)$$

where

$\hat{\phi}_{ab}(t)$ = cross-correlation function between $a(t)$ and $b(t)$ after clipping,

$\rho_{ab}(t)$ = normalized cross-correlation coefficient between $a(t)$ and $b(t)$ before clipping.

Using Equation (2.53), the real and imaginary parts of the clipped signal quadrature correlation function when $x(t) = \sigma_s s(t)$ and $y(t) = s(t - \tau)$ are:

$$\begin{aligned} \hat{\phi}_Q(2nT_s) &= \frac{2}{\pi} \sin^{-1} \left[\frac{\phi_Q(2nT_s)}{\sigma_s} \right] \\ &= \frac{2}{\pi} \sin^{-1} [\phi_{E_1 E_1}(2nT_s) \cos 2\omega_0 nT_s - \phi_{E_1 E_2}(2nT_s) \sin 2\omega_0 nT_s] \end{aligned} \quad (2.54)$$

and

$$\begin{aligned} \hat{\phi}_Q(2nT_s) &= \frac{2}{\pi} \sin^{-1} \left[\frac{\hat{\phi}_Q(2nT_s)}{\sigma_s} \right] \\ &= \frac{2}{\pi} \sin^{-1} [\phi_{E_1 E_1}(2nT_s) \sin 2\omega_0 nT_s + \phi_{E_1 E_2}(2nT_s) \cos 2\omega_0 nT_s]. \end{aligned} \quad (2.55)$$

Because clipping is a non-linear operation, the correlation envelope cannot be computed as the square root of the sum of the squares of $\hat{\phi}_Q$ and $\hat{\phi}_I$. However, the peak of the correlation envelope can be found from Equation (2.54) for $n = 0$, since $\hat{\phi}_Q(0) = 0$; i.e.,

$$(\xi_Q)_{\max} = \overset{\sim}{\phi}_Q(0) = \frac{2}{\pi} \sin^{-1}(1) = 1 \quad (2.56)$$

Equations (2.56) and (2.52) illustrate a basic normalization property of clipping; i.e., the correlation function for clipped signals has a range of -1 to +1, while for the unclipped signal, the range is $-\sigma_s$ to $+\sigma_s$, a function of the signal amplitude.

For Case (2), if $y(t) = s(t)$ and $x(t) = \sigma_n n(t)$, a member of a stationary gaussian random process, the average value of the quadrature correlation function for the unclipped case is zero and its variance as given by Equation (2.46) is:

$$\begin{aligned} \sigma_Q^2 = & \frac{\sigma_n^2}{M} + \frac{2}{M} \sum_{m=1}^{M/2} [\phi_{N_1 N_1}(2mT_s) \phi_{E_1 E_1}(2mT_s) \\ & + \phi_{N_1 N_2}(2mT_s) \phi_{E_1 E_2}(2mT_s)] (1 - \frac{2m}{M}). \end{aligned} \quad (2.57)$$

If $n(t)$ is assumed to have a rectangular spectrum of width W Hz, Figure 2.7 shows that, for any $\hat{f}_s \geq W$,

$$\sigma_Q^2 \approx \frac{\sigma_n^2}{2TW}, \quad (2.58)$$

where T is the signal duration in seconds.

The correlation function variance for the clipped signal case can be found by computing $\overset{\sim}{\sigma}_Q^2$ from Equation (2.42) as a function of $u(t)$ and $v(t)$ and then using Equation (2.53) to express $\overset{\sim}{\sigma}_Q^2$ in terms of $s(t)$ and $n(t)$.

$$\begin{aligned}
\sigma_Q^2 &= \frac{2}{M^2} \sum_{k=1}^{M/2} \sum_{m=1}^{M/2} \left\{ \overline{\phi_{uu}}[2(k-m)T_s] \overline{\phi_{vv}}[2(k-m)T_s] \right. \\
&\quad \left. + \overline{\phi_{uu}}[2(k-m)T_s] \overline{\phi_{vv}}[2(k-m)T_s] \right\} \\
&= \frac{1}{M} + \frac{2}{M} \sum_{m=1}^{M/2} \left(1 - \frac{2m}{M} \right) \left(\overline{\phi_{uu}}(2mT_s) \overline{\phi_{vv}}(2mT_s) \right. \\
&\quad \left. + \overline{\phi_{uu}}(2mT_s) \overline{\phi_{vv}}(2mT_s) \right) \\
&= \frac{1}{M} + \frac{2}{M} \frac{4}{\pi^2} \sum_{m=1}^{M/2} \left(1 - \frac{2m}{M} \right) \left\{ \left[\sin^{-1} \frac{\phi_{nn}(2mT_s)}{2} \right] \left[\sin^{-1} \phi_{ss}(2mT_s) \right] \right. \\
&\quad \left. + \left[\sin^{-1} \frac{\phi_{nn}(2mT_s)}{2} \right] \left[\sin^{-1} \phi_{ss}(2mT_s) \right] \right\}. \quad (2.59)
\end{aligned}$$

A plot of the variance given by Equation (2.59) for a random process $n(t)$ with a rectangular spectrum of bandwidth W Hz and center frequency f_0 Hz is shown in Figure 2.9 for $\frac{f_0}{W} = 9$ and $M = 2TW = 50$. The equations for this example are derived in the Appendix. Figure 2.9 shows that, for the Shannon sampling rate of $\hat{f}_s = W$, the variance is given by

$$\sigma_Q^2 = \frac{1}{2TW}, \quad (2.60)$$

but if the sampling rate is increased sufficiently, a variance of approximately

$$\sigma_Q^2 = \frac{1}{4TW} \quad (2.61)$$

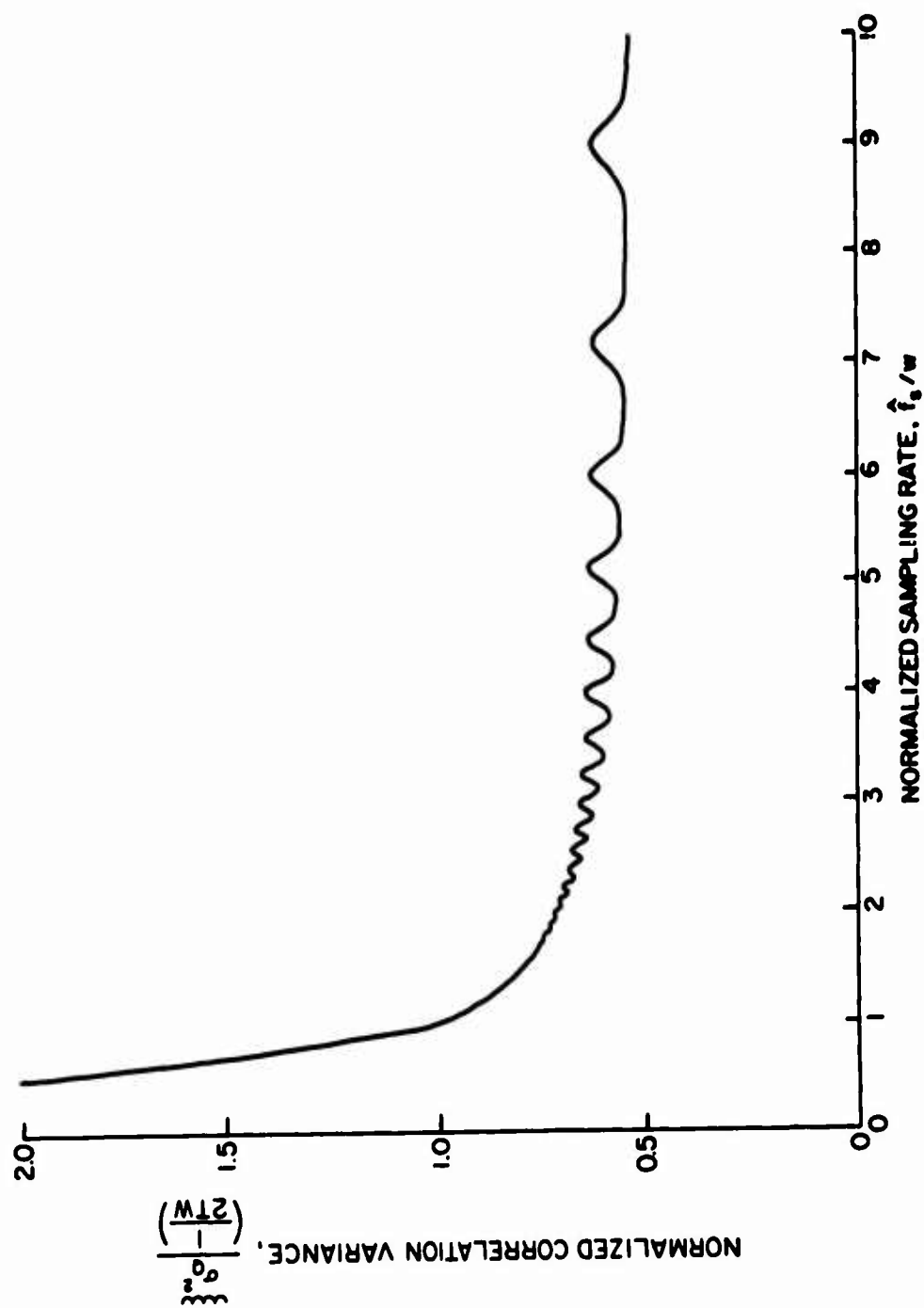


Figure 2.9 Clipped Signal Quadrature Correlation Function
Variance Vs. Sampling Rate

can be achieved. The small ripples in Figure 2.9 occur when integer multiples of the sampling rate are equal to the second harmonic of the signal center frequency. Because of the non-linearity of the limiters, these ripples were not completely eliminated as were those of Figure 2.7 for the unclipped signal case.

For comparison with Figure 2.9, the variance for the regular clipped correlation function is shown in Figure 2.10 for the same example. The curve of Figure 2.10 shows the same asymptote for large f_s as the quadrature correlation curve of Figure 2.9, but it exhibits ripples of about 3 dB instead of approximately 0.5 dB for the latter case.

A comparison of Figure 2.7 and 2.9 shows that clipping permits a reduced correlation variance for random signals if sampling is increased sufficiently beyond the Shannon rate. In summary, the two principal effects of clipping are seen to be correlation function normalization and reduced correlation variance for high sampling rates.

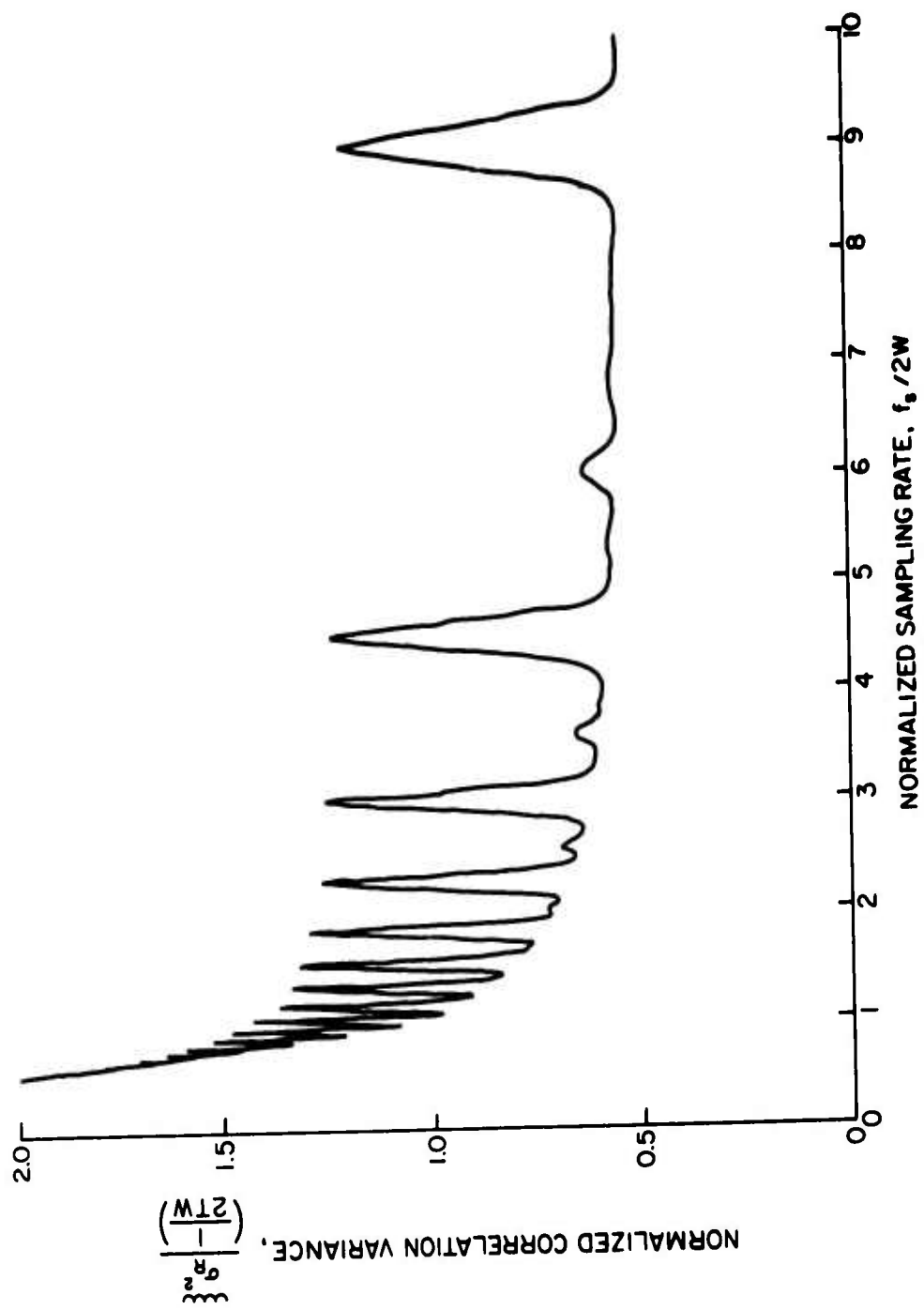


Figure 2.10 Clipped Signal Regular Correlation Function
Variance Vs. Sampling Rate

CHAPTER III

QUADRATURE CORRELATION FUNCTION PROPERTIES FOR SINUSOIDAL SIGNALS AND UNIFORM SAMPLING

3.1 Quadrature Correlation Function for Sinusoidal Signals

In this chapter, the uniform sampling quadrature correlation results of Chapter II for narrowband functions with large TW products will be extended to the case of sinusoidal signals. After examining the correlation properties of sinusoidal signals, the effects of uniform sampling and hard limiting will be derived separately and, finally, the combined effects of both sampling and hard limiting will be examined. The problem of spurious odd harmonic correlation resulting from clipping and sampling will be investigated in detail and a solution to the problem by the use of non-uniform sampling will be introduced.

Consider the quadrature correlation function model with finite integration time T shown in Figure 3.1 for two infinitely long sinusoidal signals with different frequencies. Let the input and reference signals be given by

$$x(t) = \cos \omega_1 t, -\infty < t < \infty,$$

and

$$y(t) = \cos \omega_0 t, -\infty < t < \infty,$$

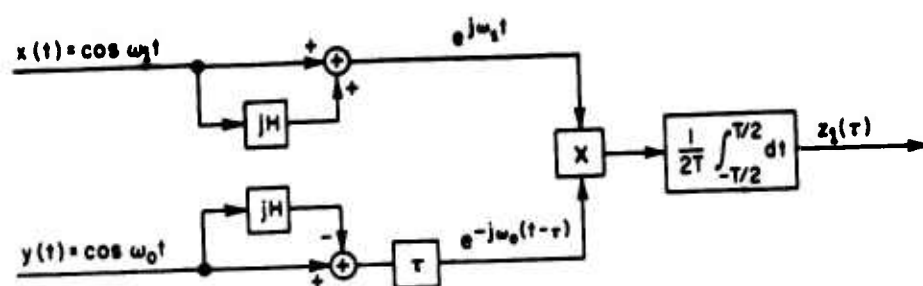


Figure 3.1 Quadrature Correlation Function Model for Sinusoidal Signals

where $\omega_1 = 2\pi f_1$ and $\omega_0 = 2\pi f_0$ are the sinusoidal frequencies. As discussed in Chapter II, the real and imaginary parts of the complex correlation function $z_1(\tau)$ of Figure 3.1 represent the "in-phase" and "quadrature phase" correlation components and $|z_1(\tau)|$ represents the envelope of the correlation function. From Figure 3.1, $z_1(\tau)$ is:

$$\begin{aligned} z_1(\tau) &= \frac{1}{2T} \int_{-T/2}^{T/2} e^{j\omega_1 t} e^{-j\omega_0(t-\tau)} dt \\ &= \frac{1}{2} e^{j\omega_0 \tau} \frac{\sin \pi T(f_1 - f_0)}{\pi T(f_1 - f_0)}. \end{aligned} \quad (3.1)$$

The correlation envelope peak at $\tau = 0$,

$$\left| z_1(0) \right| = \frac{1}{2} \left| \frac{\sin \pi T(f_1 - f_0)}{\pi T(f_1 - f_0)} \right|, \quad (3.2)$$

is plotted in Figure 3.2 as a function of the frequency difference $(f_1 - f_0)$. This plot shows that, except for frequencies f_1 within about $\frac{1}{T}$ of the fixed frequency f_0 , the correlation-envelope peaks, as a function of input frequency f_1 , never exceed the sidelobe peaks of the $\frac{\sin x}{x}$ function. Only the first two peaks are greater than 10 percent of the main lobe value at $f_1 = f_0$. For large T , therefore, this correlation function has a very selective frequency characteristic, since it has appreciable amplitude only for frequencies f_1 which are within about $\frac{1}{T}$ of the reference frequency f_0 .

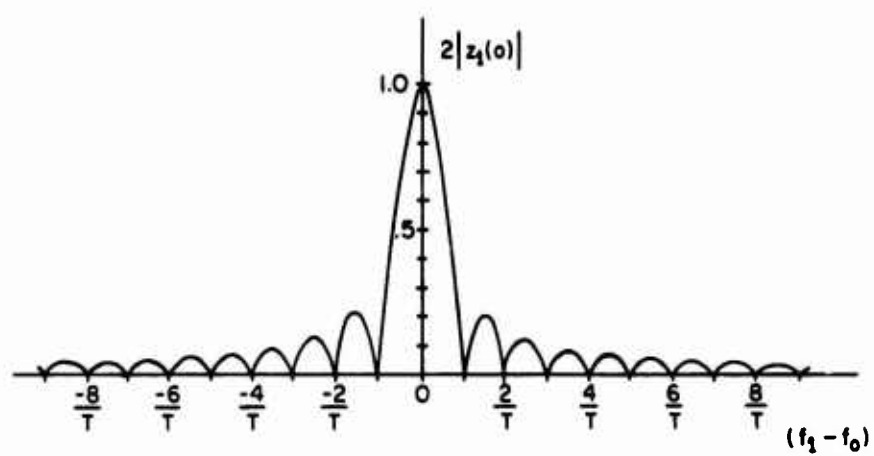


Figure 3.2 Frequency Selectivity of Quadrature Correlation Function

The correlation function given by Equation (3.1) assumes an input signal, $\cos \omega_1 t$, of infinite duration. For a sinusoid signal of finite duration T , an additional linear weighting factor is present giving

$$z_1(\tau) = \frac{1}{2} e^{j\omega_0 \tau} \frac{\sin \pi T(f_1 - f_0)}{\pi T(f_1 - f_0)} \left(1 - \frac{|\tau|}{T}\right).$$

Note that the correlation peak at $\tau = 0$ is the same as that given by Equation (3.2) for the infinite duration case, justifying the use of infinite duration sinusoids for finding the frequency response for small τ such that $\tau \ll T$.

3.2 Uniform Sampling Effects

Next, consider the quadrature correlation of sinusoidal signals with uniform sampling. Figure 3.5 shows a quadrature correlation function model with uniform sampling intervals of $2T_s$ seconds and with input and reference sinusoidal signals of $\cos \omega_1 t$ and $\cos \omega_0 t$, respectively. The complex quadrature correlation function $z_1(\tau)$ for infinite duration input sinusoids is:

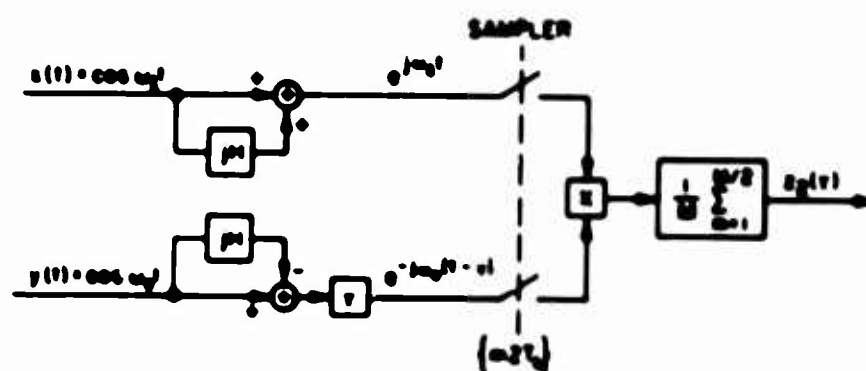


Figure 5.3 Quadrature Correlation Function Model for Sampled Sinusoidal Signals

$$\begin{aligned}
 z_2(\tau) &= \frac{1}{M} \sum_{m=1}^{M/2} e^{j\omega_1 2mT_s} e^{-j\omega_0 2mT_s} e^{j\omega_0 \tau} \\
 &= \frac{e^{j\omega_0 \tau}}{M} \sum_{m=1}^{M/2} e^{j2mT_s(\omega_1 - \omega_0)} \\
 &= \frac{e^{j\omega_0 \tau}}{M} \frac{\sin \pi MT_s(f_1 - f_0)}{\sin \pi 2T_s(f_1 - f_0)} e^{jT_s \left(\frac{M}{2} + 1\right) 2\pi(f_1 - f_0)} \quad (3.3)
 \end{aligned}$$

where $\frac{M}{2}$ is the number of sample pairs taken during the finite averaging time of T seconds. The correlation function for $\tau = 0$,

$$\left| z_2(0) \right| = \frac{1}{2} \left| \frac{\sin \pi T(f_1 - f_0)}{\frac{1}{2} M \sin \pi 2T_s(f_1 - f_0)} \right|, \quad (3.4)$$

shown in Figure 3.4 approximates the $\frac{\sin x}{x}$ envelope characteristic of Figure 3.2 but with a repetition interval of $\hat{f}_s = \frac{1}{2T_s}$, as expected from sampling theory [36]. The sidelobe peaks midway between the mainlobes are equal to about $1/M$, where M is the total number of samples. This correlation function also has a very selective frequency characteristic as long as the input frequency f_1 does not differ from the reference frequency f_0 by greater than \hat{f}_s Hertz.

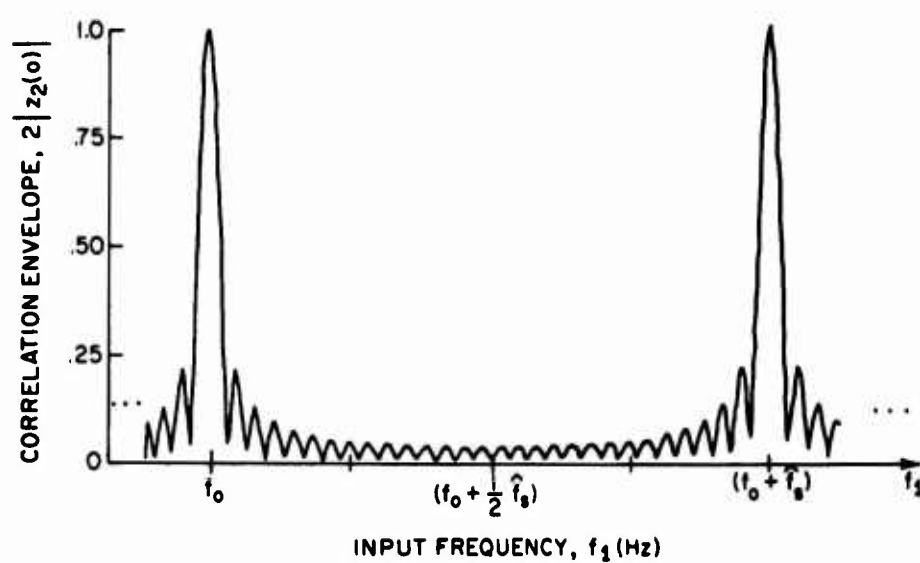


Figure 3.4 Frequency Selectivity of Quadrature Correlation Function with Uniform Sampling

3.3 Generation of Odd Harmonics by Clipping

Next, consider the effect of hard-limiting on the correlation of two sinusoidal functions as shown in Figure 3.5. The clipped sinusoidal signals $x(t)$ and $y(t)$ are square waves of unit amplitude which can be represented by a Fourier series of odd harmonics of the fundamental input frequencies f_0 and f_1 ,

$$x(t) = \text{sgn}(\cos \omega_1 t) = \frac{4}{\pi} \sum_{n=0}^{\infty} \frac{(-1)^n}{(2n+1)} \cos (2n+1) \omega_1 t.$$

and

$$y(t) = \text{sgn}(\cos \omega_0 t) = \frac{4}{\pi} \sum_{k=0}^{\infty} \frac{(-1)^k}{(2k+1)} \cos (2k+1) \omega_0 t.$$

If the boxes labeled " H_f " of Figure 3.5 are assumed to shift the input square wave by 90 degrees of the fundamental frequencies ω_1 and ω_0 , then the pre-envelopes $p_x(t)$ and $p_y^*(t-\tau)$ become:

$$p_x(t) = x(t) + j\hat{x}(t) = \frac{4}{\pi} \sum_{n=0}^{\infty} \frac{(-1)^n}{(2n+1)} e^{j(-1)^n(2n+1) \omega_1 t} \quad (3.5)$$

and

$$\begin{aligned} p_y^*(t-\tau) &= y(t-\tau) - jy(t-\tau) \\ &= \frac{4}{\pi} \sum_{k=0}^{\infty} \frac{(-1)^k}{(2k+1)} e^{-j(-1)^k(2k+1) \omega_0 (t-\tau)}, \end{aligned} \quad (3.6)$$

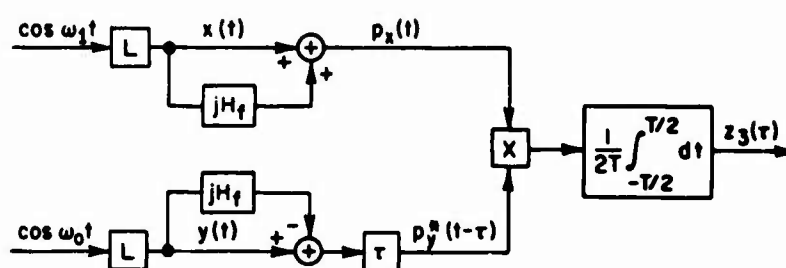


Figure 3.5 Quadrature Correlation Function Model for Clipped Sinusoidal Signals

and the complex correlation function is:

$$\begin{aligned}
 z_3(\tau) &= \frac{1}{2T} \int_{-T/2}^{T/2} p_x(t) p_y^*(t-\tau) dt \\
 &= \frac{8}{\pi^2} \sum_{n=0}^{\infty} \sum_{k=0}^{\infty} (-1)^{n+k} \frac{e^{j(-1)^k(2k+1)\omega_0\tau}}{(2n+1)(2k+1)} \\
 &\quad \cdot \left[\frac{1}{T} \int_{-T/2}^{T/2} e^{j\Omega_{kn}t} dt \right], \tag{3.7}
 \end{aligned}$$

where

$\Omega_{kn} = [(-1)^n(2n+1)\omega_1 - (-1)^k(2k+1)\omega_0]$ represents differences between the odd harmonics of ω_1 and ω_0 for given values of n and k . Table 3.1, which shows some typical values that Ω_{kn} can assume, contains all the values of Ω_{kn} with amplitude weighting factors, $\frac{1}{(2n+1)(2k+1)}$, greater than 0.1.

Note from the definition of Ω_{kn} that the odd harmonic frequencies alternate sign; i.e., ω_1 is positive, $3\omega_1$ is negative, $5\omega_1$ is positive, etc. This is the result of the fact that the H_f boxes in Figure 3.5 time shift $x(t)$ and $y(t)$ by a time equivalent to 90 degrees of their fundamental frequencies ω_0 and ω_1 . However, this same time shift is equivalent to 270 degrees (or -90 degrees) for the third harmonic component of the square wave, to 450 degrees or +90 degrees for the fifth harmonic component, etc. Thus, positive Hilbert transforms are obtained for the fundamental, fifth harmonic, ninth harmonic, etc., while negative Hilbert transforms

TABLE 3.1
 ODD HARMONIC DIFFERENCE FREQUENCIES WITH
 WEIGHTING FACTORS OVER 10 PERCENT

n	k	Input Harmonic (ω_1)	Ref. Harmonic (ω_0)	Ω_{kn}	Amplitude Weighting Factor $\frac{1}{(2n+1)(2k+1)}$
0	0	FUND.	FUND.	$\omega_1 - \omega_0$	1.000
0	1	FUND.	THIRD	$\omega_1 - 3\omega_0$	$1/5 = 0.200$
0	2	FUND.	FIFTH	$\omega_1 - 5\omega_0$	$1/9 = 0.111$
0	3	FUND.	SEVENTH	$\omega_1 - 7\omega_0$	$1/25 = 0.040$
0	4	FUND.	NINTH	$\omega_1 - 9\omega_0$	$1/49 = 0.020$
1	0	THIRD	FUND.	$-3\omega_1 - \omega_0$	$1/5 = 0.200$
1	1	FIFTH	FUND.	$-5\omega_1 - \omega_0$	$1/25 = 0.040$
1	2	SEVENTH	FUND.	$-7\omega_1 - \omega_0$	$1/49 = 0.020$
1	3	NINTH	FUND.	$-9\omega_1 - \omega_0$	$1/81 = 0.012$
1	1	THIRD	THIRD	$-3\omega_1 - 3\omega_0$	$\frac{1}{(3)(3)} = 0.111$

are obtained for the third harmonic, seventh harmonic, etc. This phenomenon appears as alternating positive and negative odd harmonic frequencies in the spectrums shown in Figure 3.6 of the pre-envelopes $p_x(t)$ and $p_y^*(t)$ obtained by taking the Fourier transforms of Equations (3.5) and (3.6) and given by:

$$P_x(\omega) = \mathcal{F}[p_x(t)] = \frac{b}{\pi} \sum_{n=0}^{\infty} \frac{(-1)^n}{(2n+1)} \delta(\omega - (-1)^n (2n+1) \omega_1)$$

and

$$P_y^*(\omega) = \mathcal{F}[p_y^*(t)] = \frac{b}{\pi} \sum_{k=0}^{\infty} \frac{(-1)^k}{(2k+1)} \delta(\omega - (-1)^k (2k+1) \omega_0).$$

Performing the integration indicated in Equation (3.7) gives

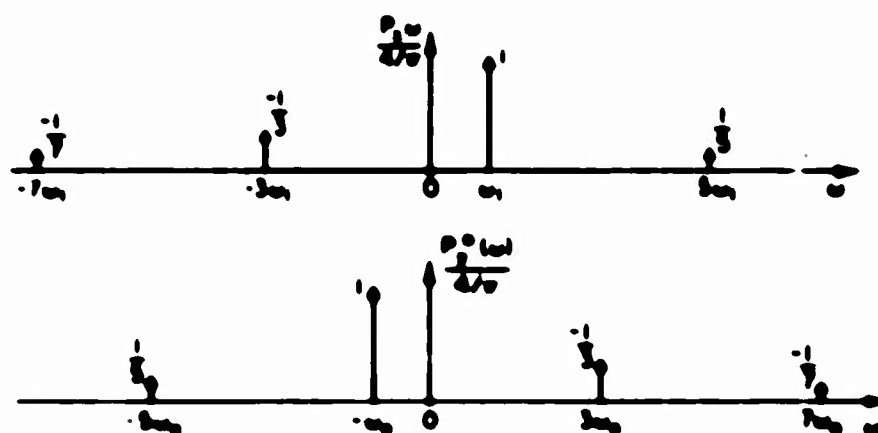


Figure 3.6 Spectra of the Pre-Envelopes $p_x(t)$ and $p_y(t)$

$$\begin{aligned}
 z_3(\tau) &= \frac{8}{\pi^2} \sum_{n=0}^{\infty} \sum_{k=0}^{\infty} (-1)^{n+k} \frac{e^{j(-1)^k(2k+1)\omega_0\tau}}{(2n+1)(2k+1)} \cdot \frac{\sin \Omega_{kn} \frac{T}{2}}{\Omega_{kn} \frac{T}{2}} \\
 &= \frac{8}{\pi^2} \left[\frac{\sin(\omega_1 - \omega_0) \frac{T}{2}}{(\omega_1 - \omega_0) \frac{T}{2}} e^{j\omega_0\tau} \right. \\
 &\quad - \frac{1}{3} \frac{\sin(3\omega_1 + \omega_0) \frac{T}{2}}{(3\omega_1 + \omega_0) \frac{T}{2}} e^{j\omega_0\tau} \\
 &\quad - \frac{1}{3} \frac{\sin(\omega_1 + 3\omega_0) \frac{T}{2}}{(\omega_1 + 3\omega_0) \frac{T}{2}} e^{-j3\omega_0\tau} \\
 &\quad + \frac{1}{5} \frac{\sin(5\omega_1 - \omega_0) \frac{T}{2}}{(5\omega_1 - \omega_0) \frac{T}{2}} e^{j\omega_0\tau} \\
 &\quad + \frac{1}{5} \frac{\sin(\omega_1 - 5\omega_0) \frac{T}{2}}{(\omega_1 - 5\omega_0) \frac{T}{2}} e^{j5\omega_0\tau} \\
 &\quad \left. + \dots \right].
 \end{aligned}$$

	<u>input harmonic</u>	<u>reference harmonic</u>
where	FUND.	FUND.
	THIRD	FUND.
	FUND.	THIRD
	FIFTH	FUND.
	FUND	FIFTH

(3.8)

where the individual contributions of all combinations of input and reference harmonics can be seen. For the special case of $\omega_1 = \omega_0$ and $\tau = 0$, all the terms in Equation (3.8) are negligible except when $k = n$, giving:

$$z_2(0) = \frac{8}{\pi^2} \sum_{n=0}^{\infty} \frac{1}{(2n+1)^2} = 1 \text{ for } \omega_0 = \omega_1.$$

Likewise, for $\omega_0 = -3\omega_1$ and $\tau = 0$, all terms are negligible except when $n = (3k+1)$, giving:

$$z_2(0) = \frac{8}{\pi^2} \sum_{n=0}^{\infty} \frac{1}{3} \frac{-1}{(2n+1)^2} = \frac{-1}{3} \text{ for } \omega_0 = -3\omega_1.$$

If we consider just the peaks of $z_2(0)$ for frequencies at which $\Omega_{kn} = 0$, we can express the contribution due to the principal pairs of input and reference odd harmonics by:

$$\begin{aligned} z_2(0)_{\text{peak}} \approx & \sum_{n=0}^{\infty} \frac{(-1)^n}{(2n+1)} \delta[\omega_1 - (-1)^n (2n+1) \omega_0] \\ & + \sum_{k=1}^{\infty} \frac{(-1)^k}{(2k+1)} \delta[\omega_0 - (-1)^k (2k+1) \omega_1] \end{aligned} \quad (3.9)$$

as shown in Figure 3.7. Equation (3.9) neglects differences between higher order odd harmonics of ω_0 and ω_1 , the most significant of which (for $n = 3, k = 5$) has an amplitude of only $\frac{1}{(3)(5)} = \frac{1}{15}$. As shown in Equation (3.9), the principal terms are of two types: (1) differences between the input fundamental ω_1 and the odd harmonics of ω_0 (the terms indexed by n), and (2) differences between the reference fundamental ω_0 and odd harmonics of ω_1 (the

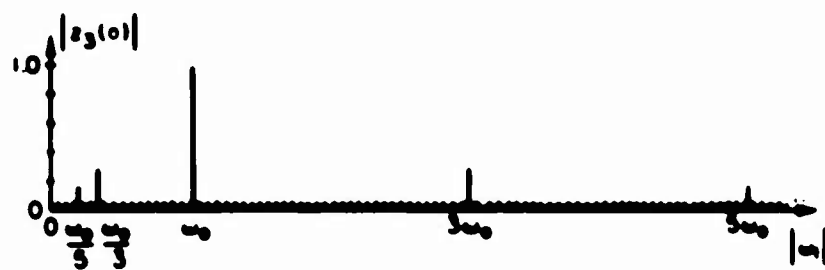


Figure 3.7 Frequency Selectivity of Correlation Function for Clipped Sinusoidal Signals

terms indexed by n). In all cases, the correlation amplitude of the odd harmonic terms is equal to the inverse of the order of the harmonic; i.e., to $1/3$ for third harmonics, $1/5$ for fifth harmonics, etc.

The next section will consider the effect of uniform sampling on the model shown in Figure 3.5. It will be shown that for the sampled case, the odd harmonic terms shown in Figure 3.7 at $\omega_1 = (-1)^n (2n+1) \omega_0$ will be repeated at multiples of the sampling frequency $2\hat{f}_s$, and the sub-harmonic terms at $\omega_1 = (-1)^n \frac{\omega_0}{(2n+1)}$ will be repeated at multiples of $\frac{2\hat{f}_s}{(2n+1)}$.

3.4 Effect of Uniform Sampling of Clipped Sinusoids

To examine the effect of uniform sampling of clipped sinusoids, consider the quadrature correlation function model shown in Figure 3.6. The expressions for $p_x(t)$ and $p_y^*(t-\tau)$ are given by Equations (3.9) and (3.6). The sampler output signals are

$$p_x(2mT_s) = \frac{b}{\pi} \sum_{n=0}^{\infty} \frac{(-1)^n}{(2n+1)} \cdot j(-1)^n (2n+1) \omega_1(2mT_s) \quad (3.10)$$

and

$$p_y^*(2mT_s - \tau) = \frac{b}{\pi} \sum_{k=0}^{\infty} \frac{(-1)^k}{(2k+1)} \cdot -j(-1)^k (2k+1) \omega_0(2mT_s - \tau) \quad (3.11)$$

where $2T_s = 1/\hat{f}_s$ is the quadrature pairs sampling interval. The complex correlation function is

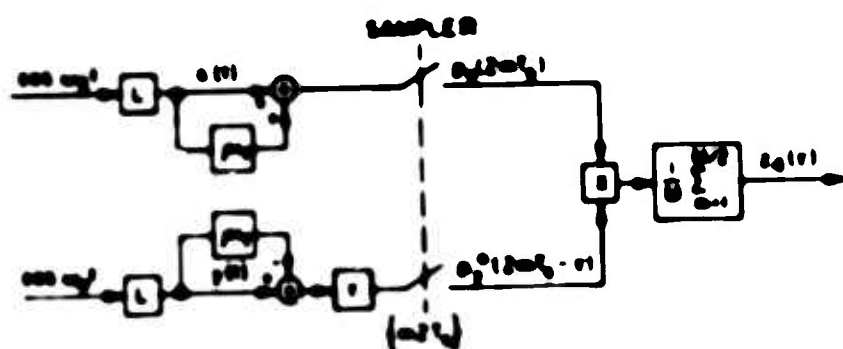


Figure 3.6 Quadrature Correlation Function Model for Clipped Sinusoidal Signals with Uniform Sampling

$$\begin{aligned}
z_h(\tau) &= \frac{1}{M} \sum_{m=1}^{M/2} p_x(2mT_s) p_y^*(2mT_s - \tau) \\
&= \frac{16}{\pi^2} \sum_{n=0}^{\infty} \sum_{k=0}^{\infty} (-1)^{n+k} \frac{e^{j(-1)^k(2k+1)\omega_0\tau}}{(2n+1)(2k+1)} \\
&\quad \cdot \left[\frac{1}{M} \sum_{m=1}^{M/2} e^{j2mT_s\Omega_{kn}} \right], \tag{3.12}
\end{aligned}$$

where

$$\Omega_{kn} = [(-1)^n(2n+1)\omega_1 - (-1)^k(2k+1)\omega_0] \text{ as before.}$$

Putting the bracketed series of Equations (3.12) in closed form gives

$$\begin{aligned}
z_h(\tau) &= \frac{16}{\pi^2} \sum_{n=0}^{\infty} \sum_{k=0}^{\infty} (-1)^{n+k} \frac{e^{jT_s(\frac{M}{2}+1)\Omega_{kn}}}{(2n+1)(2k+1)} \\
&\quad \cdot \left[\frac{\sin \frac{1}{2} MT_s \Omega_{kn}}{\frac{1}{2} M \sin T_s \Omega_{kn}} \right] e^{j(-1)^k(2k+1)\omega_0\tau} \tag{3.13}
\end{aligned}$$

where $MT_s = T$.

Writing Equation (3.13) in terms of individual odd harmonics contributions gives:

$$\begin{aligned}
 z_4(\tau) = & \frac{8}{\pi^2} \left[\frac{\sin(\omega_1 - \omega_0) T/2}{M/2 \sin(\omega_1 - \omega_0) T_s} e^{jT_s(\frac{M}{2} + 1)(\omega_1 - \omega_0)} e^{j\omega_0 \tau} \right. \\
 & - \frac{1}{3} \frac{\sin(3\omega_1 + \omega_0) T/2}{M/2 \sin(3\omega_1 + \omega_0) T_s} e^{-jT_s(\frac{M}{2} + 1)(3\omega_1 + \omega_0)} e^{j\omega_0 \tau} \\
 & - \frac{1}{3} \frac{\sin(\omega_1 + 3\omega_0) T/2}{M/2 \sin(\omega_1 + 3\omega_0) T_s} e^{jT_s(\frac{M}{2} + 1)(\omega_1 + 3\omega_0)} e^{-j3\omega_0 \tau} \\
 & + \frac{1}{5} \frac{\sin(5\omega_1 - \omega_0) T/2}{M/2 \sin(5\omega_1 - \omega_0) T_s} e^{jT_s(\frac{M}{2} + 1)(5\omega_1 - \omega_0)} e^{j\omega_0 \tau} \\
 & + \frac{1}{5} \frac{\sin(\omega_1 - 5\omega_0) T/2}{M/2 \sin(\omega_1 - 5\omega_0) T_s} e^{jT_s(\frac{M}{2} + 1)(\omega_1 - 5\omega_0)} e^{j5\omega_0 \tau} \\
 & \left. + \dots \right]. \quad (3.14)
 \end{aligned}$$

This equation shows that $z_4(\tau)$ contains repetitive terms due to sampling similar to those shown in Figure 3.4 about each odd harmonic difference frequency satisfying the relation $\Omega_{kn} = 0$.

Neglecting terms with amplitudes of the order of $1/15$ and smaller, an equation analogous to Equation (3.9) can be written approximating principal peaks of $z_4(0)$ as

$$\begin{aligned}
 [z_k(0)]_{\text{peak}} \approx & \sum_{m=-\infty}^{\infty} \left\{ \sum_{k=0}^{\infty} \frac{(-1)^k}{(2k+1)} \cdot [\omega_1 - (-1)^k(2k+1)\omega_0 + m\hat{f}_s] \right. \\
 & \left. + \sum_{n=1}^{\infty} \frac{(-1)^n}{(2n+1)} \cdot [\omega_0 - (-1)^n(2n+1)\omega_1 + m\hat{f}_s] \right\}.
 \end{aligned}
 \tag{3.15}$$

If the reference frequency $\omega_0 = 2\pi f_0$ in Equation (3.15) is held fixed while the input frequency $\omega_1 = 2\pi f_1$ is varied, the complex pattern of odd harmonic correlation terms typified by those shown in Figure 3.9 for the fundamental, third and fifth harmonics will result. This figure illustrates that, because of uniform sampling, many odd harmonic correlation peaks are produced for input frequencies f_1 which differ from f_0 by only a fraction of the sampling rate \hat{f}_s . This could be a highly undesirable situation if a correlation function with good frequency selectivity is necessary.

The exact location of the input frequencies f_1 that give rise to spurious odd harmonic correlation peaks as a function of f_0 and \hat{f}_s is shown in Figure 3.10. This figure shows that in any of the fixed f_1 frequency intervals $[N\hat{f}_s, (N+1)\hat{f}_s]$ of length \hat{f}_s , where N is an arbitrary integer, there are one fundamental, 4 third harmonic, 6 fifth harmonic, etc., frequencies giving spurious correlations. For fixed values of f_0 and \hat{f}_s , the location of each of these response frequencies can be located from Figure 3.10 once the

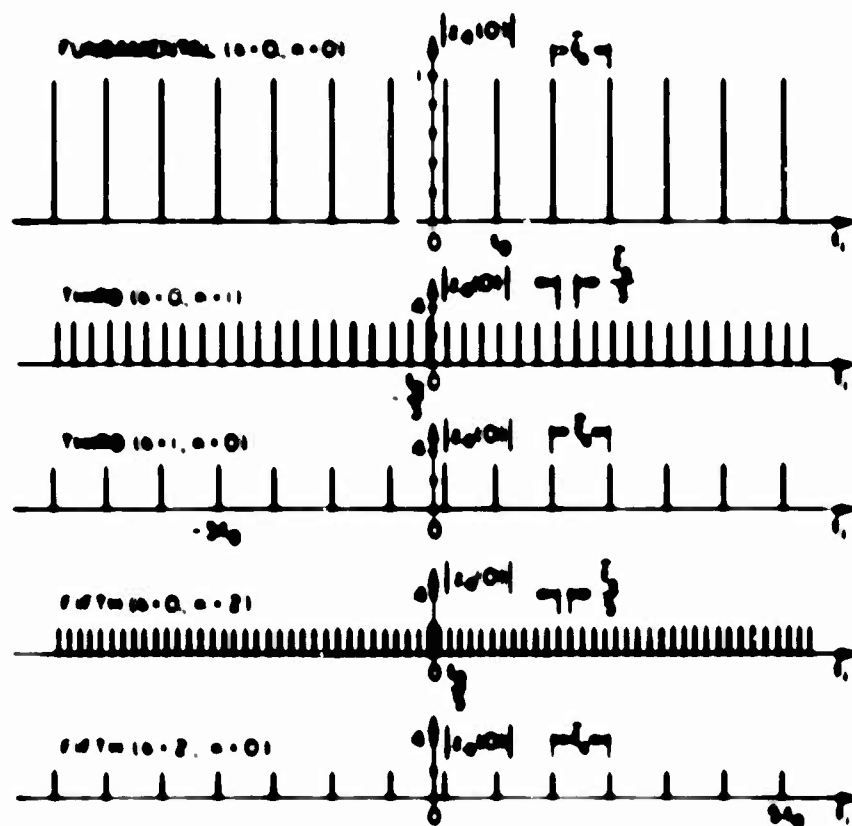


Figure 3.9 Fundamental, 3rd, and 5th Harmonic Correlation Response Frequencies for Clipped Sinusoids with Uniform Sampling

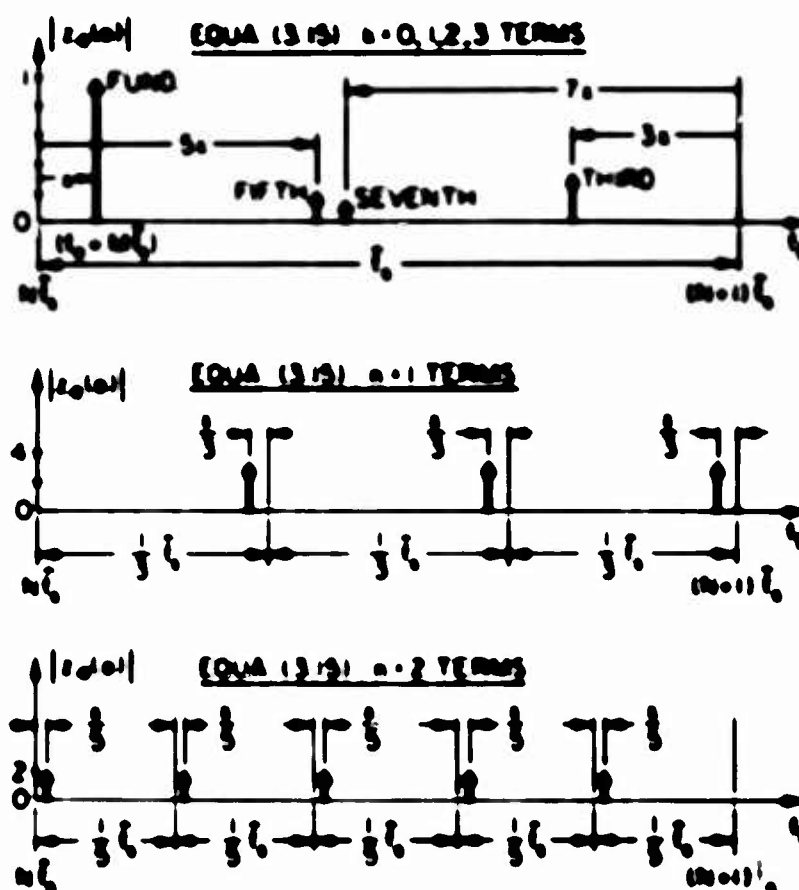


Figure 3.10 Location of Odd Harmonic Response Frequencies in Any T_0 Interval

position of the fundamental response at $(f_0 + N\hat{\Delta}f_0)$ for some integer N is established and its distance x from the left-hand edge of the interval $\hat{\Delta}f_0$ is determined. The significance of the alternating positive and negative odd harmonic frequencies shown in Figure 5.6 is apparent in Figure 5.10 in that, if the fundamental response frequency were moved to the right by an amount Δx , the third, seventh, eleventh, etc., harmonic frequencies would move to the left, while the fifth, ninth, etc., harmonic frequencies would move to the right by the amount indicated in Figure 5.10.

5.9 Correlation Function Variance for Narrowband Random Process

Input Functions

The correlation function variance, σ_y^2 , defined as the variance of the real part of $z_y(\tau)$ of Figure 3.8 when the input $x(t) = m(t)$ is a clipped narrowband random process and $y(t)$ is a clipped sinusoidal function is given by Equation (2.94) as

$$\sigma_y^2 = \frac{1}{\pi^2} \sum_{n=1}^{M/2} \sum_{m=1}^{M/2} \left\{ \left(\frac{1}{n} - \frac{1}{m} \right)^2 \left(\frac{1}{n} - \frac{1}{m} \right)^2 + \left(\frac{1}{n} + \frac{1}{m} \right)^2 \left(\frac{1}{n} + \frac{1}{m} \right)^2 \right\} \quad (5.16)$$

For the case of $m(t)$ with a rectangular spectrum of bandwidth B centered around f_c ,

$$\phi_{\text{in}}(t) - \phi_{\text{out}}(t) = \frac{2}{\pi} \sin^{-1} \left(\frac{\sin \pi W t}{\pi W t} \cos \omega_c t \right),$$

$$\phi_{\text{in}}(t) - \phi_{\text{out}}(t) = \frac{2}{\pi} \sin^{-1} (\cos \omega_c t),$$

$$\phi_{\text{in}}(t) - \phi_{\text{out}}(t) = \frac{2}{\pi} \sin^{-1} \left(\frac{\sin \pi W t}{\pi W t} \sin \omega_c t \right)$$

and

$$\phi_{\text{in}}(t) - \phi_{\text{out}}(t) = \frac{2}{\pi} \sin^{-1} (\sin \omega_c t).$$

Equation (2.16) thus becomes:

$$\begin{aligned} \epsilon^2 = \frac{1}{\pi} \left\{ 1 + \frac{W/2}{\pi} \right. & \left. 1 + \frac{W/2}{\pi} \right. \\ & \cdot \left[\sin^{-1} \frac{\sin \pi W t}{\pi W t} \cos \omega_c 2\pi t, \sin^{-1} (\cos \omega_c 2\pi t) \right. \\ & \left. \left. + \sin^{-1} \frac{\sin \pi W t}{\pi W t} \sin \omega_c 2\pi t, \sin^{-1} (\sin \omega_c 2\pi t) \right] \right\}. \end{aligned} \quad (2.17)$$

The plot of ϵ^2 vs. sampling rate of Figure 2.11 for $\omega_c = \omega_s$ shows the presence of the same second harmonic ripples seen in Figure 2.10 for the large W signal case. The amplitude of the ripples for the sinusoidal signal case is greater than that for the large W case because the small sinusoidal signal bandwidth increases the second harmonic error effects. Also, because of the narrower

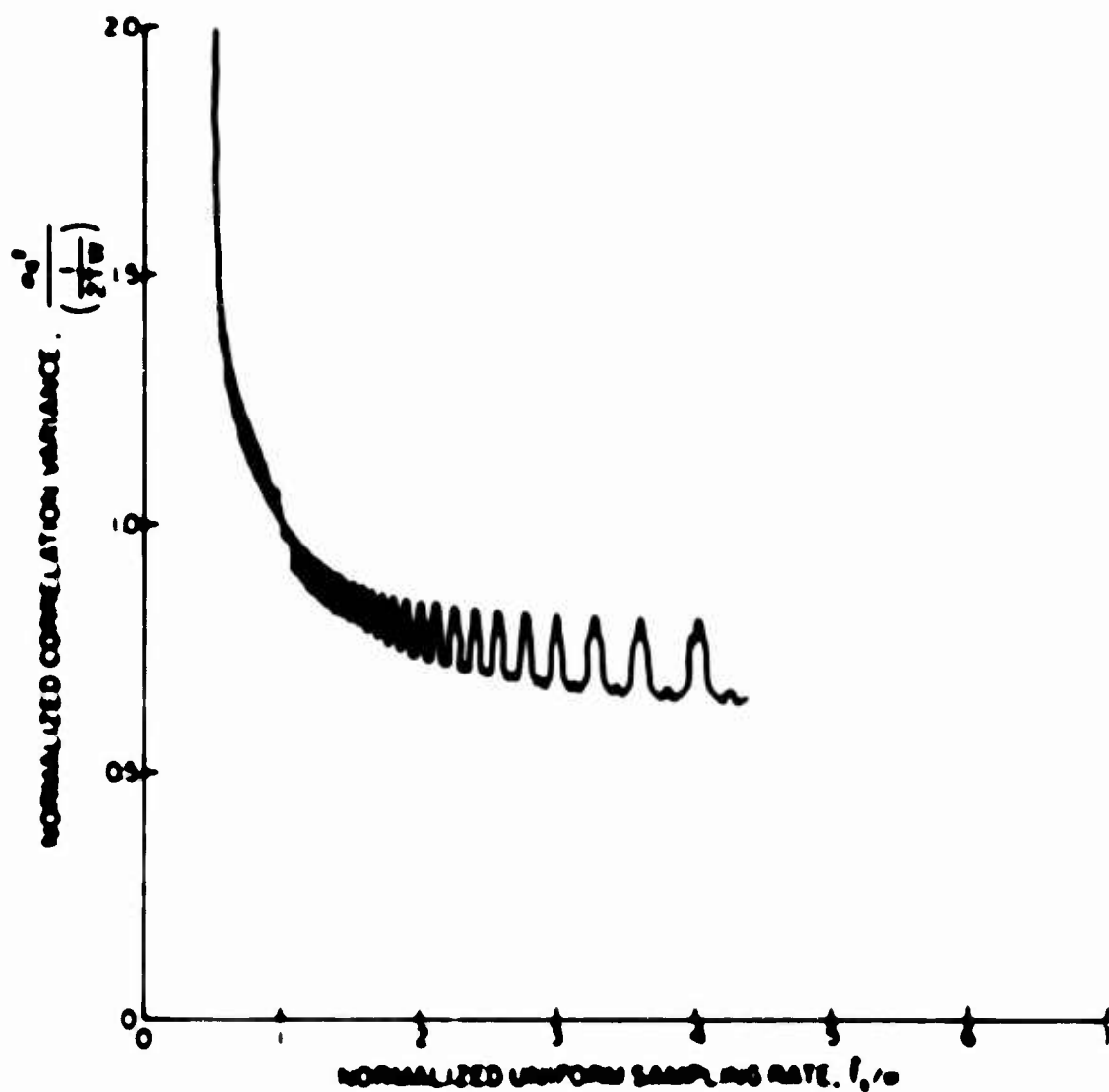


Figure 3.11 Clipped Sinusoidal Signal Quadrature Correlation Function
Noise Variance Vs. Sampling Rate

bandwidth, the variance of Figure 3.11 approaches the first sampling rate asymptotic value of $1/4TW$ more slowly than the corresponding large TW case of Figure 2.9.

3.6 Use of Nonuniform Sampling to Eliminate Odd Harmonic Responses

In the next two chapters, we will consider the use of nonuniform time sampling to reduce the effect of spurious odd harmonic correlations caused by the clipping and sampling of sinusoids. The general sampling technique considered is that of "Block Sampling"; i.e., the use of short sequences (or blocks) of nonuniform time samples which are repeated at periodic intervals. The nonuniform sampling destroys the synchronism between the sampling periodicity and the signal periodicity which cause the odd harmonic responses for the uniform sampling case. Some general theoretical properties of block sampling will be developed in Chapter IV, and the use of block sampling to reduce spurious odd harmonic effects in quadrature correlation functions of clipped sinusoidal signals will be discussed in Chapter V.

CHAPTER IV

SPECTRAL ANALYSIS OF NONUNIFORM BLOCK SAMPLING

4.1 Introduction

The use of repetitive nonuniform sampling (block sampling) has been considered for various applications in the literature. Tou [36] uses Z-transforms to analyze sampled-data control systems with "cyclic variable-rate" sampling. Yen [41] and Kohlenberg [24] derive sampling theorems for the reconstruction of signals which have been sampled by various nonuniform sampling schemes, one of which is "recurrent nonuniform sampling." In this chapter, we will examine some of the basic properties of block sampling, concentrating on the sampling frequency spectrum properties. The importance of studying the sampling function spectrum is evident from the fact that the spectrum of a sampled signal is equal to the convolution of the spectrum of the unsampled signal with the sampling function spectrum. In Chapter V, the sampling spectrum results from this chapter will be applied to the problem of reducing odd harmonic correlation peaks for a correlation function between two sinusoidal signals.

Before deriving the block sampling time and frequency equations, the analogous uniform sampling equations will be obtained for comparison. Consider the infinite train of uniformly spaced ideal sample pulses shown in Figure 4.1 and given by the sampling function

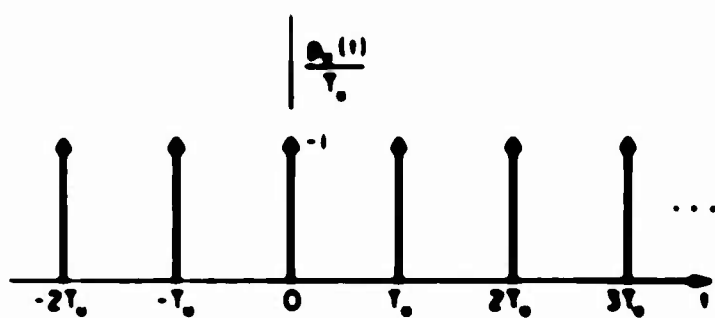


Figure 4.1 Uniform Sample Train

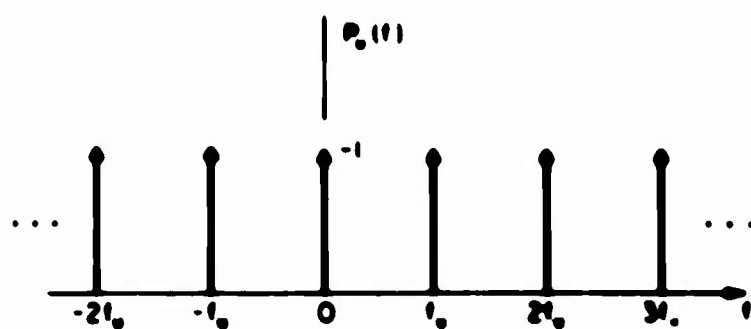


Figure 4.2 Uniform Sampling Spectrum

$$p_u(t) = \sum_{n=-\infty}^{\infty} \delta(t - nT_u) \quad (4.1)$$

where T_u is the uniform sample spacing in seconds. Since $p_u(t)$ is periodic, it can be equivalently represented by the Fourier series

$$p_u(t) = \sum_{k=-\infty}^{\infty} c_k e^{j2\pi k t / T_u} \quad (4.2)$$

Taking the Fourier transform of Equation (4.2) the uniform sampling function amplitude spectrum is found to be

$$P_u(f) = \sum_{k=-\infty}^{\infty} c_k \delta(f - k f_u) \quad (4.3)$$

where $f_u = \frac{1}{T_u}$ is the uniform sampling rate in samples per second. The plot of $P_u(f)$ in Figure 4.2 shows that the ideal uniform sampling function has a discrete line spectrum consisting of an infinite train of constant amplitude delta functions at multiples of the sampling rate f_u .

4.2 Definition of Block Sampling

Consider the periodic sampling function $p(t)$ shown in Figure 4.3 of period T_p consisting of an infinite sampling train containing N samples with arbitrary sampling times t_1, t_2, \dots, t_N in each "block" interval of T_p seconds. As shown in Figure 4.4,

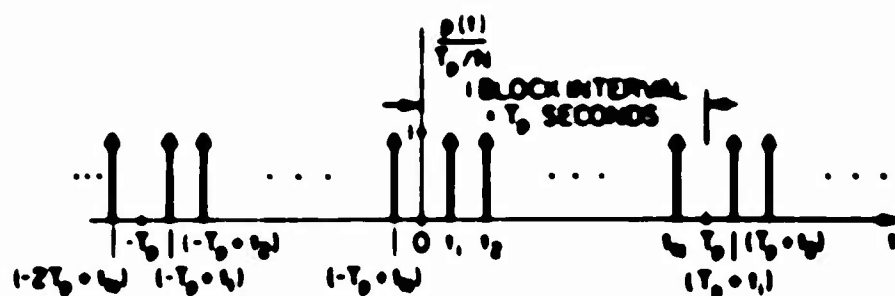


Figure 4.1 Arbitrary Uniform Sampling Function with Period T_p

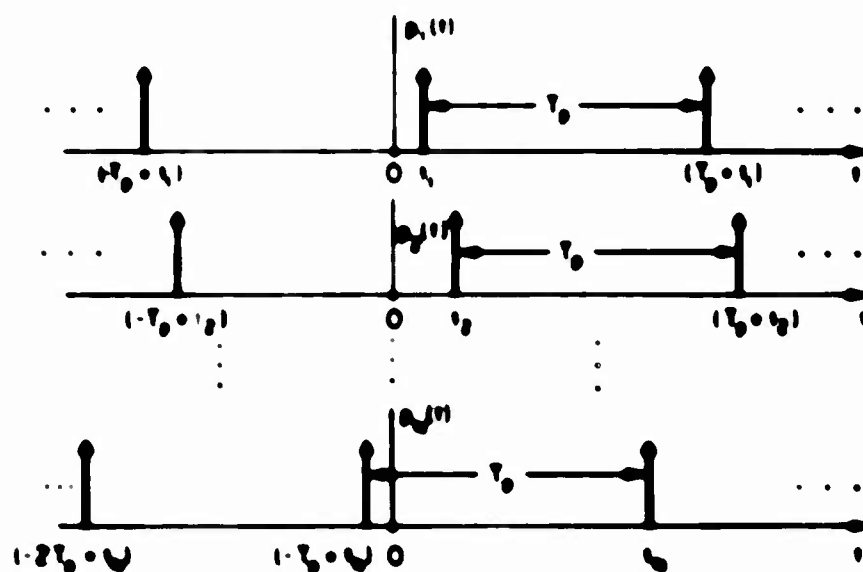


Figure 4.2 Decomposition of Arbitrary Uniform Sampling Function into Sum of Uniform Sampling Functions

$p(t)$ can be decomposed into the sum of N uniform sampling functions each of period T_p

$$p(t) = \sum_{n=1}^N p_n(t) \\ = \sum_{n=1}^N \sum_{k=-\infty}^{\infty} \frac{1}{N} \delta(t - k T_p - t_n), \quad (4.4)$$

where T_p/N is the average sampling interval taken over the blocks of length T_p . Since $p(t)$ is a periodic function of period T_p , it can be represented by its Fourier series expansion by

$$p(t) = \sum_{n=1}^N \sum_{k=-\infty}^{\infty} \frac{1}{N} \delta(t - k T_p - t_n) \\ = \sum_{k=-\infty}^{\infty} \sum_{n=1}^N \frac{1}{N} \delta(t - k T_p - t_n) \quad (4.5)$$

where the complex nonuniform sampling coefficient, a_k , given by

$$a_k = \sum_{n=1}^N \frac{1}{N} e^{-j 2 \pi k T_p^{-1} t_n} \quad (4.6)$$

for all integers k plays an important role in the study of nonuniform sampling as will be shown in this chapter and in Chapter 5.

The nonuniform sampling spectrum $P(f)$ which can be obtained by taking the Fourier transform of $p(t)$ from Equation (4.5) is:

$$P(f) = \sum_{k=-\infty}^{\infty} a_k \delta(f - k f_p), \quad (4.7)$$

where $f_p = \frac{1}{T_p}$ is the block sampling rate in samples per second. Equation (4.7) shows that the nonuniform sampling spectrum is a discrete spectrum with components of amplitude a_k at multiples, $k f_p$, of the block sampling rate f_p , as shown in the example of Figure 4.9.

A comparison of the uniform sampling spectrum of Figure 4.2 and the nonuniform sampling spectrum of Figure 4.9 shows that basically the nonuniform sampling spectrum contains 3 times as many spectral components, each of which has a complex amplitude which is variable from component to component and is always equal to or less than 1 in absolute value. To illustrate this, consider uniform sampling with a constant sampling interval equal to the average nonuniform sampling interval in Equation (4.4); i.e., let

$$T_s = T_p$$

The sampling times $\left\{ t_n \right\}_{n=1}^N$ reduce to

$$t_n = n T_p$$

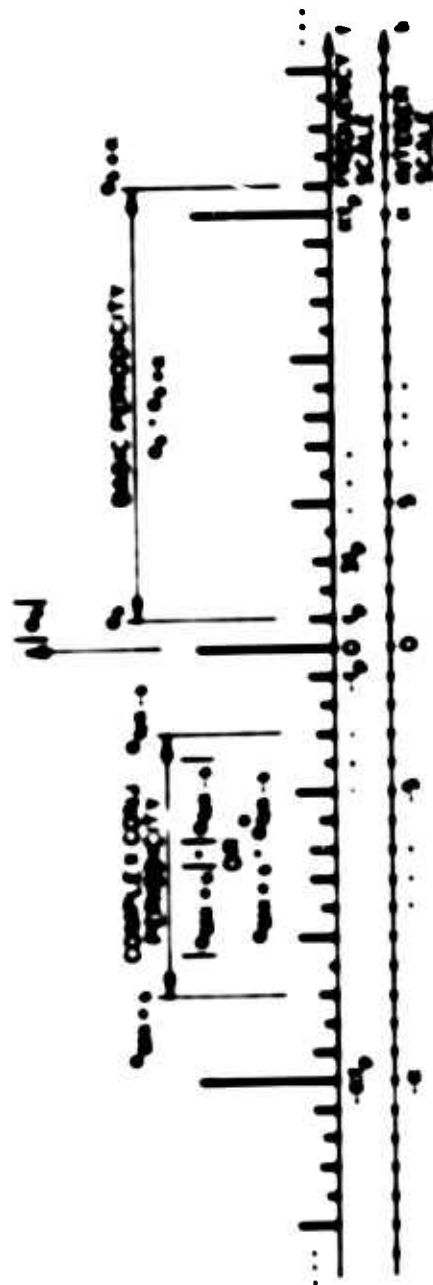


Figure 1.1. Typical Nonuniform Band Sampling Spectrum
Illustrating Periodicity

and the nonuniform sampling coefficient a_k reduces to:

$$a_k = \frac{1}{N} \sum_{n=1}^N e^{-j2\pi k t_n} = \begin{cases} 1 & \text{for } k = \text{any multiple of } N, \\ 0 & \text{for all other } k. \end{cases} \quad (4.6)$$

The nonuniform time and frequency equations (4.5 and 4.7) thus reduce to the uniform sampling equations (4.2 and 4.3). Equation (4.6) shows that the nonuniform sampling spectrum (Figure 4.5) has N times as many spectral lines as the uniform sampling spectrum (Figure 4.2).

Equation (4.7) shows that the detailed structure of the nonuniform sampling spectrum $P(f)$ is completely described by the complex coefficients a_k , which will be the topic of study for the remainder of this chapter. Two interpretations of a_k as given by Equation (4.6) are useful: (1) as a finite exponential series, and (2) as the average of N unit vectors in the complex plane. These interpretations will be helpful in the analysis problem of determining the sampling spectrum properties for a given set of nonuniform sampling times $\{t_n\}_{n=1}^N$, and in the discussion of the synthesis problem of finding a set of nonuniform sampling times which optimize the sampling spectrum in some specified way.

4.5 Sampling Spectrum Periodicity Properties

In this section, we wish to consider the conditions for periodicity of the nonuniform sampling spectrum given by Equations (4.6) and (4.7).

$$P(f) = \sum_{k=-\infty}^{\infty} a_k \delta(f - k f_p) \quad (4.7)$$

and

$$a_k = \frac{1}{N} \sum_{n=1}^N e^{-j2\pi k n \frac{T}{p}} \quad (4.6)$$

where $T_p = 1/f_p$ is the block sampling period. Finding the conditions for the periodicity of a_k is equivalent to finding the smallest integer K , such that:

$$a_k = a_{k+K} \quad (4.9)$$

for all k . From Equation (4.6), a_{k+K} is given by

$$a_{k+K} = \frac{1}{N} \sum_{n=1}^N e^{-j2\pi (k+K) n \frac{T}{p}} = \frac{1}{N} \sum_{n=1}^N e^{-j2\pi k n \frac{T}{p}} e^{-j2\pi K n \frac{T}{p}} = \frac{1}{N} \sum_{n=1}^N e^{-j2\pi k n \frac{T}{p}} e^{-j2\pi K n \frac{T}{p}} \quad (4.10)$$

From this equation, the necessary and sufficient condition for the periodicity of a_k amounts to finding the smallest integer K , such that:

$$e^{-j2\pi K n \frac{T}{p}} = 1, \text{ for all } n = 1, 2, \dots, N. \quad (4.11)$$

or, equivalently, finding the smallest K such that

$$\frac{t_n}{T_p} = \frac{M_n}{K}, \text{ for all } n = 1, 2, \dots, N, \quad (4.12)$$

where M_n is an integer which is dependent upon t_n . The sufficiency is obvious from Equation (4.10). The necessity exists because Equation (4.10) must be equal to a_k for all values of k .

In addition to the basic periodicity $a_k = a_{k+K}$, a complex conjugate symmetry about $k = 0$ follows directly from the definition of a_k given in Equation (4.6); i.e.,

$$a_k = \frac{1}{N} \sum_{n=1}^N \frac{t_n}{T_p} e^{-j2\pi k \frac{t_n}{T_p}} \\ = \frac{1}{N} \sum_{n=1}^N \frac{t_n}{T_p} e^{j2\pi (-k) \frac{t_n}{T_p}} \\ = a_{-k}^* \quad \text{for all } k. \quad (4.13)$$

Using Equations (4.9) and (4.13), the complex conjugate symmetry can be generalized to

$$a_{MK+L} = a_{-MK-L}^* \quad \text{for all } L, \quad (4.14)$$

where M and K are arbitrary integers.

A corollary to Equation (4.14) is:

$$|a_{N-k}| = |a_{k}|, \text{ for all } k.$$

which follows directly from complex conjugate properties. The symmetry properties of Equations (4.14) and (4.9) are illustrated in Figure 4.5.

An examination of the periodicity condition of Equation (4.12) will illustrate the relationships between the nonuniform sampling times $\{t_n\}_{n=1}^N$ and the sampling spectrum coefficients, a_k .

Equation (4.12) shows that all ratios $\frac{t_n}{T_p}$ ($n = 1, 2, \dots, N$) must be rational numbers if a_k is to be a periodic function. This property can be summarized by the following theorem:

THEOREM: The function $a_k = \frac{1}{N} \sum_{n=1}^N e^{-j2\pi k \frac{t_n}{T_p}}$ is periodic if,

and only if, $\frac{t_n}{T_p}$ is a rational number for all

$n = 1, 2, \dots, N$.

PROOF: To show sufficiency, let $\frac{t_n}{T_p}$ be rational numbers for all n and represent these rational numbers as the ratio of two integers, i.e., let $\frac{t_1}{T_p} = \frac{a_1}{b_1}$, $\frac{t_2}{T_p} = \frac{a_2}{b_2}$, \dots ,

$\frac{t_N}{T_p} = \frac{a_N}{b_N}$ where a_i and b_i are integers for

$i = 1, 2, \dots, N$. We need only exhibit one value of K' [not necessarily the minimum K defined by Equation (4.10)] which will satisfy Equation (4.12) for all n to prove

periodicity. One such K' is $K' = b_1 \cdot b_2 \dots b_N$

$= \prod_{i=1}^N b_i$. To show necessity, consider Equation (4.11).

If $\frac{t_n}{T_p}$ is an irrational number for any n , then

$e^{-j2\pi K' \frac{t_n}{T_p}}$ could not be unity for that n and periodicity of a_k would not be possible.

In practice, where sampling times cannot be determined with infinite accuracy, approximate periodicity rather than precise periodicity must be considered. This topic, which could be an area of further study, is not considered in this thesis.

Assume that a set of sampling times, $\{t_n\}_1^N$, is specified and that we wish to determine its spectral period K . Let K' be the smallest common demoninator simultaneously satisfying the N equations:

$$\begin{aligned} \frac{t_1}{T_p} &= \frac{M_1}{K'} \\ \frac{t_2}{T_p} &= \frac{M_2}{K'} \\ &\vdots \\ \frac{t_N}{T_p} &= \frac{M_N}{K'} \end{aligned} \tag{4.15}$$

for some set of integers M_i , $i = 1, 2, \dots, N$. Then, the spectral period K is equal to K' . This is equivalent to saying that K is the smallest number of equally spaced time instants into which each block sampling interval T_p can be divided such that each of the N nonuniform sample points $\{t_n\}_1^N$ occurs at one of these K uniformly spaced time instants. This is illustrated in Figure 4.6.

If, instead of the sample times $\{t_n\}$ being specified, a desired periodicity K is given, the acceptable sets of sampling times giving this periodicity can be found by dividing the block sampling interval T_p into K equally spaced time instants T_p/K seconds apart as shown in Figure 4.6. From this set of K possible sampling times, any selected set of N sampling times would yield a sampling spectrum of period equal to K/m , where m is some positive integer. We are interested here only in those sets of sampling times for which $m = 1$. These will be the sets satisfying Equation (4.15); i.e., those sets for which K is equal to the smallest common denominator K' of the N equations given by Equation (4.15). Of course, the actual values of the spectral coefficients a_k depend on the specific set of N sampling times chosen. Since the number of possible unique sets of N sample times from K possible sampling times (the number of combinations of K things taken N at a time is $\left[\frac{K!}{N!(K-N)!} \right]$) becomes very large for large K and N with $K \gg N$, additional criteria beyond periodicity may be necessary to be able to select an optimum set of N sampling instants.

(K POSSIBLE SAMPLING TIMES PER BLOCK)
 (N SAMPLES PER BLOCK)

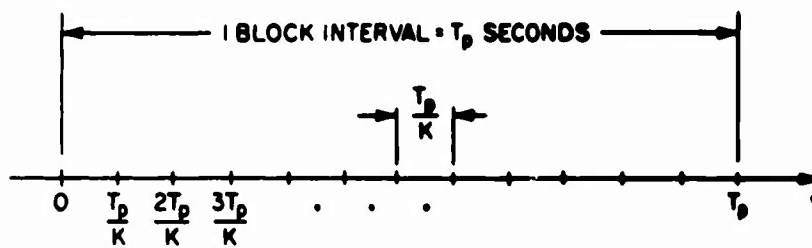


Figure 4.6 Division of Block Interval T_p into K Possible Sampling Instants

An important example of such a criterion is that of spectral shaping; i.e., of controlling the amplitude of x_p in certain frequency regions. The remainder of this chapter will be devoted to spectral shaping considerations of this type.

4.4 Spectrum Conservation Properties

A comparison of the uniform sampling spectrum of Figure 4.2 with the nonuniform sampling spectrum of Figure 4.3 shows, in general, that the power in a uniform sampling spectrum is equally distributed over a few widely spaced frequencies, while the power in a nonuniform sampling spectrum is distributed unequally over a greater number of closely spaced frequencies. In this section, we will analyze this distribution of spectral power and will show that the average power in any sampling spectrum depends only upon the average sampling rate and not upon the precise sampling scheme. This is equivalent to saying that all sampling schemes with the same average sampling rate merely redistribute a fixed amount of power in the frequency domain. In addition, a similar property will be shown for the complex amplitude spectrum.

Consider any nonuniform block sampling function similar to that of Figure 4.3 with N samples per block interval T_p and with a periodicity K . The spectrum of each such sampling function is completely described by a knowledge of the complex spectral coefficients

$$a_k = \frac{1}{N} \sum_{n=1}^N e^{-j2\pi k \frac{t_n}{T_p}}$$

at the frequencies $f = \frac{n}{p}$. The power associated with each a_n is given by:

$$|a_n|^2 = \frac{1}{K} \sum_{n=1}^K \sum_{m=1}^K \cos \frac{2\pi n}{p} (t_n - t_m).$$

Summing $|a_n|^2$ over one period, K , gives

$$\sum_{n=1}^K |a_n|^2 = \frac{1}{K} \sum_{n=1}^K \sum_{m=1}^K \left[\sum_{k=1}^K \cos \frac{2\pi k}{p} (t_n - t_m) \right]. \quad (4.16)$$

The summation in brackets in Equation (4.16) can be shown to be zero by making use of the periodicity condition of Equation (4.12). From this periodicity condition, it is seen that

$$t_n - t_m = K \cdot \frac{p}{K}.$$

for all n and m , where K is an integer ($K \neq 0$) which is dependent upon the values of n and m . The summation in brackets in Equation (4.16) can thus be written

$$\sum_{k=1}^K \cos \frac{2\pi k}{p} (t_n - t_m) = \sum_{k=1}^K \cos \frac{2\pi K}{K} k$$

$$\begin{cases} K & \text{if } \frac{(t_n - t_m)}{p} = 0 \text{ or } 1 \\ 0 & \text{otherwise.} \end{cases}$$

The case $\frac{t_n - t_m}{T} = 1$ does not arise because the sum over n and m in Equation 4.16 does not include the $n = m$ terms and the case $\frac{t_n - t_m}{T} = 0$ likewise cannot exist since, if $t_1 = t_2 = \dots = t_N = T$, we would not get N samples per block. Equation 4.16 thus reduces to:

$$\frac{1}{N} \sum_{k=1}^N |a_k|^2 = \frac{1}{N} \quad (4.17)$$

Equation 4.17 shows that the average sampling spectrum power (over one periodicity interval and, thus, also over any integral multiple of the basic period) is a function only of the number of samples per block N , and is independent of the exact sampling instants t_n , and of the periodicity interval T . This is equivalent to saying that all nonuniform block sampling schemes with N samples per block have the same average spectral power, and only the distribution of that fixed power as a function of frequency depends upon the exact set of sampling instants $\{t_n\}_{n=1}^N$. This property provides the basis for spectral "shaping" of the sampling spectrum by the choice of sample times $\{t_n\}$ as will be discussed in the remaining sections of this chapter.

Although Equation 4.17 shows that the average value of $|a_k|^2$ is a constant independent of the specific sampling instants $\{t_n\}$, the variance of $|a_k|^2$, which is one measure of the uniformity of $|a_k|^2$ as a function of frequency, is strongly dependent upon the

exact sampling times. In Section 4.6, it will be shown that the variance of $|a_k|^2$ can be kept low by careful selection of the sample times t_n , and that the minimum variance of $|a_k|^2$ is given by $\frac{1}{N} (1 - \frac{1}{N})$.

A spectrum conservation property similar to that of Equation (4.16) for $|a_k|^2$ can also be proven for the complex amplitude spectrum a_k . The average value of a_k over one periodicity interval K is given by:

$$\frac{1}{K} \sum_{k=1}^K a_k = \frac{1}{K} \sum_{k=1}^K \left(\frac{1}{N} \sum_{n=1}^N e^{-j2\pi \frac{k}{N} t_n} \right). \quad (4.18)$$

Again, using the periodicity relation of Equation (4.12) and interchanging the order of summation, Equation (4.18) becomes:

$$\frac{1}{K} \sum_{k=1}^K a_k = \frac{1}{N} \sum_{n=1}^N \left[\frac{e^{-j2\pi \frac{k}{N} t_n}}{1 - e^{-j2\pi \frac{k}{N} t_n}} \right]. \quad (4.19)$$

The term in brackets in Equation (4.19) is equal to zero if $\frac{k}{N} \neq 1$ and unity if $\frac{k}{N} = 1$. But, since $\frac{k}{N} \leq 1$, the condition

$\frac{N}{T_p} = 1$ can only occur when the last N^{th} sample in each block occurs at the end point $t_N = T_p$. Thus, Equation (4.17) reduces to

$$\frac{1}{T_p} = \begin{cases} \frac{1}{T_p} & \text{if } \frac{t_N}{T_p} = 1 \\ 0 & \text{if } \frac{t_N}{T_p} \neq 1 \end{cases}$$

The property of Equation (4.20) is dependent upon the arbitrary selection of the time origin of the block sampling interval as will be illustrated by the examples in Section 4.5.

4.5 Block Sampling Spectrum Examples

In this section, some specific examples are given to illustrate the effects of various nonuniform sampling parameters on the sampling spectrum. Consider first a basic uniform sampling function as shown in Figure 4.7(a) as a special case of nonuniform sampling. A total of $N = 10$ samples are assumed in each block sampling interval of arbitrary length T_p . For this uniform sampling example, Equations (4.7) and (4.8) show that uniform unity amplitude spectral spikes a_k exist for k multiples of 10, i.e., at frequencies which are multiples of $\frac{1}{T_p}$ as illustrated in the spectral plot of Figure 4.7(a).

Next, consider breaking the block interval T_p up into 2 possible sampling times with a uniform spacing of $0.5 T_p$ seconds from which $N = 10$ nonuniform sampling instants will be chosen for the four examples shown in Figure 4.7(b) - 4.7(d). In the previous

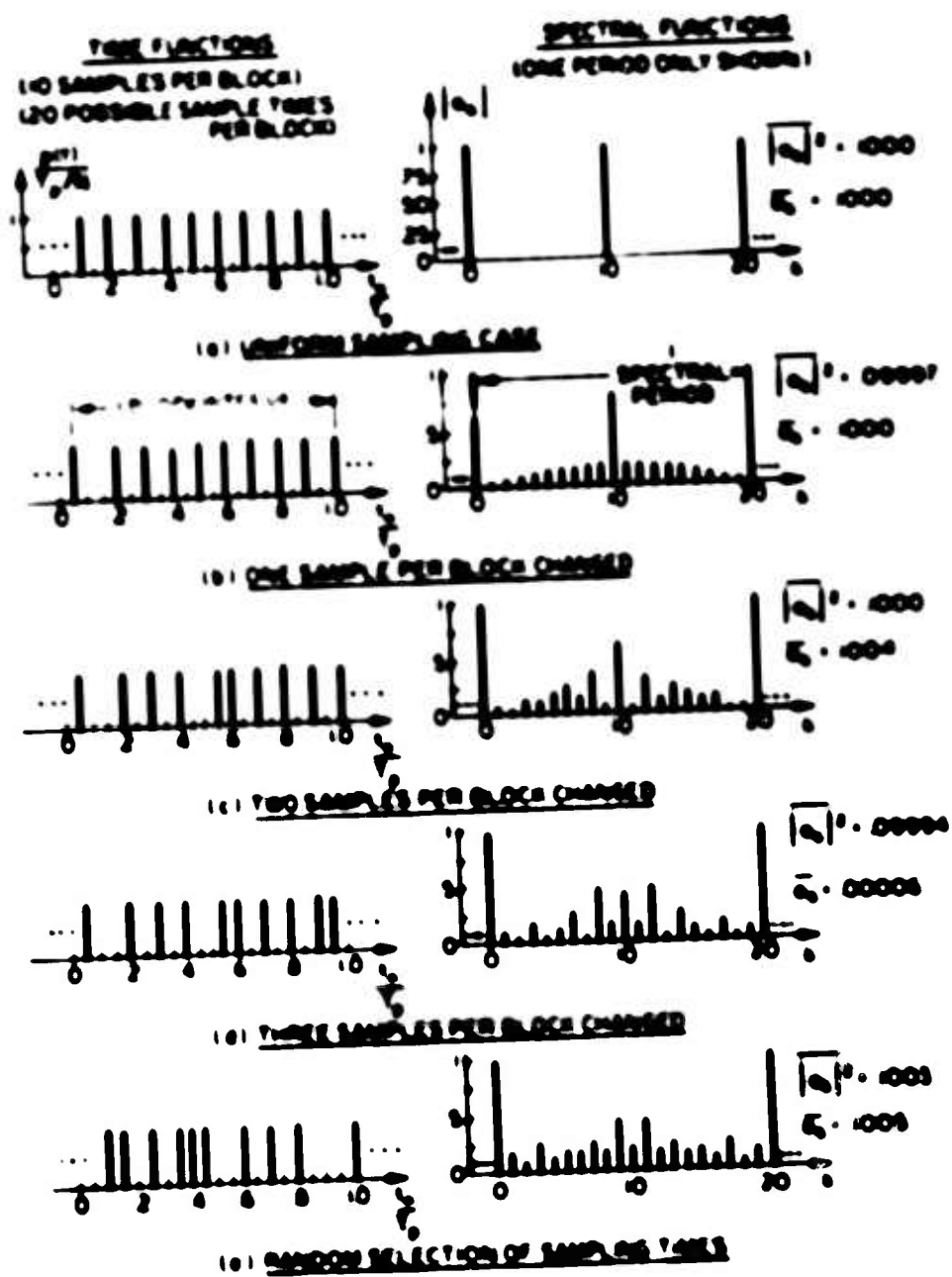


Figure 4.1 Block Sampling Examples

section, it was shown that regardless of which 10 of the 20 possible sampling instants are selected, x_q will have a periodicity of $K = 20$, although a shorter period is possible in some cases. For example, in the uniform sampling case of Figure 4.7(a). Thus, in general, the nonuniform sampling spectrum examples of Figure 4.7(b) - 4.7(e) will have 10 times as many non-zero spectral components as the uniform sampling spectrum of Figure 4.7(a). In order to examine the spectral changes in stages as uniform sampling is gradually reduced to a random nonuniform pattern, Examples (b) - (d) of Figure 4.7 consist of changing, respectively, one, two, and three samples per block from uniform sampling.

In Example (b), only the location of the first sample in each repetitive block interval is changed. As shown in the frequency plot of Figure 4.7(b), small spectral components appear at all values of k . As expected, the spectral component at $k = 10$ is still relatively large since the sampling time function differs only slightly from uniform sampling.

Examples (c) and (d), with two and three sample points displaced from uniform sampling, exhibit frequency spectra in which the large uniform component at $k = 10$ rapidly disappears into the background.

Example (e) consists of a random selection of 10 sampling points from the 20 possible sampling instants. The spectral plot for this example is typical of that generally produced by nonuniform random sampling in that, although the sampling power is distributed fairly uniformly in frequency, a rather wide amplitude spread between

the largest and smallest spectral components is noticeable. As will be seen later, the presence of excessively large spectral components may be undesirable in some applications and a more uniform distribution of power versus frequency required.

The complex conjugate symmetry about the midpoint $k = 10$ given by Equation (4.14) is evident in all the examples of Figure 4.7. The

$$\text{computed values of } \overline{|a_k|^2} = \frac{1}{K} \sum_{k=1}^K |a_k|^2 \quad \text{and} \quad \overline{a_k} = \frac{1}{K} \sum_{k=1}^K a_k,$$

as shown on Figure 4.7 for each example, can be compared with the theoretical values from Equation (4.17) and (4.20) of $\overline{|a_k|^2} = \frac{1}{N} = 0.1$ for all examples and $\overline{a_k} = 0$ for Example (d) and $\overline{a_k} = \frac{1}{N} = 0.1$ for the remaining examples since $\frac{t_N}{T_p} = 1$ for these examples. All computed values are seen to be within $\pm 0.5\%$ of the theoretical values--well within computational accuracy.

Another important special case of nonuniform sampling (see Figure 4.8) is that of moving every second sample of a uniform sampling function by a constant amount. For example, this could describe the quadrature sampling process in Chapter II and III of taking quadrature pairs of samples at a uniform rate. This example can be assumed to be the sum of two uniform sampling functions with a fixed time origin offset. Accordingly, the frequency spectrum for this sampling function is equal to the vector sum of the contributions from each uniform sampling function. For the example of Figure 4.8, the uniform spacing between corresponding samples is $0.2 T_p$ which, in

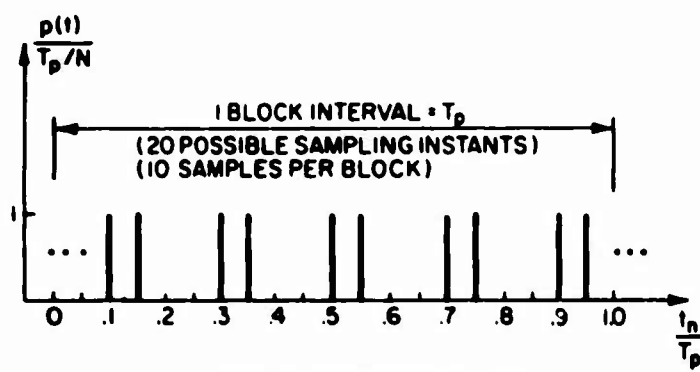
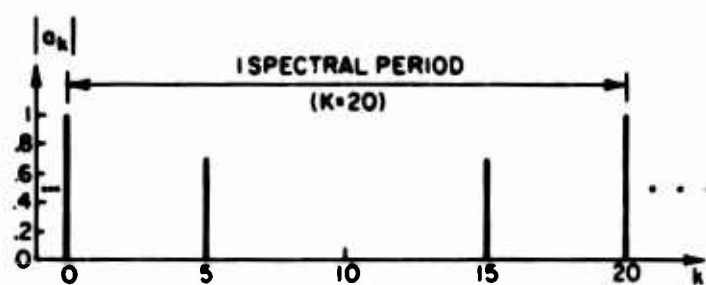
(a) SAMPLING TIME FUNCTION(b) SAMPLING SPECTRUM

Figure 4.8 Uniform Pairs Sampling Example

general, results in a non-zero component for $k = \text{multiples of } 5$. The zero spectral component at $k = 10$ occurs because the vector contributions of the two uniform sampling function cancel each other. The periodicity of $K = 20$ follows from Equation (4.15) since there are 20 possible sampling instants per block and $N = 10$. Performing the following sums over one spectral period:

$$\overline{|a_k|^2} = \frac{1}{K} \sum_{k=1}^{20} |a_k|^2 = 0.1$$

and

$$\overline{a_k} = \frac{1}{K} \sum_{k=1}^{20} a_k = 0$$

likewise is consistent with Equations (4.17) and (4.20).

The concept of the complex frequency spectrum a_k , as a vector sum of complex spectral contributions from two uniform sampling functions in the example of Figure 4.8 can be extended in the general case of Figures 4.3 and 4.4 to the sum of contributions from N uniform sampling functions. This is equivalent to considering a_k as a resultant vector equal to the average of N unit vectors with varying phases. The maximum value of $a_k = 1$ occurs when all N vectors have the same (zero) phase. If the N vector contributions are uniformly distributed in phase over 2π radians, the resultant a_k is zero [e.g., see spectrum of Figure 4.7(a) for $1 \leq k \leq 9$].

4.6 Minimizing the Spectrum Variance by Choice of Sample Times

In Section 4.4, it was noted that although the average power $|a_k|^2$ of the sampling spectrum components is a constant which depends only upon the number N of samples per block, the variance of $|a_k|^2$ is strongly a function of the specific sampling times $\{t_n\}$. In this section, it will be shown that the variance of $|a_k|^2$ can be minimized by proper choice of $\{t_n\}$ and the conditions on $\{t_n\}$ for minimum variance will be derived.

The power associated with each a_k is given by:

$$\begin{aligned}
 |a_k|^2 &= \frac{1}{N^2} \sum_{n=1}^N \sum_{m=1}^N e^{-j2\pi k \frac{(t_n - t_m)}{T_p}} \\
 &= \frac{1}{N} + \frac{1}{N^2} \sum_{\substack{n=1 \\ n \neq m}}^N \sum_{m=1}^N \cos \frac{2\pi k}{T_p} (t_n - t_m) \quad (4.21)
 \end{aligned}$$

Since the mean value of $|a_k|^2$ was found to be equal to $\frac{1}{N}$ in Equation (4.17), the variance σ_K^2 of $|a_k|^2$ over one period of k can be defined as:

$$\sigma_K^2 = \frac{1}{K} \sum_{k=1}^K \left(|a_k|^2 - \frac{1}{N} \right)^2 \quad (4.22)$$

Substituting the expression for $\left(|a_k|^2 - \frac{1}{N} \right)$ from Equation (4.21) into Equation (4.22) gives σ_K^2 as:

$$\sigma_K^2 = \frac{1}{K} \sum_{k=1}^K \frac{1}{N^4} \sum_{\substack{n=1 \\ n \neq m}}^N \sum_{m=1}^N \sum_{\substack{i=1 \\ i \neq j}}^N \sum_{j=1}^N \cos \frac{2\pi k}{T_p} (t_n - t_m) \cos \frac{2\pi k}{T_p} (t_i - t_j). \quad (4.23)$$

If the terms for which $(t_n - t_m) = (t_i - t_j)$ are isolated and the summation over k is interchanged with the other four summations, Equation (4.23) becomes:

$$\begin{aligned} \sigma_K^2 = & \frac{2}{N^4} \sum_{\substack{n=1 \\ n \neq m}}^N \sum_{m=1}^N \left[\frac{1}{K} \sum_{k=1}^K \cos^2 \frac{2\pi k}{T_p} (t_n - t_m) \right] \\ & + \frac{2}{N^4} \sum_{\substack{n=1 \\ n \neq m \\ (i,j) \neq (n,m) \\ (i,j) \neq (m,n)}}^N \sum_{\substack{m=1 \\ m \neq n}}^N \sum_{\substack{i=1 \\ i \neq j}}^N \sum_{j=1}^N \\ & \cdot \left[\frac{1}{K} \sum_{k=1}^K \cos \frac{2\pi k}{T_p} (t_n - t_m) \cos \frac{2\pi k}{T_p} (t_i - t_j) \right]. \quad (4.24) \end{aligned}$$

The conditions for minimizing σ_K^2 by choice of $\{t_n\}$ can be found by examining the two bracketed sums of Equation (4.24). Let

$$S_1 = \frac{1}{K} \sum_{k=1}^K \cos^2 \frac{2\pi k}{T_p} (t_n - t_m)$$

and

$$S_2 = \frac{1}{K} \sum_{k=1}^K \cos \frac{2\pi k}{T_p} (t_n - t_m) \cos \frac{2\pi k}{T_p} (t_i - t_j).$$

Using trigonometric identities, S_1 and S_2 can be written as:

$$S_1 = \frac{1}{2} + \frac{1}{2K} \sum_{k=1}^K \cos \frac{4\pi k}{T_p} (t_n - t_m) \quad (4.25)$$

and

$$\begin{aligned} S_2 = & \frac{1}{2K} \sum_{k=1}^K \cos \frac{2\pi k}{T_p} (t_n - t_m + t_i - t_j) \\ & + \frac{1}{2K} \sum_{k=1}^K \cos \frac{2\pi k}{T_p} (t_n - t_m - t_i + t_j). \end{aligned} \quad (4.26)$$

An examination of Equations (4.25) and (4.26) shows that because of the periodicity of Equation (4.12), the three summations over k are always either zero or positive depending upon the choices of t_n , t_m , t_i , and t_j . Therefore, minimizing σ_K^2 is equivalent to minimizing S_1 and S_2 separately over all sampling instants.

First, consider S_1 as given by Equation (4.25). Using the periodicity condition of Equation (4.12) in an analogous manner to that done in Section 4.4, it can be shown that

$$\frac{1}{K} \sum_{k=1}^K \cos \frac{4\pi k}{T_p} (t_n - t_m) = \begin{cases} 1 & \text{whenever } (t_n - t_m) = \pm \frac{T_p}{2} \\ 0 & \text{otherwise.} \end{cases} \quad (4.27)$$

Equation (4.27) shows that to minimize σ_K^2 , the sampling times should be selected to minimize the number of occurrences of the condition

$$(t_n - t_m) = \frac{T_p}{2}, \quad (4.28)$$

where t_n and t_m are any two sampling times with $t_n > t_m$.

Next, consider the sum S_2 given by Equation (4.26). Again, using the periodicity relationship of Equation (4.12), the two S_2 equations analogous to Equation (4.27) are

$$\frac{1}{K} \sum_{k=1}^K \cos \frac{2\pi k}{T_p} (t_n - t_m + t_i - t_j) = \begin{cases} 1 & \text{whenever } (t_n - t_m + t_i - t_j) = -T_p, \\ & 0, \text{ or } T_p, \\ 0 & \text{otherwise,} \end{cases} \quad (4.29)$$

and

$$\frac{1}{K} \sum_{k=1}^K \cos \frac{2\pi k}{T_p} (t_n - t_m + t_i - t_j) = \begin{cases} 1 & \text{whenever } (t_n - t_m - t_i - t_j) = -T_p, \\ & 0, \text{ or } T_p, \\ 0 & \text{otherwise.} \end{cases} \quad (4.30)$$

To minimize σ_K^2 , the sampling times should be selected to minimize the number of occurrences of the conditions given by Equations (4.29) and (4.30). These two conditions on t_n , t_m , t_i , and t_j can be

combined into an alternate equivalent criterion that covers all cases and is easier to compute in general. Consider any four sampling instants t_1, t_2, t_3, t_4 , at most, two of which can be equal, order them such that

$$t_1 \leq t_2 \leq t_3 \leq t_4 \quad (4.31)$$

and form the six linear combinations

$$L_1 = (t_4 - t_3) \pm (t_2 - t_1),$$

$$L_2 = (t_4 - t_2) \pm (t_3 - t_1)$$

and

$$L_3 = (t_4 - t_1) \pm (t_3 - t_2). \quad (4.32)$$

Then, from Equation (4.26), S_2 is increased by $1/2$ whenever L_1, L_2 , or L_3 equals T_p or zero.

For the case above where two of the four sampling instants in Equation (4.31) are equal, Equations (4.31) and (4.32) reduce to:

$$t_1 < t_2 < t_3 \quad (4.33)$$

and

$$L_1 = (t_3 - t_2) \pm (t_2 - t_1),$$

$$L_2 = (t_3 - t_2) \pm (t_3 - t_1)$$

and

$$L_3 = (t_3 - t_1) \pm (t_2 - t_1). \quad (4.34)$$

To summarize, in order to minimize σ_K^2 , it is necessary to minimize the number of occurrences of the following three conditions:

$$(1) \quad (t_n - t_m) = \frac{T_p}{2}, \text{ for } t_n > t_m, \quad (4.35)$$

$$(2) \quad L_1, L_2, \text{ or } L_3 = T_p \quad (4.36)$$

and

$$(3) \quad L_1, L_2, \text{ or } L_3 = 0, \quad (4.37)$$

where L_1, L_2, L_3 are given by Equations (4.32) or (4.34).

Consider a given sampling function $\{t_i\}_{i=1}^N$ consisting of N distinct sampling instants. In order to determine the total number of occurrences of the conditions of Equations (4.35) - (4.37) for all combinations of sampling instants, the following procedure can be used:

- (1) Form all possible pairs of two distinct sample points t_n and t_m such that $t_n > t_m$ and, for each pair, compute the difference $(t_n - t_m)$. Count the total number of occurrences M_2 of the condition of Equation (4.35); i.e., the number of times that $(t_n - t_m) = T_p/2$.
- (2) Form all possible sets of three distinct sample points t_1, t_2 , and t_3 and order each set according to Equation (4.33). For each set, compute the six numbers represented by L_1, L_2 , and L_3 of Equation (4.34). Count the total number of occurrences M_3 of either Equation (4.36) or Equation (4.37); i.e., the number of times that L_1, L_2 , or L_3 equals 0 or T_p .

- (3) Form all possible sets of four distinct sample points t_1, t_2, t_3, t_4 and order each set according to Equation (4.31). For each set, compute the six numbers represented by L_1, L_2 , and L_3 of Equation (4.32). Count the total number of occurrences M_4 of either Equation (4.36) or Equation (4.37).

If no occurrences of the conditions of Equations (4.35) - (4.37) are found for all possible combinations of sampling times; i.e., if $M_2 = M_3 = M_4 = 0$, then $S_1 = \frac{1}{2}$, $S_2 = 0$ and the minimum value of the variance σ_K^2 is attained. From Equation (4.24), this value is:

$$(\sigma_K^2)_{\min} = \frac{2}{N^2} \sum_{n=1}^N \sum_{\substack{m=1 \\ n \neq m}}^N \left(\frac{1}{2}\right) = \frac{1}{N^2} \left(1 - \frac{1}{N}\right). \quad (4.38)$$

Equation (4.38) is useful as a standard against which the variance of any non-optimum (i.e., non-minimum variance) sampling scheme can be compared.

A simplified expression for σ_K^2 from Equation (4.24) for any non-optimum sampling scheme can be written in terms of M_2, M_3 , and M_4 . An examination of Equation (4.24) shows that each M_2 violation results in two non-zero S_1 terms and each M_3 or M_4 violation results in four non-zero S_2 terms. Thus, σ_K^2 for the general case in terms of M_2, M_3 , and M_4 is:

$$\begin{aligned}
 \sigma_K^2 &= \frac{1}{N^2} \left(1 - \frac{1}{N}\right) + \frac{2}{N^4} (M_2) + \frac{4}{N^4} (M_3 + M_4) \\
 &= (\sigma_K^2)_{\min} + \frac{2}{N^4} (M_2 + 2M_3 + 2M_4). \quad (4.39)
 \end{aligned}$$

The examples of Figure 4.9 illustrate the variance minimization concepts discussed in this section. Example (1) shows one of many possible sample time choices (for $N = 4$ samples per block and 20 possible sampling times per block) which yield a minimum variance spectrum. Since $N = 4$ for these examples, the minimum variance from Equation (4.38) is $(\sigma_K^2)_{\min} = \frac{1}{N^2} \left(1 - \frac{1}{N}\right) = 0.0469$. Examples (2) - (4) show some typical non-minimum variance cases. The table at the bottom of Figure 4.9 gives the values of M_2 , M_3 , and M_4 for each example and compares the computed variance with the theoretical variance from Equation (4.39). In all cases, the computed variance was accurate to within computational accuracy. Note that the minimum variance spectrum of Example (1), while not perfectly uniform over k , has fewer extremely large or extremely small values compared with the other examples. The uniform sampling case, Example (5), illustrates the upper extreme of maximum variance because all of the spectral power is concentrated at the minimum number of frequencies. The value of σ_K^2 for the uniform sampling case is given by $\sigma_K^2 = 1/N (1 - 1/N)$. Therefore, the range of σ_K^2 is given by:

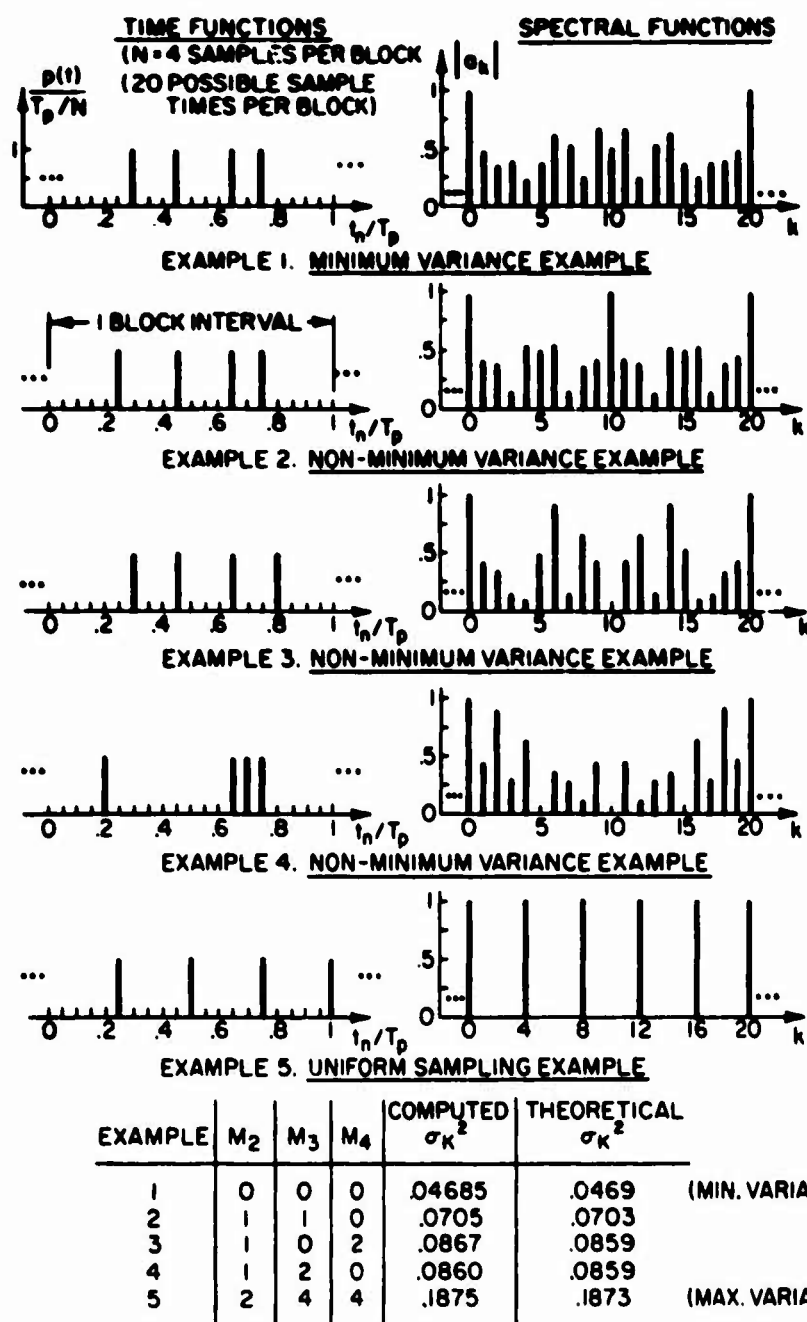


Figure 4.9 Examples of Variance Minimization Principles

$$\frac{1}{N^2} \left(1 - \frac{1}{N}\right) \leq \sigma_K^2 \leq \frac{1}{N} \left(1 - \frac{1}{N}\right).$$

The minimum variance sampling points shown in Example (1) of Figure 4.9 were relatively easy to find by trial and error because of the relatively small number of possible sets (eleven) of 2, 3, and 4 samples which had to be checked against the conditions of Equations (4.35) - (4.37). However, as the number of samples per block N becomes large, this method rapidly becomes unmanageable except perhaps with a digital computer. If minimum variance solutions do exist for large N , it seems probable that a computer algorithm could be devised that would find them. Investigation of this topic is left as a possible area for further research.

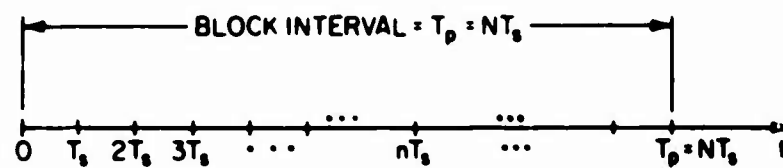
Even if minimum variance solutions cannot readily be found or are not practical for a given application, the minimum variance concept is important because the minimum σ_K^2 given by Equation (4.38) and the σ_K^2 for the uniform sampling case give two extremes against which any practical sampling scheme can be compared. This will be done in the next section for a unique nonuniform sampling technique which uses a pseudo-random number generator to select the sampling times $\{t_n\}$.

4.7 Sampling Time Selection Using Pseudo-Random Number Generators

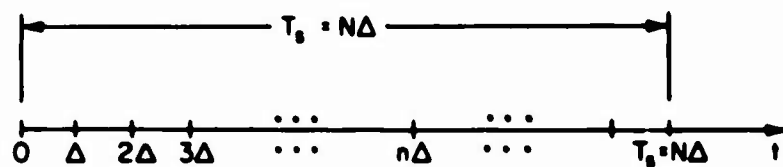
This section describes a nonuniform sampling scheme which uses a pseudo-random number generator [19] to select the nonuniform sampling times $\{t_i\}_{i=1}^N$. Although the scheme does not generate a minimum

variance sampling spectrum, it achieves an important unique spectrum shaping by suppressing the amplitude of the a_k spectral components for small values of k , it is easily reproducible, and it can be readily modified to obtain any desired number of samples per block, N . In this section, the basic pseudo-random sampling function will be analyzed.

Let each block sampling time T_p be divided into N equal segments of duration $T_s = T_p/N$ as shown in Figure 4.10(a). One sampling instant is to be selected at some point in each T_s interval to give the required total of N sampling times per block interval. Now, let each segment of length T_s be subdivided into N uniformly spaced possible sampling instants spaced $\Delta = T_s/N$ apart as shown in Figure 4.10(b). Only one of these N possible sampling instants will be selected by the sampling logic during each T_s second time segment. The choice of which of the N possible sampling instants to select during each T_s segment is made by a pseudo-random number generator as shown in Figure 4.11. In this figure, a pulse train with a period of Δ seconds between pulses drives a binary counter which counts to N in $T_s = N\Delta$ seconds before being reset to zero to repeat the count during each T_s second interval. The Pseudo-Random Number Generator (PRNG) which is assumed to have a repetition cycle of N states is driven by the pulse train divided by N . The PRNG thus changes states at the beginning of each T_s second segment shown in Figure 4.10(b) at the same time at which the binary counter is reset. At some time during each T_s second interval in which the PRNG remains



(a) SUBDIVISION OF BLOCK INTERVAL, T_p ,
INTO N EQUAL SEGMENTS



(b) SUBDIVISION OF EACH SEGMENT OF LENGTH T_s
INTO N POSSIBLE SAMPLING TIMES

Figure 4.10 Construction of Possible Sampling Times for Pseudo-Random Sampling

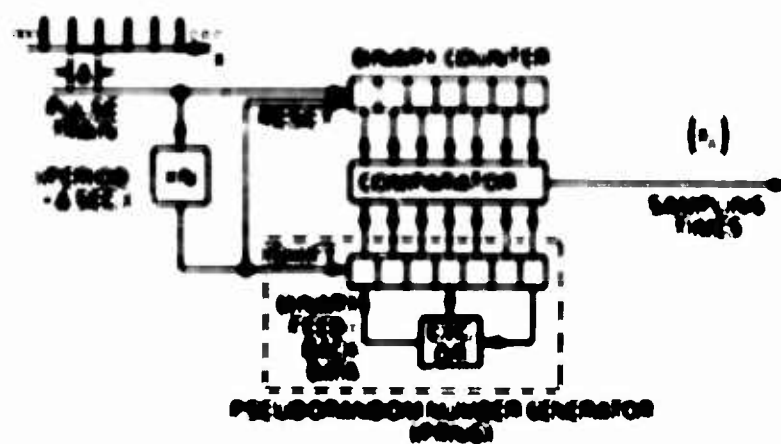


Figure 4.11 Sampling Time Generation Scheme Using a PRCG

constant, the binary counter state and the PRNG state will be identical. Whenever this condition exists, the comparator will produce an output pulse indicating that another sampling instant has been selected. Thus, one sampling instant is chosen during each T_p second interval at a multiple of T_p seconds from the start of that interval determined by the state of the PRNG. Since the PRNG has N states, one complete set of nonuniform sampling times $\{t_i\}_{i=1}^N$ is generated in T_p seconds (one block interval) and the entire process is repeated indefinitely since the PRNG is periodic.

The PRNG could be connected in a variety of ways to give sequences of varying lengths. For example, the PRNG feedback could be connected to give a maximal length sequence for which the theory has been well developed [19]. If the PRNG has an m stage shift register, the maximal length code length is $(2^m - 1)$. Thus, by making the block length N equal to the code length $(2^m - 1)$, an effective sampling time generator can be made whose sampling spectrum, although not of minimum variance, exhibits a high degree of randomness. With minor modifications, a PRNG can be made to generate shorter repetitive sequences of varying lengths, thus giving more freedom in the selection of a sampling scheme.

Assuming the system shown in Figure 4.11 is used to generate a set of repetitive nonuniform sampling times with N samples per block, the results of this chapter can be used to predict the properties of the sampling spectrum. The expression for the sampling coefficients a_k can be found by letting

$$t_n = (n-1)T_s = \frac{(n-1)T_p}{N}, \quad n = 1, 2, 3, \dots, N \quad (4.40)$$

in Equation (4.3), where t_n is n^{th} number in the PRNG output sequence and satisfies $1 \leq t_n \leq N$. Equation (4.6) thus reduces to

$$a_k = \frac{1}{N} \sum_{n=1}^N \exp \left[-j2\pi k \frac{(n-1)T_p}{N} \right] \quad (4.41)$$

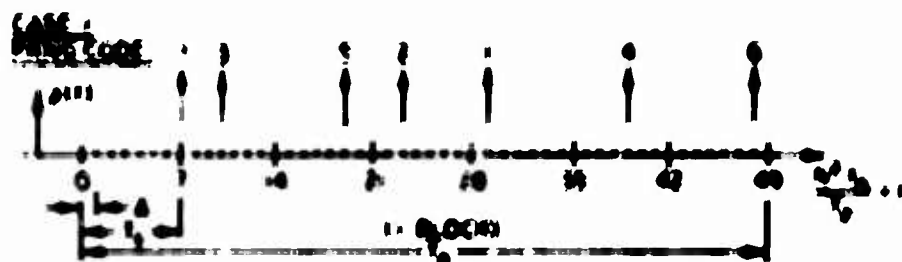
in this case, since $T_s = T_p/N$ and $\Delta = T_p/N^2$. Since the block interval T_p is subdivided into N^2 possible equally spaced sampling times as shown in Figure 4.10, the periodicity K of a_k as given by Equation (4.15) is $K = N^2$ and the spectral period in Hz is $N^2 f_p$, where $f_p = \frac{1}{T_p}$. The average power of a_k as given by Equation (4.17) is a constant equal to

$$\frac{1}{K} \sum_{k=1}^K |a_k|^2 = \frac{1}{N}$$

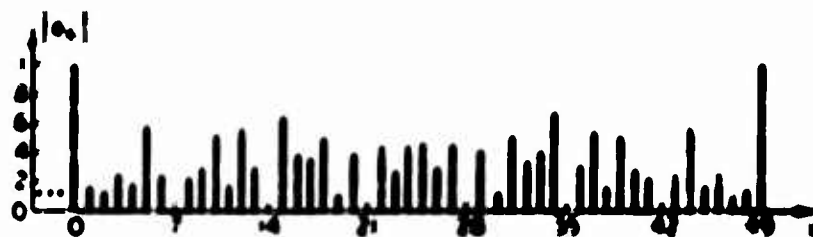
and the average value of a_k as given in Equation (4.20) is either $1/N$ or 0 depending on whether or not the last sample t_N occurs at the end point of the block interval T_p .

As an example of this technique, a computer program was written to simulate the sampling time generator of Figure 4.11. A PRNG with a 3-stage shift register was simulated with feedback connections to give a maximal length sequence of length $N = 7 = 2^3 - 1$.

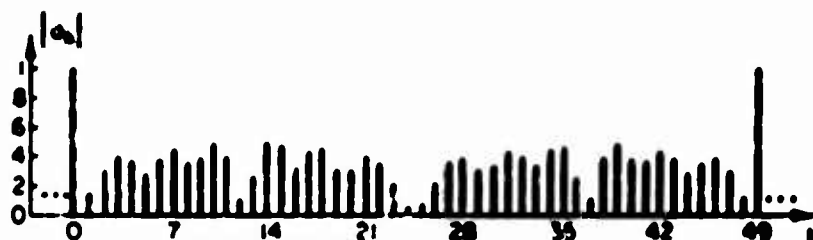
Figure 4.12(a) shows that each basic block interval of length T_p



(a) EXAMPLE OF SAMPLING TIME SELECTION
USING PRNG CODE (CASE - SAMPLE TIMES SHOWN)



(b) CASE 1 - SPECTRUM (PRNG CODE)



(c) CASE 6 - SPECTRUM (NON-PRNG CODE)

CASE	σ_K^2	M_3 OR M_4	MAX. $ a_k $	CODE SOURCE	PRNG CODE
1	.02915	7	.64	PRNG (1,3 FEEDBACK)	7 3 5 2 4 6
2	.03082	8	.68	PRNG (1,3 FEEDBACK) COMPLEMENTARY CODE	7 6 5 2 1 1 3
3	.03582	11	.76	PRNG (2,3 FEEDBACK)	7 3 1 4 2 5 6
4	.03082	8	.71	PRNG (2,3 FEEDBACK) COMPLEMENTARY CODE	7 6 4 1 2 5 3
5	.02915	7	.64	CASE 1-DIFFERENT STARTING PHASE	5 2 1 4 6 7 3
6	.01916	1	.47	BEST TRIAL & ERROR CODE	(EQUIV. PRNG CODE) 7 1 -1 1 5 5 1
MIN.	.01749	0	-	THEORETICAL MIN. VARIANCE	
MAX.	.12245	63	1.00	UNIFORM SAMPLING	(EQUIV. PRNG CODE) 7 7 7 7 7 7 7

(d) SUMMARY OF N=7 CASES STUDIED

Figure 4.12 Examples of Sampling Functions Generated by 5 Stage PRNG

The comparison in Cases 1 and 2 also indicated in Figure 4.12.4) is the maximum value of $|a_k|$ including the value of the end points, the computed spectral estimates \hat{a}_k^2 are given by Equation 4.29), and the computed values of \hat{a}_k are \hat{a}_k , the number of times the comparison of cases Equation 4.29) is Equation 4.29) are collected. The number of comparisons of Equation 4.29) is \hat{a}_k is given for all cases because $\hat{a}_k/2$ is not an integer multiple of 1, 2, 3, ..., $\hat{a}_k/2 = 24$ for

The computed spectrum for Case 1 is shown in Figure 4.12.5) where $|a_k|$ of Equation 4.29) is plotted versus k for the spectral peak of $k = 3^2 = 9$ is shown in the table, the estimate \hat{a}_k^2 of this spectrum is not as good as the spectral estimate computed from the maximum estimate comparison shown at the end of the table is that \hat{a}_k . This is also evident by comparing the 'smoothness' of spectrum of Case 1 with the 'noisy' spectrum shown in Figure 4.12.6) for the same maximum estimate spectrum of Case 1.

The spectral spectrum of Figure 4.12.6) illustrates the important property of spectral amplitude suppression for small k which is exhibited by all spectra generated by the pseudo-random sampling scheme described in this section. This example of the spectral shaping is demonstrated in Figure 4.12.6) by the fact that the amplitude of the first four spectral components ($k = 1$ to 4) are all well below the average level. This property has been experimentally found to be most effective for $k = \frac{1}{2}$ (approximately), where k is the number of samples per tone. The explanation for this suppression effect can be

can be considered each ϕ_k to be the average of N samples as shown by Equation (4.6). Since one sample is chosen from each of the N equal time segments in each time interval, the completion of ϕ_k consists of averaging N samples chosen each according to Equation (4.6) phase region of area $\frac{2\pi}{N}$ for which ϕ_k also covers the N samples in the first, middle, last, and the entire 2π phase region of the unit circle. The average amplitude of ϕ_k will be small. This argument is also applicable to saying that each phase region of area $\frac{2\pi}{N}$ contains N samples whose phase distribution is determined by the JNMC noise. For example, when $N = 1$, each $\frac{2\pi}{N}$ phase region contains one sample and maximum amplitude suppression is obtained when $N = \frac{1}{2}$, each $\frac{2\pi}{N}$ phase region contains half of the samples and a moderate amount of suppression is achieved when $N = 3$, each sector has a full phase range of 2π , the suppression effect is no longer present and maximum fluctuation of ϕ_k versus k is observed. This suppression effect will be better illustrated later in Figure 4.13 where a JNMC sampling spectrum is plotted for $N = 96$. In Chapter 5, this effect will be shown to have important implications in the reduction of odd harmonic responses for correlation functions of clipped sinusoidal signals.

The sampling function shown in Figure 4.12(c) for Case 6, which has only one occurrence of zero in Equation (4.36) or Equation (4.37), was the best that could be found by a limited trial and error search. The question of existence of a true minimum variance sampling function for $N = 7$ and $N = 49$ is still open.

The sampling spectrum of Figure 4.12(b) shows spectral characteristics possessed by all finite generated sampling functions with $k = 2^2$, i.e., the existence of zero spectral components at $k = \text{multiples of } 4$ (in this case). This property follows from Equation (4.4) by setting $k = 4n$, where n is an integer giving

$$S_k = \frac{1}{N} \sum_{n=0}^{N-1} e^{-j2\pi k n / N} = \frac{1}{N} \sum_{n=0}^{N-1} e^{-j2\pi 4n} = \frac{1}{N} \sum_{n=0}^{N-1} 1 = 0 \quad (4.43)$$

For all k values k assumes all possible integer values in the interval $1 \leq k \leq N$. The summation of Equation (4.43) can be considered to be the addition of N vectors uniformly distributed in phase over 2π and is thus equal to zero.

A comparison of Cases 1-4 shows that the spectral shape and variance σ_k^2 vary with the choice of maximal length PN code. Thus, in a practical problem, all possible codes should be examined in order to make a "best" choice. The sampling code for Case 5 is identical to that of Case 1 except that a different initial starting point in the sequence was assumed, which is equivalent to a redefinition of the time origin of the sampling block. The variance σ_k^2 and all spectral components $|a_k|$ were found to be identical independent of the starting point.

The results of the comparison of the examples of Figure 4.12 can be summarized as follows:

- (1) The spectral shape and f_s^2 are independent upon the specific PNNG code used.
- (2) The sampling spectrum and f_s^2 are independent of the PNNG lattice sampling rates.
- (3) The PNNG generated spectrum are not minimum resistance spectrum but do possess a slight degree of irregularities.
- (4) PNNG generated spectrum exhibit a small, a significant suppression effect which is more effective for $k > \frac{N}{2}$.
- (5) A common characteristic of all PNNG generated spectrum with $k = 1^2$ is that all spectral components at $k =$ multiples of N are zero.
- (6) Non-PNNG generated sampling functions can be found with lower f_s^2 , but minimum resistance sampling functions, if they exist, are difficult to find.

Another computer example of a PNNG generated sampling function is represented by Figure 4.13 which shows the initial portion of the sampling spectrum generated by a 7-stage PNNG. The PNNG code of length $(2^7 - 1) = 127$ is used to select which of 127 possible sampling times in each T_s interval (see Figure 4.10(b)) is chosen. However, only $N = 96$ samples per block interval are used, so the PNNG is reset after the 96th number in its code and the sampling process is repeated. The sampling spectrum thus has a period $K = 96(127) = 12,192$ which is equal to the total number of possible sampling times. Although only about 1/12 of a total spectral period is shown in Figure 4.13, the section from $k = 100$ to

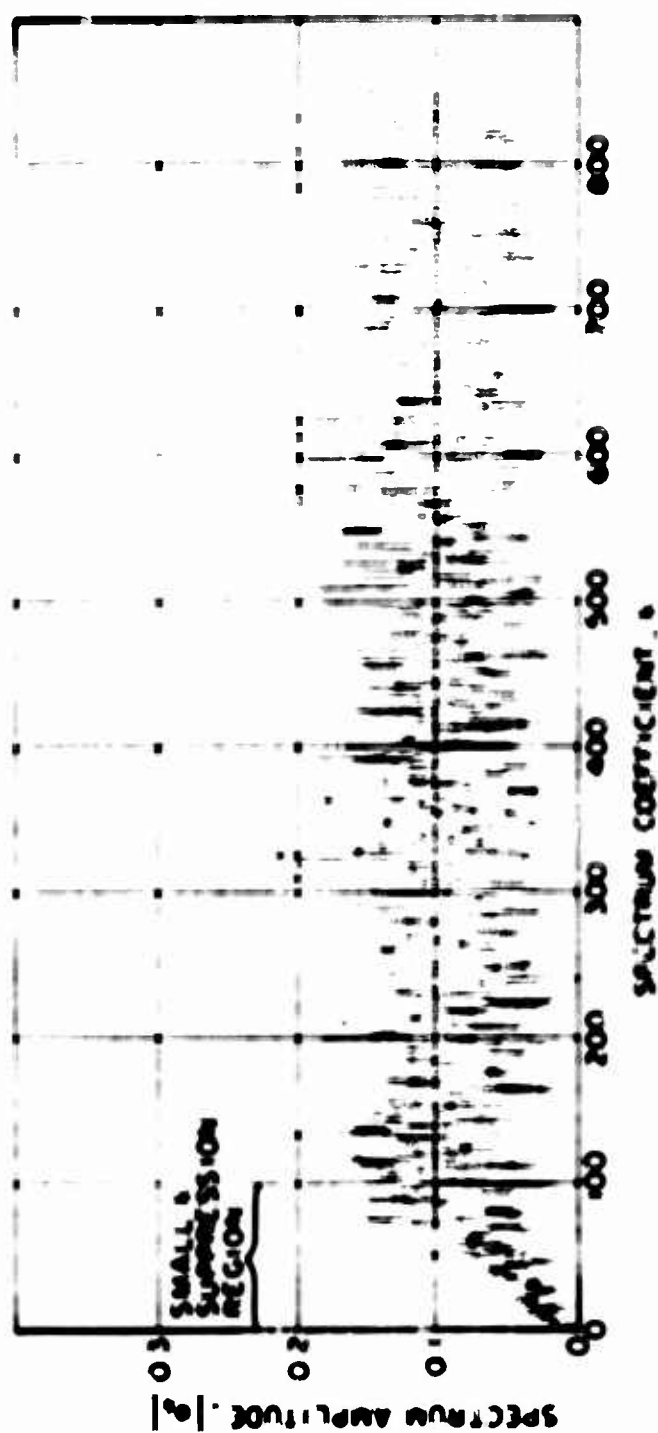


Figure 4.13 Sampling Spectrum for RMS Sampling Function. (X - 20)

$N = 800$ is typical of the general shape of the remaining uncharted portion of the spectrum. Since each spectral component a_k is formed by averaging a large number of unit vectors with essentially random phases, one would suspect that, if the initial region for $1 \leq k \leq N$ is eliminated, the probability distribution function for the remaining spectral components $|a_k|$ should be approximately Rayleigh with the following parameters for $N = 96$:

$$\overline{|a_k|^2} = \frac{1}{N} = 0.010417$$

and

$$\overline{|a_k|^4} = \sqrt{\frac{2}{\pi}} = 0.0905.$$

This was experimentally shown to be a valid assumption for large N . The following table compares the measured spectrum parameters shown for this example with the theoretical values derived in this chapter.

<u>Parameter</u>	<u>Measured Value</u>	<u>Theoretical Value</u>
$\frac{1}{K} \sum_{k=1}^K a_k ^2$	0.0104182	$\frac{1}{N} = 0.0104167$
$\sigma_K^2 = \frac{1}{K} \sum_{k=1}^K (a_k ^2 - \frac{1}{N})^2$	0.0001818	$(\sigma_K^2)_{\min} = 0.0001074$ $(\sigma_K^2)_{\max} = 0.010308$

The property of spectral suppression for small k is well illustrated by the spectrum of Figure 4.13 which shows an approximate linear growth of $|a_k|$ for $1 \leq k \leq 96$ with the region of the maximum suppression effectiveness for $1 \leq k \leq 48$. The importance of the small k suppression effect in the reduction of odd harmonic responses in correlation functions of clipped sinusoidal signals will be discussed in the next chapter.

CHAPTER V

APPLICATION OF BLOCK SAMPLING TO CORRELATION

FUNCTIONS OF CLIPPED SINUSOIDAL SIGNALS

5.1 Introduction

In Chapter III, correlation function properties of clipped sinusoidal signals with uniform sampling were investigated. As shown in Figure 3.10, the uniform sampling produced undesirably large correlations for some reference frequencies due to the presence of odd harmonics caused by clipping. For example, the frequencies that respond to the third harmonics have nominal correlations of $1/3$ of the fundamental correlation. Likewise, the fifth harmonics generate correlations of about $1/5$ of the fundamental response at some frequencies and, in general, the $(2n + 1)^{\text{st}}$ harmonic produces a correlation of about $\frac{1}{(2n + 1)}$ relative to the fundamental response. In Section 3.5, the use of nonuniform "block" sampling was proposed to reduce these odd harmonic correlations by destroying the synchronism between the uniform sampling periodicity and the periodicity of the odd signal harmonics.

In Chapter IV, "block sampling" was defined and some of its properties were developed; namely, the spectral periodicity properties, the average power spectrum properties, the requirements for minimum variance of the sampling coefficient power spectrum and small k

spectral amplitude suppression for PRNG sampling. In this chapter, these block sampling results will be applied to the reduction of odd harmonic responses in correlation functions of clipped sinusoids. A specific correlation function example is included using a PRNG generated sampling function similar to the one discussed in Section 4.7.

This chapter considers the basic reasons for the ability of block sampling to reduce the odd harmonic responses of correlation functions of clipped sinusoidal signals. In the next section, a qualitative correlation function analysis with block sampling will be made to help develop insight into the problem and to help predict which of the reference frequencies will have the greatest response for a given input frequency.

5.2 Qualitative Analysis of Correlation Functions with Block Sampling

The ideal block sampling quadrature correlation function model of Figure 5.1 is useful for analyzing the relationships between the input frequency f_I and the reference frequencies f_R which produce significant correlations. Since the frequency difference $(f_R - f_I)$ is the important parameter in this chapter, we will adopt the point of view of holding the input frequency f_I constant while varying the reference frequency f_R to study the correlation function dependence upon the frequencies f_I and f_R . The spectra of the pre-envelopes $p_x(t)$ and $p_y^*(t-\tau)$ at the sampler inputs are shown in Figure 3.6, while the spectrum of a typical block sampling function

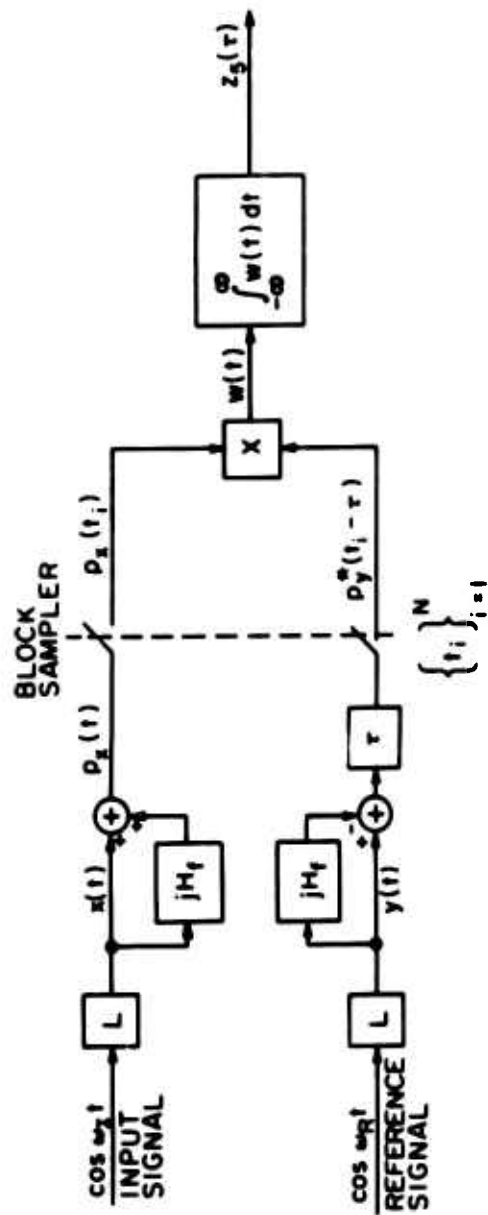


Figure 5.1 Ideal Block Sampling Quadrature Correlation Function Model with Clipped Sinusoidal Inputs

is shown in Figure 4.5. The spectrums of the sampler outputs $p_x(t_i)$ and $p_y^*(t_i - \tau)$ are equal to the convolution of the sampler input spectrum (Figure 3.6) and the sampling spectrum (Figure 4.5). Thus, if $X(f)$ and $Y^*(f)$ represent the Fourier Transforms of $p_x(t)$ and $p_y^*(t)$ and $P(f)$ is the block sampling spectrum given by Equation (4.7), then

$$\begin{aligned} X(f) &= \frac{4}{\pi} \sum_{n=0}^{\infty} \frac{(-1)^n}{(2n+1)} P[f - (-1)^n (2n+1) f_I] \\ &= \frac{4}{\pi} \sum_{n=0}^{\infty} \sum_{k=-\infty}^{\infty} \frac{(-1)^n a_k}{(2n+1)} \delta[f - (-1)^n (2n+1) f_I - k f_p], \end{aligned} \quad (5.1)$$

$$\begin{aligned} Y^*(f) &= \frac{4}{\pi} \sum_{q=0}^{\infty} \frac{(-1)^q}{(2q+1)} P[f + (-1)^q (2q+1) f_R] \\ &= \frac{4}{\pi} \sum_{q=0}^{\infty} \sum_{l=-\infty}^{\infty} \frac{(-1)^q a_l}{(2q+1)} \delta[f + (-1)^q (2q+1) f_R - l f_p], \end{aligned} \quad (5.2)$$

where

a_k = sampling spectrum coefficient (see Equation 4.6), and

$T_p = 1/f_p$ = block sampling period in seconds.

The complex spectrum $Z_5(f)$ of the correlation function $z_5(\tau)$ of Figure 5.1 is given by:

$$\begin{aligned}
 Z_5(f) &= X(f) Y^*(-f) \\
 &= \frac{16}{\pi^2} \sum_{n=0}^{\infty} \sum_{q=0}^{\infty} \sum_{k=-\infty}^{\infty} \sum_{l=-\infty}^{\infty} \frac{(-1)^{n+q} a_k a_l}{(2n+1)(2q+1)} \\
 &\quad \cdot \delta[f - (-1)^n (2n+1) f_I - \frac{k}{T}] \delta[f - (-1)^q (2q+1) f_R - \frac{l}{T}].
 \end{aligned}
 \tag{5.3}$$

Although Equation (5.3) is not a useful analytic expression for computing the actual correlation function, it is useful for determining which reference frequencies f_R , combined with a given input frequency f_I , can cause the largest odd harmonic correlations.

Typical plots of $X(f)$ and $Y^*(-f)$ from Equations (5.1) and (5.2) are shown in Figures 5.2 and 5.3. These plots show that the total spectrum of each sampler output consists of the sum of contributions from all odd harmonics (only the fundamental, third, and fifth of which are shown in each figure). The spectral contribution of each n^{th} odd harmonic is seen from these figures to be the complete block sampling spectrum of Figure 4.5, modified in amplitude by $\frac{4}{\pi} \frac{1}{(2n+1)}$ and centered about $f = (-1)^n (2n+1) f_I$ for the input frequency harmonics and about $f = (-1)^q (2q+1) f_R$ for the reference frequency harmonics. Each spectral component can be computed using Equation (4.6) for a specific block sampling function. Thus, all of the properties derived for block sampling

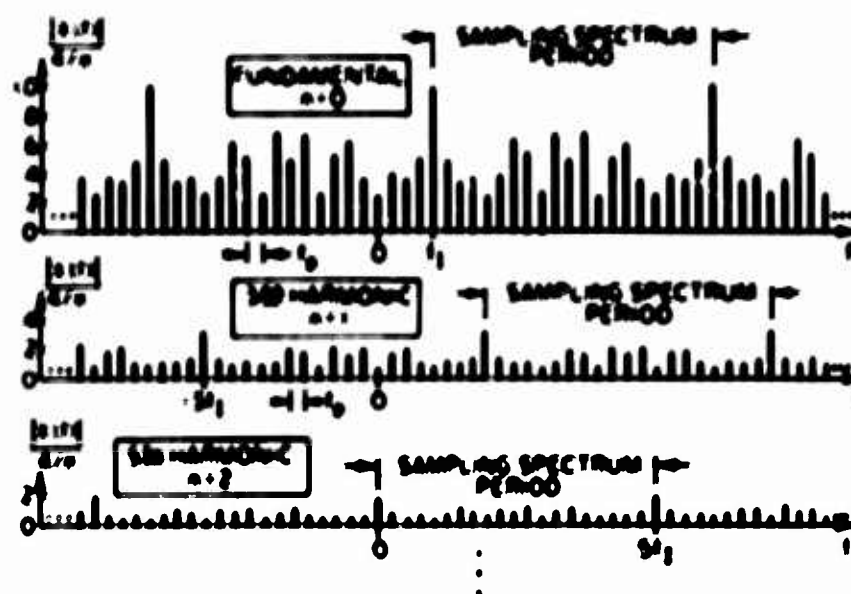


Figure 5.2 Typical Spectrum of Sampled Input Pre-Envelope

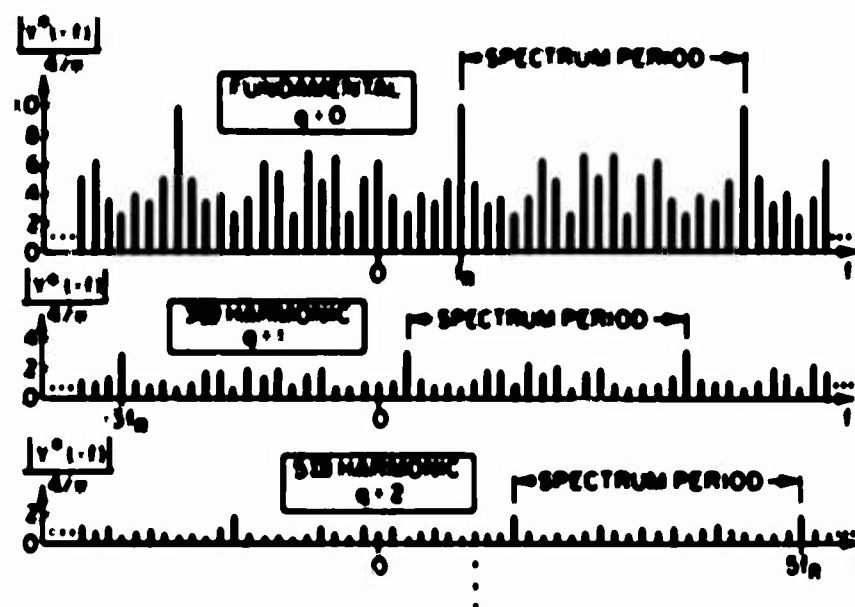


Figure 5.3 Typical Spectrum of Sampled Reference Pre-Envelope

spectra in Chapter IV can be applied to the analysis of correlation functions for clipped sinusoidal signals with block sampling.

Since the correlation function spectrum, by Equation (5.3), is equal to the product of the two discrete spectrums shown in Figures 5.2 and 5.3, it is obvious that some values of f_I and f_R will produce greatly different output spectra than other values. For example, values of f_I and f_R can be picked such that no frequency components of $X(f)$ and $Y^*(-f)$ align, and the resulting correlation function spectrum (and also the correlation amplitude) will be zero. On the other hand, for some combinations of f_I , f_R , and f_p , maximum alignment of input and reference spectral components will occur which will tend to maximize the correlation. More precisely, since each component a_k of the block sampling spectrum is a complex quantity, the spectrum $Z_5(f)$ consists of complex components which are products of two or more complex coefficients. Since the correlation function is proportional to the integral $\int_{-\infty}^{\infty} Z_5(f) e^{j2\pi f\tau} df$, the peak correlation depends upon the relative phases and amplitudes of all of the complex components in $Z_5(f)$. Although precise equations will be derived in the following sections, it is, in general, qualitatively true that values of f_I , f_R , and f_p that minimize alignment of spectral components result in lower average correlations than values which maximize spectral component alignment.

Using this as a rough criterion, we can derive some relationships between f_I , f_R , and f_p which result in maximum

alignment of spectral components and, hence, larger average correlations. Considering first the spectrum of the pre-envelope of the input signal as shown in Figure 5.2, it can be seen that the relation

$$4f_I = m_I f_p, \quad (5.4)$$

where m_I is any positive integer, is a sufficient condition to insure alignment of all input odd harmonic spectral components on a set of frequencies with f_p separation. For this special case, the spectrum of $X(f)$ reduces to one similar to the example shown in Figure 5.4.

In the same manner, the relation

$$4f_R = m_R f_p, \quad (5.5)$$

where m_R is any positive integer, assures the alignment of all reference odd harmonics on the set of frequencies shown in Figure 5.5. Each of the complex spectral components represented in Figures 5.4 and 5.5 is thus the vector sum of an infinite number of weighted complex coefficients, one for each odd harmonic. These cases, represented by Equation (5.4) and (5.5), can be thought of as "Worst Cases" in the sense that the spectral energy is distributed over the fewest possible frequencies rather than being distributed over a greater number of frequencies with smaller average amplitude.

Even though $4f_I$ and $4f_R$ are multiples of f_p as given by Equations (5.4) and (5.5), the product spectrum will be zero unless

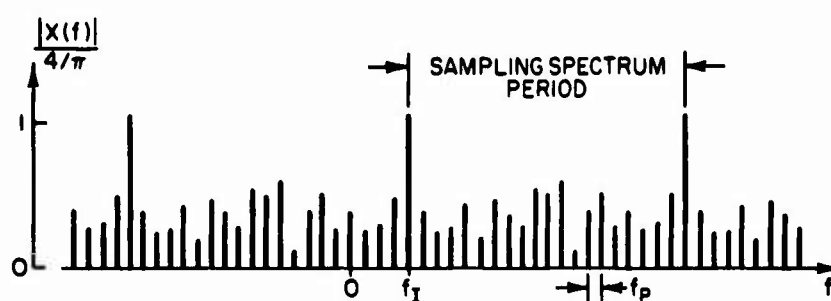


Figure 5.4 Typical Input Pre-Envelope Spectrum When $4f_I = m_I f_p$

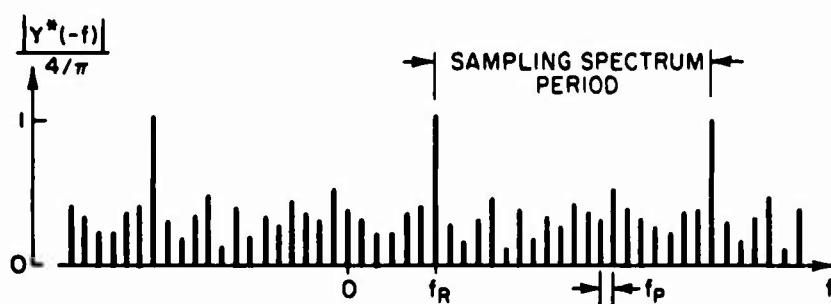


Figure 5.5 Typical Reference Pre-Envelope Spectrum When $4f_R = m_R f_p$

the non-zero spectral components of f_I shown in Figure 5.4 align with those of f_R shown in Figure 5.5; i.e., unless

$$(f_I - f_R) = m_d f_p, \quad (5.6)$$

where m_d is any positive or negative integer.

Equations (5.4), (5.5) and (5.6) thus define the conditions on f_I , f_R , and f_p which result in the Worst Case correlation responses. Let the input frequency f_I be fixed and satisfy Equation (5.4), and consider the problem of finding all the reference frequencies f_R , satisfying Equations (5.5) and (5.6).

It should be noted that just because a reference frequency satisfies the Worst Case criteria does not necessarily imply that the corresponding peak correlation will be high. The actual correlation amplitude for given values of f_I and f_R is proportional to the vector sum of a large number of complex numbers (spectral coefficients) and thus can be relatively small or relatively large. It will be shown later, however, that the average correlation is the largest for the Worst Case frequency conditions, and that the correlation variance about the average value over all Worst Case frequencies can be relatively large.

If f_I is a fixed input frequency satisfying $lf_I = m_I f_p$, then the Worst Case reference frequencies satisfying Equations (5.5) and (5.6) are given by

$$f_R = f_I \pm m f_p, \quad (5.7)$$

where $m = 1, 2, 3, \dots$. Thus, the Worst Case reference frequencies are f_p Hz apart for a fixed input frequency f_I . Each time the input frequency f_I is incremented by $1/4 f_p$ from its initial value, a new set of reference frequencies, each separated by f_p Hz, will satisfy the Worst Case conditions.

It is also of interest to briefly consider other combinations of f_I , f_R and f_p which lead to a non-zero correlation function spectrum $Z(f)$, but which do not meet the Worst Case criteria. For example, we can let the input frequency satisfy the Worst Case condition, $4f_I = m_I f_p$, and ask how many non-zero reference frequencies exist between each pair of Worst Case reference frequencies given by Equation (5.7). If f_I is held fixed and f_R is moved from its Worst Case value by $1/3 f_p$, the third harmonic spectral components of f_R (see Figure 5.3) will align with the spectral components of f_I (see Figure 5.4) and a non-zero correlation function spectrum will result whose average power (as will be shown in Section 5.4) is about $1/3$ of the Worst Case average power. Moving f_R by another increment of $1/3 f_R$ produces a similar result. Using a similar argument for the higher order odd harmonics, the set of non-zero response frequencies shown in Figure 5.6 can be constructed. Although only the non-zero reference frequencies caused by the third, fifth, and seventh harmonics are shown in Figure 5.6, similar responses due to all higher order odd harmonics are also present.

Now, consider the case where the input frequency does not satisfy the Worst Case condition $4f_I = m_I f_p$. Let f_I be an

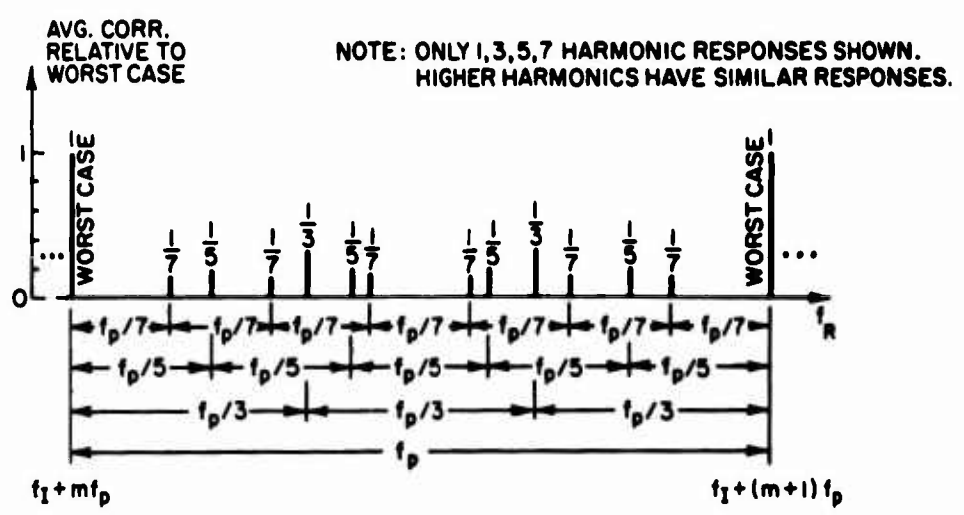


Figure 5.6 Non-Zero Reference Frequencies When $4f_I = m_I f_p$

arbitrary distance x away from the nearest Worst Case frequency as shown in Figure 5.7(a). For this general case, the input and reference harmonic spectra will not align as shown in Figures 5.4 and 5.5, but will be similar to those shown in Figures 5.2 and 5.3. The odd harmonic reference response pattern similar to that of Figure 5.6 now becomes more complex because the alignment of all possible pairs of reference and input odd harmonics must now be considered. However, it is instructive to consider the most significant alignment combinations as shown in Figure 5.7(b). This figure includes all possible alignment combinations of the fundamental, third and fifth harmonics of the input and reference frequencies. Figure 5.7(b) shows that, relative to Figure 5.6, two more reference frequencies respond to both the third and fifth harmonic terms and that the average responses of Figure 5.7(b) are somewhat lower (by about 20 percent) than the corresponding responses of Figure 5.6.

Figures 5.6 and 5.7 both show that, although minor responses are present due to the odd harmonics, the dominant terms are those for which

$$f_R = f_I + m f_p,$$

where $m = \pm 1, \pm 2, \pm 3, \dots$. Although the Worst Case correlation responses shown in Figure 5.6 are somewhat higher (about 20 percent) on the average than the corresponding terms in Figure 5.7, the correlation variance (fluctuation) at these frequencies will be shown to be large enough to make this difference less significant.

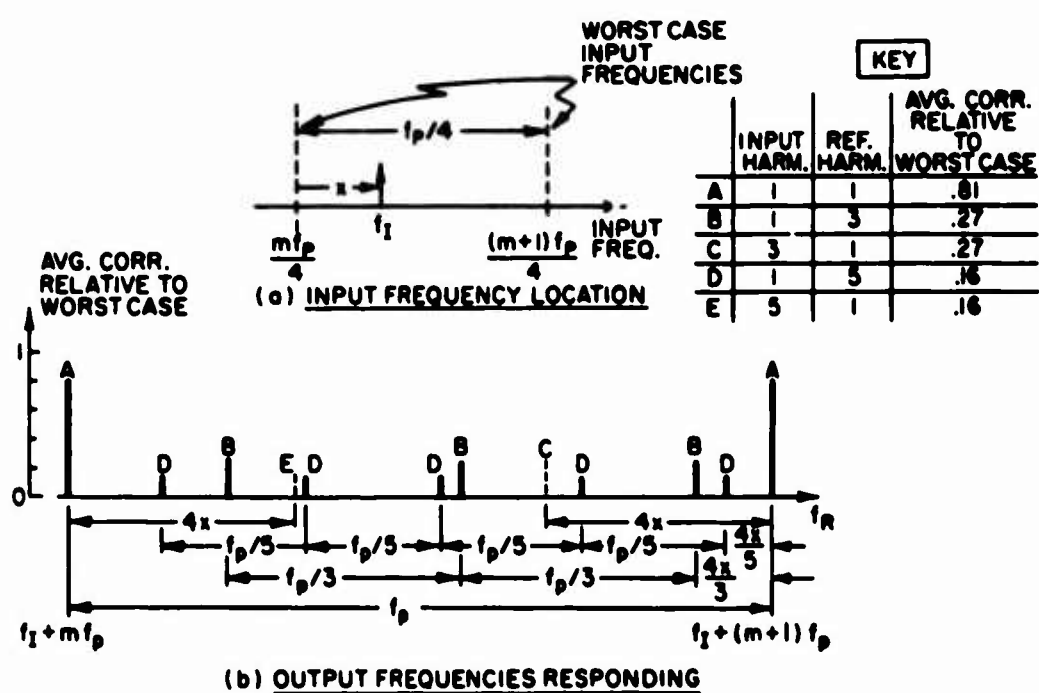


Figure 5.7 Non-Zero Reference Frequencies When $4f_I \neq m f_p$

Careful selection of the sampling spectrum periodicity K is important if undesirably large extraneous correlations, equal to those for the uniform sampling case of Chapter III, are to be avoided. For example, if the Worst Case conditions are met and if the third harmonic periodicity (see Figures 5.2 and 5.3) of the input spectrum coincides with some reference frequency f_R , then that reference frequency will produce a peak correlation of about 33 percent relative to the fundamental response of unity. That is, if $(-3f_I + NKf_p) = f_R$ for some reference frequency f_R , where N is any integer, then this undesirable situation exists. Similar conditions for the fifth harmonic results in approximately a 20 percent correlation. Since the periodicity K is usually controllable by choice of sampling times, undesirable fundamental, third, and fifth harmonic responses can be avoided by choosing K to satisfy the following inequalities:

$$f_I + NK f_p \neq f_R,$$

$$f_I - NK f_p \neq 3f_R,$$

$$f_R - NK f_p \neq -3f_I,$$

$$f_I + NK f_p \neq 5f_R$$

and

$$f_R + NK f_p \neq 5f_I$$

for any f_I or f_R in the range of interest where N is any positive or negative integer. Similar conditions can be derived for higher harmonics.

The qualitative remarks based on the model of Figure 5.1 and the frequency plots of Figures 5.2 through 5.7 have been based on the assumption of sinusoidal signals of infinite time duration and thus of spectral lines of zero width. For signals of finite duration T , each of these spectral lines have a finite width of approximately $1/T$ Hz and, therefore, the spectral picture becomes a continuous "smeared" one instead of a discrete one as described by this model. The real value of this model lies in its ability to help us gain qualitative insight into some of the complexities of the system response and to help predict the Worst Case reference frequencies for a given input frequency.

5.3 Deterministic Analysis

In order to obtain a useful quantitative correlation function expression with block sampling, consider the model of Figure 5.8. This model, based on a similar model in Tou [36], represent nonuniform block sampling as parallel uniform sampling (at the block rate T_p) of N delayed versions of the signal, where the delays are equal to the N nonuniform sampling times $\{t_i\}_{i=1}^N$ in each block interval. $w(mT_p)$ represents the average of the N samples in each block interval and the correlation function $z_G(\tau)$ is formed by averaging over a signal duration time of M blocks or T seconds where $M = T/T_p$. Since the input and reference are both deterministic sinusoidal signals and since the sampling instants $\{t_i\}$ are assumed known, the complex output correlation $z_G(\tau)$ is a deterministic function whose real and imaginary parts are equal to the quadrature

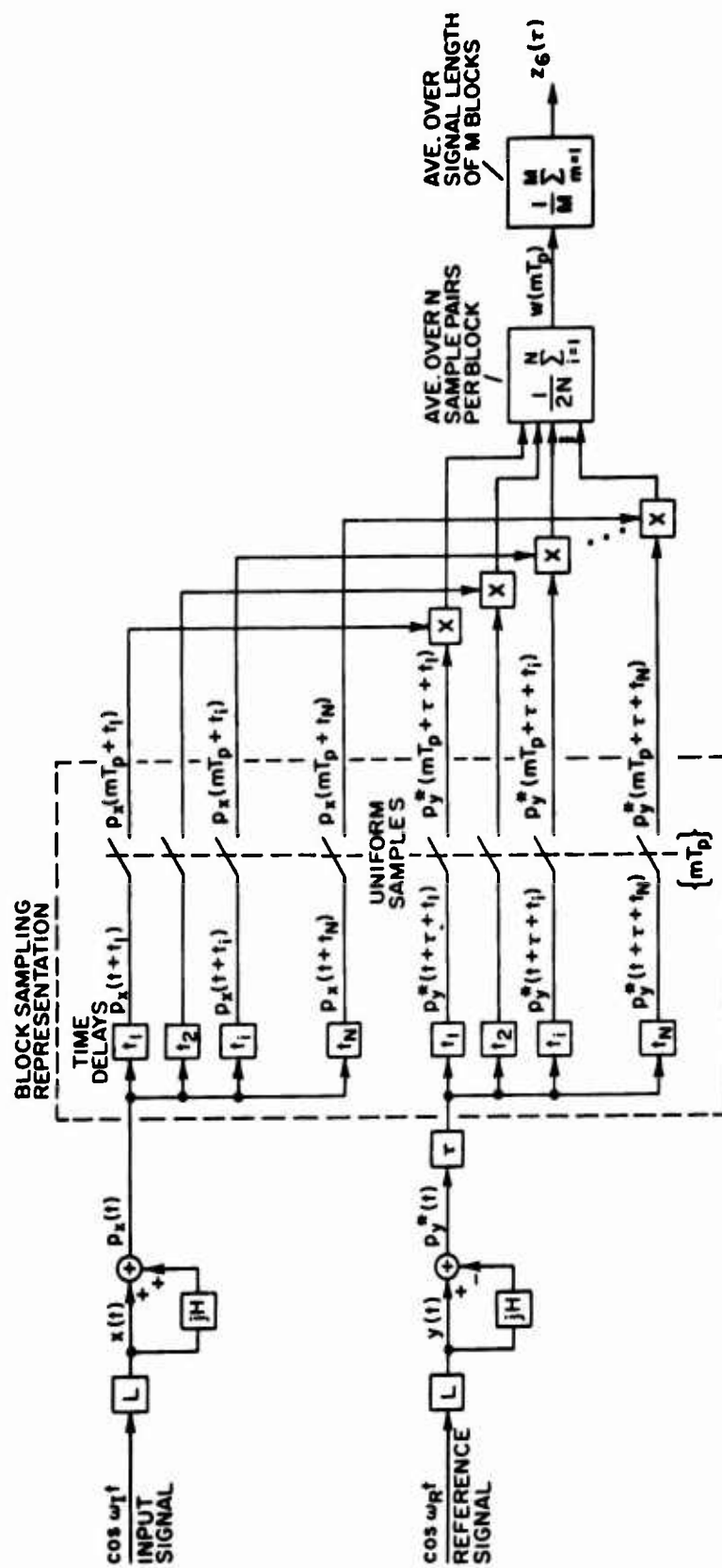


Figure 5.8 Quadrature Correlation Function Model with Block Sampling

phase of the correlation function between $x(t)$ and $y(t)$. The relative phase θ between the input and reference sinusoids is chosen to be zero without loss of generality since any value of θ can be represented by an equivalent value of time delay τ .

If the pre-envelopes of the clipped sinusoidal signals are represented as in Chapter III by the Fourier Series representation:

$$p_x(t) = \frac{4}{\pi} \sum_{n=0}^{\infty} \frac{(-1)^n}{(2n+1)} e^{j(-1)^n (2n+1) \omega_I t} \quad (5.8)$$

and

$$p_y^*(t) = \frac{4}{\pi} \sum_{q=0}^{\infty} \frac{(-1)^q}{(2q+1)} e^{-j(-1)^q (2q+1) \omega_R t}, \quad (5.9)$$

then, from Figure 5.8, the correlation function $z_G(\tau)$ is

$$\begin{aligned} z_G(\tau) &= \frac{1}{M} \sum_{m=1}^M \frac{1}{2N} \sum_{i=1}^N p_x(mT_p + t_i) p_y^*(mT_p + t_i + \tau) \\ &= \frac{8}{\pi^2} \frac{1}{MN} \sum_{m=1}^M \sum_{i=1}^N \sum_{n=0}^{\infty} \sum_{q=0}^{\infty} \frac{(-1)^{n+q}}{(2n+1)(2q+1)} \\ &\quad \cdot e^{j(-1)^n (2n+1) \omega_I (mT_p + t_i)} \cdot e^{-j(-1)^q (2q+1) \omega_R (mT_p + t_i + \tau)} \end{aligned} \quad (5.10)$$

where n denotes the input odd harmonics and q denotes the reference odd harmonics. Changing the order of summation of Equation (5.10) gives

$$\begin{aligned}
z_6(\tau) &= \frac{8}{\pi} \sum_{n=0}^{\infty} \sum_{q=0}^{\infty} \frac{(-1)^{n+q} e^{-j(-1)^q(2q+1)\omega_R\tau}}{(2n+1)(2q+1)} \\
&\cdot \frac{1}{N} \sum_{i=1}^N e^{-j2\pi t_i [(-1)^q(2q+1)f_R - (-1)^n(2n+1)f_I]} \\
&\cdot \frac{1}{M} \sum_{m=1}^M e^{-j2\pi m T_p [(-1)^q(2q+1)f_R - (-1)^n(2n+1)f_I]}. \quad (5.11)
\end{aligned}$$

For specific values of f_R and f_I , Equation (5.11) gives the deterministic correlation function as a function of time delay τ . This equation shows that, in general, $z_6(\tau)$ contains contributions from all input and reference odd harmonics. Each of these terms has an amplitude and a phase which are functions of the harmonic order (n and q), the specific frequencies (f_R and f_I), the nonuniform sampling instants (t_i), the block sampling period (T_p), the number of samples per block (N), and the number of blocks in a signal length (M). The real part of $z_6(\tau)$, $\phi_6(\tau)$, which represents the "in-phase" correlation function, thus consists of the sum of an infinite number of sinusoidal terms whose amplitudes, frequencies, and phases are determined by these parameters. As will be shown later by a specific example, this results in a correlation function with a "noisy" carrier; i.e., the basic sinusoidal carrier term at frequency f_R ($k = n = 0$) in Equation (5.11) is modified by the other odd harmonic terms to create a resultant correlation function which is deterministic but irregular in shape.

Although Equation (5.11) is exact for all frequencies f_I and f_R , it is quite cumbersome to work with, in general, because of the four summations. However, a considerable simplification results for the important Worst Case frequencies described by Equations (5.4), (5.5), and (5.6); i.e., when

$$4f_I = m_I f_p,$$

$$4f_R = m_R f_p$$

and

$$(f_I - f_R) = m_d f_p,$$

(5.12)

where m_I , m_R , and m_d are integers. This simplification results because, when these three conditions are satisfied, the term $[(-1)^q (2q + 1) f_R - (-1)^n (2n + 1) f_I]$, which represents the frequency difference between the $(2q + 1)$ reference harmonic and the $(2n + 1)$ input harmonic, reduces to a multiple of f_p ; i.e., whenever the conditions of Equation (5.12) are satisfied, it can be shown that

$$[(-1)^q (2q + 1) f_R - (-1)^n (2n + 1) f_I] = k f_p = \frac{k}{T_p} \quad (5.13)$$

where k is a positive or negative integer which depends on m_I , m_R , and m_d . When the Worst Case conditions described by Equations (5.12) and (5.13) exist, the final summation over m in Equation (5.11) reduces to

$$\begin{aligned}
\frac{1}{M} \sum_{m=1}^M e^{-j2\pi m T_p [(-1)^q (2q+1) f_R - (-1)^n (2n+1) f_I]} \\
= \frac{1}{M} \sum_{m=1}^M e^{-j2\pi m k} = 1
\end{aligned} \tag{5.14}$$

for all k and n , and the summation over i can be expressed in terms of the sampling coefficients of Chapter IV as

$$\begin{aligned}
\frac{1}{N} \sum_{i=1}^N e^{-j2\pi t_i [(-1)^q (2q+1) f_R - (-1)^n (2n+1) f_I]} \\
= \frac{1}{N} \sum_{i=1}^N e^{-j2\pi \frac{t_i}{T_p} k} = a_k,
\end{aligned} \tag{5.15}$$

where k is an integer given by $k = [(-1)^q (2q+1) \frac{m_R}{4} - (-1)^n (2n+1) \frac{m_I}{4}]$.

Thus, for the Worst Case frequencies, described by Equation (5.12), Equation (5.11) reduces to

$$z_6(\tau) = \frac{8}{\pi^2} \sum_{n=0}^{\infty} \sum_{q=0}^{\infty} \frac{(-1)^{n+q} a_k}{(2n+1)(2q+1)} e^{-j(-1)^q (2q+1) \omega_R \tau}. \tag{5.16}$$

Equation (5.16) shows that the correlation function for this case can be written in terms of the odd input and reference harmonics and of the nonuniform sampling coefficients a_k , discussed in Chapter IV, thus illustrating the important role of these coefficients. The

distinguishing feature of the Worst Case Frequencies is that the summation over m in Equation (5.14) is equal to its maximum value of unity for all q and n which is equivalent to saying that corresponding samples t_i in all sampling blocks occur at the same input and reference phase. For non-worst case frequencies, this summation over m serves as an attenuation factor which reduces the average correlation envelope response as will be shown in Section 5.4.

If the coefficients a_k are written as $a_{k(q,n)}$ to show the dependence of k on the odd harmonic indices q and n , Equation (5.14) can be expanded to illustrate the contribution of each odd harmonic

$$\begin{aligned}
 \frac{\pi^2}{8} z_6(\tau) = & a_{k(0,0)} e^{-j\omega_R \tau} - \frac{1}{3} a_{k(0,1)} e^{-j\omega_R \tau} + \frac{1}{5} a_{k(0,2)} e^{-j\omega_R \tau} + \dots \\
 & - \frac{1}{3} a_{k(1,0)} e^{j3\omega_R \tau} + \frac{1}{(3)(3)} a_{k(1,1)} e^{j3\omega_R \tau} \\
 & - \frac{1}{(3)(5)} a_{k(1,2)} e^{j3\omega_R \tau} + \dots + \frac{1}{5} a_{k(2,0)} e^{-j5\omega_R \tau} \\
 & - \frac{1}{(5)(3)} a_{k(2,1)} e^{-j5\omega_R \tau} + \frac{1}{(5)(5)} a_{k(2,2)} e^{-j5\omega_R \tau} + \dots \\
 & - \frac{1}{7} a_{k(3,0)} e^{j7\omega_R \tau} + \dots
 \end{aligned} \tag{5.17}$$

Equation (5.17) shows that the correlator output $z_6(\tau)$ is equal to the sum of sinusoidal (or exponential) terms whose amplitudes are equal to $\frac{|a_{k(q,n)}|}{(2q+1)(2n+1)}$, whose frequencies are given by $(2q+1)f_R$,

and whose phases are determined by the phase of the complex coefficient $a_{k(q,n)}$. Since, by Chapter IV, the a_k terms can vary greatly in both amplitude and phase from term to term, the summation given by Equation (5.17), in general, leads to an irregularly shaped waveform which is periodic at the period of the reference frequency f_R ; i.e., which has a period of $1/f_R$.

Because of the amplitude weighting of unity, the most significant term in Equation (5.17) is the $a_{k(0,0)}$ term at the fundamental frequency f_R . One point of view might be to consider the $a_{k(0,0)} e^{-j\omega_R \tau}$ term of Equation (5.17) as the principal carrier term and the remaining terms as additive "noise" terms, although for some small values of $a_{k(0,0)}$ the noise terms may be larger than the principal term. Adopting this point of view, if we wish to minimize the odd harmonic correlation responses, we should try to keep $a_{k(0,0)}$ uniformly low in some sense for all the Worst Case frequency conditions. The $a_{k(0,0)}$ coefficient is a single efficient in the block sampling spectrum where the integer $k_{(0,0)}$ is given by

$$k(0,0) = \frac{(f_R - f_I)}{f_p} . \quad (5.18)$$

If a number of reference frequencies and input frequencies are to be considered, Equation (5.18) can be used to compute all applicable values of k .

One approach to finding an optimum set of $a_{k(0,0)}$ coefficients would be to try to choose the sampling times $\{t_i\}$ to minimize the

variance of $|a_k|^2$ over the k 's given by Equation (5.18). In Chapter IV, a technique for minimizing the variance of $|a_k|^2$ over an entire period of the sampling spectrum was developed. The problem of minimizing the variance of $|a_k|^2$ over an arbitrary set of k 's is a considerably more complicated problem and is not considered in this thesis. Although the PRNG sampling technique described in Section 4.7 does not minimize the variance of $|a_k|^2$ in a localized k region, it has a similar property in that the values of $|a_k|^2$ are suppressed well below the average spectral level of the localized region $1 \leq k \leq N/2$. If the differences between the values of f_R and f_I in Equation (5.18) are small so that all $k(0,0)$ terms of interest occur in the region $1 \leq k(0,0) \leq N/2$, the PRNG sampling technique is effective in substantially reducing the contribution of the principal term, $a_{K(0,0)} e^{-j\omega_R \tau}$, in the correlation function expansion of Equation (5.17).

At the same time, the PRNG sampling spectrum is reasonably uniform in amplitude for large k so that no higher order odd harmonic terms of Equation (5.17) will dominate and create an unusually large correlation peak.

5.4 Statistical Analysis

Although the correlation function $z_G(\tau)$ of Figure 5.8 for fixed values of f_R and f_I is a deterministic function given by Equation (5.11), it is sometimes useful to consider the statistical problem of finding the average properties of the correlation functions for all reference frequencies which respond to a given input frequency

as a function of the average properties of a_k developed in Chapter IV. For example, let the fixed input frequency f_I satisfy the Worst Case condition $4f_I = m_I f_p$ of Equation (5.12) and consider all reference frequencies which satisfy Worst Case conditions $4f_R = m_R f_p$ and $(f_I - f_R) = m_d f_p$. The corresponding correlation functions as given by Equation (5.16) are

$$z_6(\tau) = \frac{8}{\pi^2} \sum_{n=0}^{\infty} \sum_{q=0}^{\infty} \frac{(-1)^{n+q} a_k}{(2n+1)(2q+1)} e^{-j(-1)^q (2q+1) \omega_R \tau}$$

Since the a_k 's vary for each set of Worst Case frequencies f_I and f_R , this analysis will assume that the a_k 's are random variables with a mean and mean square given by Equations (4.20) and (4.17) as

$$\overline{a_k} = \frac{1}{K} \sum_{k=1}^K a_k = 0$$

$$\overline{|a_k|^2} = \frac{1}{K} \sum_{k=1}^K |a_k|^2 = \frac{1}{N},$$

where N is the number of samples per block interval T_p , and K is the assumed period of the sampling spectrum a_k . Choosing $\tau = 0$ as an arbitrary value of carrier phase, the average value of $z_6(\tau)$ at $\tau = 0$ is

$$\overline{z_6(0)} = \frac{8}{\pi^2} \sum_{n=0}^{\infty} \sum_{q=0}^{\infty} \frac{(-1)^{n+q} \overline{a_k}}{(2n+1)(2q+1)} = 0 \quad (5.18)$$

where the average is taken over all Worst Case input and reference frequencies. The average squared value of $z_6(0)$ taken over the same frequencies is

$$\begin{aligned} \overline{|z_6(0)|^2} &= \overline{\left| \frac{8}{\pi^2} \sum_{n=0}^{\infty} \sum_{q=0}^{\infty} \frac{(-1)^{n+q} a_k}{(2n+1)(2q+1)} \right|^2} \\ &= \frac{64}{\pi^4} \sum_{n=0}^{\infty} \sum_{q=0}^{\infty} \sum_{p=0}^{\infty} \sum_{r=0}^{\infty} \frac{(-1)^{n+q+p+r} \overline{a_{k(q,n)} a_{k(p,r)}^*}}{(2n+1)(2q+1)(2p+1)(2r+1)}, \end{aligned} \quad (5.19)$$

where the notation $a_{k(q,n)}$ is used to denote the dependence of a_k on the indices n and q .

Consider the average $\overline{a_{k(q,n)} a_{k(p,r)}^*}$ in Equation (5.19) over all input and reference frequencies satisfying $4f_I = m_I f_p$ and $(f_I - f_R) = m_d f_p$. We can consider all possible Worst Case input and reference frequencies by averaging both m_I and m_d over one sampling spectrum period K ; i.e., by considering

$$\overline{a_{k(q,n)} a_{k(p,r)}^*} = \frac{1}{K} \sum_{m_I=1}^K \frac{1}{K} \sum_{m_d=1}^K a_{k(q,n)} a_{k(p,r)}^*. \quad (5.20)$$

Substituting the expression for a_k and interchanging the order of summation, Equation (5.20) becomes

$$\overline{a_{k(q,n)} a_{k(p,r)}^*}$$

$$= \frac{1}{N^2} \sum_{i=1}^N \sum_{h=1}^N \left[\frac{1}{K} \sum_{m_I=1}^K e^{-j \frac{2\pi}{T} m_I (I_1 t_i - I_2 t_h)} \right] \\ \cdot \left[\frac{1}{K} \sum_{m_d=1}^K e^{j \frac{2\pi}{T} m_d [(-1)^q (2q+1) t_i - (-1)^p (2p+1) t_h]} \right], \quad (5.21)$$

where $I_1 = \frac{1}{4}[(-1)^q (2q+1) - (-1)^n (2n+1)]$ and $I_2 = \frac{1}{4}[(-1)^p (2p+1) - (-1)^r (2r+1)]$ are both integers for all values of q, n, p and r . But,

$$\frac{1}{K} \sum_{m_I=1}^K e^{-j \frac{2\pi}{T} m_I (I_1 t_i - I_2 t_h)} = \begin{cases} 1 & \text{whenever } (I_1 t_i - I_2 t_h) = 0, \pm 1, \pm 2, \dots \\ 0 & \text{otherwise} \end{cases} \quad (5.22)$$

and

$$\frac{1}{K} \sum_{m_d=1}^K e^{-j \frac{2\pi}{T} m_d [(-1)^q (2q+1) t_i - (-1)^p (2p+1) t_h]} \\ = \begin{cases} 1 & \text{whenever } [(-1)^q (2q+1) t_i - (-1)^p (2p+1) t_h] = 0, \pm 1, \pm 2, \dots \\ 0 & \text{otherwise.} \end{cases} \quad (5.23)$$

$\overline{a_{k(q,n)} a_{k(p,r)}^*}$ of Equation (5.21) will be non-zero only for those values of q, n, p, r, t_i and t_h which simultaneously make both Equations (5.22) and (5.23) non-zero. From Equation (5.22) and (5.23), the conditions on q, n, p, r, t_i and t_h which give non-zero contributions are:

$$\begin{aligned} \frac{1}{4} [(-1)^q (2q+1) - (-1)^n (2n+1)] t_i - \frac{1}{4} [(-1)^p (2p+1) - (-1)^r (2r+1)] t_h \\ = 0, \pm 1, \pm 2, \dots \end{aligned} \quad (5.24)$$

and

$$[(-1)^q (2q+1)] t_i - [(-1)^p (2p+1)] t_h = 0, \pm 1, \pm 2, \dots \quad (5.25)$$

The principal non-zero $\overline{a_{k(q,n)} a_{k(p,r)}^*}$ terms occur when

$$q = p,$$

$$n = r$$

and

$$t_i = t_h, \quad (5.26)$$

thus satisfying both Equations (5.24) and (5.25) by making them equal to zero. For these terms,

$$\overline{a_{k(q,n)} a_{k(p,r)}^*} = \frac{1}{N^2} \sum_{i=1}^N \sum_{\substack{h=1 \\ i=h}}^N 1 = \frac{1}{N}, \text{ 'for } q = p, h = r \text{'} \quad (5.27)$$

from Equation (5.21). In addition to the principal non-zero terms given by the Equations (5.26) and (5.27) which always exist for any set of sampling times, for a specific set of $\{t_i\}$, a few other isolated values of q, p, n, r, t_i and t_h may satisfy both Equations (5.24) and (5.25) and produce small but non-zero values of $\overline{a_{k(q,n)} a_{k(p,r)}^*}$. For most sets of sampling times $\{t_i\}$ with a reasonable degree of randomness, the effects of these isolated contributions are second order and will thus be neglected in this analysis.

Considering only the principal terms given by Equation (5.27), Equation (5.19) reduces to

$$\overline{|z_6(0)|^2} = \frac{64}{\pi^4} \sum_{n=0}^{\infty} \sum_{q=0}^{\infty} \frac{1/N}{(2n+1)^2 (2q+1)^2} = \frac{1}{N}. \quad (5.28)$$

Equations (5.18) and (5.28) show that for a fixed (arbitrary) value of τ , the average value of the Worst Case correlation function is zero and their mean squared value is equal to $\frac{1}{N}$ independent of specific sampling times t_i if the averages are taken over a complete sampling spectrum period K . Since $z_6(\tau)$ is a complex function composed of the in-phase and quadrature correlation functions $\phi_6(\tau)$ and $\hat{\phi}_6(\tau)$ (see Equations 2.4 - 2.6), $\overline{z_6(0)} = 0$ implies that both the in-phase and quadrature functions also have a zero mean. The mean squared value of $1/N$ given by Equation (5.28) is the average value of the squared "envelope" of $z_6(0)$ since by Equation (2.6) $|z_6(\tau)|$ is defined as the envelope of $z_6(\tau)$ in the usual sense of the rms

of the real and imaginary parts of $z_6(\tau)$. Equations (5.18) and (5.28) thus give the correlation function statistics for a fixed value of τ for all possible Worst Case frequency combinations. If only a limited number of reference frequencies are considered, the value of $|z_6(0)|^2 = 1/N$ given by Equation (5.28) may not be representative of these reference frequencies. For example, if PRNG sampling is used and if the principal a_k terms of Equation (5.19) occur in the small k suppression region shown in Figure 4.13, the value of $|z_6(0)|^2$ can be considerably less than $1/N$ as will be shown in Section 5.5.

Since the function $z_6(\tau)$ is composed of the sum of a large number of contributions as shown in Equations (5.11) and (5.16), one would suspect intuitively that its measured probability distribution would be approximately Gaussian. This was experimentally shown to be true by programming a digital computer to simulate the correlation function model of Figure 5.8 and then by measuring the correlation function statistics for the Worst Case input and reference frequencies. The results of these measurements are summarized in Section 5.5 for an example using PRNG sampling with $N = 96$ samples per block interval.

Although $\phi_6(0)$ was experimentally shown to be approximately Gaussian, the correlation function considered as a function of τ does not meet the requirements of narrow-band Gaussian noise [13] because its spectrum is not confined to a narrow band due to the presence of the odd harmonic response terms. As a result, the correlation function $\phi_6(\tau)$ cannot be approximated by the usual narrow-band assumptions as a sinusoidal function with a slowly varying

envelope as is evident from an examination of Equation (5.16) and of the example of Figure 5.9 in Section 5.5. Davenport and Root [13] point out, however, that the assumption of a narrow-band spectrum is not necessary to show that if $\phi_6(0)$ and $\hat{\phi}_6(0)$ have Gaussian distributions, the function defined by

$$\xi(0) \equiv |z_6(0)| = \sqrt{\{\phi_6(0)\}^2 + \{\hat{\phi}_6(0)\}^2}$$

has a Rayleigh probability distribution

$$p(\xi) = \frac{\xi}{\sigma_6^2} e^{-\frac{\xi^2}{2\sigma_6^2}}, \quad \xi \geq 0$$

whose mean, mean-square, and variance are given by

$$\overline{\xi} = \frac{\pi}{2} \sigma_6,$$

$$\text{and } \overline{\xi^2} = 2 \sigma_6^2$$

$$\overline{\xi^2} = (2 - \frac{\pi}{2}) \sigma_6^2,$$

where σ_6^2 is the variance of the Gaussian random processes $\phi_6(0)$ or $\hat{\phi}_6(0)$. Thus, if one samples the outputs $\phi_6(\tau)$ of all correlation functions which satisfy the Worst Case conditions of Equation (5.12) at any fixed time τ , those samples will have an approximate Gaussian distribution with a zero mean and a variance of $\frac{1}{2N}$. Likewise, samples of the output "envelopes" $|z_6(\tau)|$ for the same channels taken at any fixed time τ will have an approximate Rayleigh distribution

with a mean of $\sqrt{\frac{\pi}{4N}}$ and a variance of $[(2 - \frac{\pi}{2}) \cdot \frac{1}{2N}]$. This approximate statistical model of the Worst Case correlation function samples was verified experimentally as will be shown in Section 5.5.

Although the statistical model of the correlation function as a wide-band Gaussian process with a Rayleigh envelope distribution is seen to fit the system model of Figure 5.1, the concept of $|z_G(\tau)|$ as an envelope normally has real significance only for narrow-band processes. For example, if it is desired to compute the peak value of $\phi_G(\tau)$ over one period (see Figure 5.9), it might be necessary to redefine the envelope of $z_G(\tau)$ in a more meaningful way.

Equation (5.28) shows that if we relate the average properties of the correlation functions for all Worst Case frequencies to the average properties of the sampling spectrum coefficients from Chapter IV, the mean-squared value of $z_G(0)$ is given by

$$\overline{|z_G(0)|^2} = 1/N ,$$

where N is the number of samples per block. We now wish to extend this analysis to the non-worst case frequency combinations shown in Figure 5.6 and 5.7 and discussed qualitatively in Section 5.2 in order to obtain a first order comparison between the correlation function statistics in these various conditions. For signals whose duration T is long relative to a block length T_p , the key to the differences in correlation for the different frequency combinations will be shown to lie in the summation over m in Equation (5.11); i.e., in

$$F = \frac{1}{M} \sum_{m=1}^M e^{-j2\pi m T_p [(-1)^q (2q+1) f_R - (-1)^n (2n+1) f_I]} ,$$

where

M = number of sampling blocks of length T_p in one signal duration T ,

f_I = input frequency

and

f_R = reference frequency.

It was shown in Equation (5.14) that $F = 1$ for all q and n for the Worst Case frequencies because the product

$P \equiv T_p [(-1)^q (2q+1) f_R - (-1)^n (2n+1) f_I]$ is always equal to an integer for this case. If either f_R or f_I do not satisfy the Worst Case conditions, P will not be an integer for all values of k and n and the summation F will be less than unity in absolute value, thus acting as an attenuation factor in the correlation function of Equation (5.11). For large M , the attenuation factor F , whose average value is proportional to $1/M$, will be a significant smoothing factor.

As an example of the effect of the attenuation factor F , consider the third harmonic response frequencies shown in Figure 5.6; i.e., those satisfying

$$4f_I = m_I f_p$$

and

$$f_R = f_I + m_d f_p + \frac{1}{3} f_p, \quad (5.30)$$

where $i = 1$ or 2 . From Equation (5.29), F becomes:

$$\begin{aligned} F &= \frac{1}{M} \sum_{m=1}^M e^{-j2\pi m T_p [(-1)^q (2q+1) f_I - (-1)^n (2n+1) f_I + (-1)^q (2q+1) (m_d + \frac{1}{3}) f_p]} \\ &= \frac{1}{M} \sum_{m=1}^M e^{-j2\pi m \frac{1}{3} [(-1)^q (2q+1)]} \end{aligned}$$

and

$$|F| \begin{cases} = 1 & \text{when } (2q+1) = 3, 9, 15, 21, \text{ etc.} \\ \leq \frac{1}{M} & \text{otherwise if } M \geq 3. \end{cases}$$

If we assume M is large and neglect all values of n and q for which $|F| \leq \frac{1}{M}$, the correlation function at $\tau = 0$ for the frequencies satisfying the conditions of Equation (5.30) can be written [from Equation (5.11)] as:

$$z_6(0) = \frac{8}{\pi^2} \sum_{n=0}^{\infty} \sum_{q=0}^{\infty} \frac{(-1)^{n+q} a_{k(q,n)}}{(2n+1)(6q+3)},$$

and the mean squared value becomes

$$\begin{aligned}
 \overline{|z_6(0)|^2} &= \frac{64}{\pi} \sum_{n=0}^{\infty} \sum_{q=0}^{\infty} \sum_{p=0}^{\infty} \sum_{r=0}^{\infty} \frac{(-1)^{n+p+3q+1+3r+1}}{(2n+1)(6q+3)(2p+1)(6r+3)} \\
 &\quad \cdot [a_{k(n,3q+1)} a_{k(p,3r+1)}^*] \\
 &= \frac{64}{\pi} \sum_{n=0}^{\infty} \sum_{q=0}^{\infty} \frac{1/N}{(2n+1)^2(6q+3)} = \frac{1}{9N},
 \end{aligned}$$

which is $1/9$ of the Worst Case value given by Equation (5.28).

Under the same assumptions, it can be shown that for the fifth harmonic response frequencies of Figure 5.6

$$\overline{|z_6(0)|^2} = \frac{1}{25} \cdot \frac{1}{N},$$

and, in general, for the K^{th} harmonic response

$$\overline{|z_6(0)|^2} = \frac{1}{(K)^2} \cdot \frac{1}{N}.$$

Thus, for the situation represented by Figure 5.6 in which the input frequency f_I satisfies $4f_I = m_I f_p$, the output power for the correlation function corresponding to the K^{th} harmonic is inversely proportional to K^2 as a first approximation for large M .

Next, consider the conditions represented by Figure 5.7 where f_I does not satisfy the Worst Case input frequency condition; i.e.,

where $4f_I \neq m_I f_p$. The reference frequencies with the maximum response are the ones for which $f_R = f_I + m_d f_p$. For these frequencies, F from Equation (5.29) is

$$\begin{aligned} F &= \frac{1}{M} \sum_{m=1}^M e^{-j2\pi m T_p [(-1)^q (2q+1) f_I - (-1)^n (2n+1) f_I + (-1)^q (2q+1) m_d f_p]} \\ &= \frac{1}{M} \sum_{m=1}^M e^{-j2\pi m T_p [(-1)^q (2q+1) f_I - (-1)^n (2n+1) f_I]} \end{aligned}$$

and

$$|F| \begin{cases} = 1 & \text{when } q = n \\ \leq 1 & \text{otherwise.} \end{cases}$$

Although $|F|$ can occasionally be nearly equal to unity for $q \neq n$, we can neglect these terms with the result that our estimate of $|z_6(0)|^2$ will be noisy; i.e., have a larger variance. Neglecting all terms for which $F \neq 1$, the complex correlation function at $\tau = 0$ for this case becomes:

$$z_6(0) \approx \frac{8}{\pi^2} \sum_{n=0}^{\infty} \frac{a_{k(n,n)}}{(2n+1)^2}$$

and its mean squared value becomes:

$$\begin{aligned}
 \overline{|z_6(0)|^2} &= \frac{64}{\pi} \sum_{n=0}^{\infty} \sum_{k=0}^{\infty} \frac{a_{k(n,n)} a_{k(q,q)}^*}{(2n+1)^2 (2k+1)^2} \\
 &= \frac{64}{\pi} \sum_{n=0}^{\infty} \frac{1/N}{(2n+1)^4} = \frac{2}{3} \cdot \frac{1}{N} = \frac{.667}{N}, \quad (5.31)
 \end{aligned}$$

which can be compared with a value of $1/N$ for the Worst Case condition of Figure 5.6. Therefore, if the input frequency does not satisfy the condition $4f_I = m_d f_p$, samples of $\phi_6(0)$ from all reference channels satisfying $f_R = f_I + m_d f_p$ approximately satisfy a Gaussian distribution with a zero mean and a variance of $\frac{1}{3N}$, which is $2/3$ of the Worst Case variance of $\frac{1}{2N}$ as shown in Figure 5.6. Likewise, the envelope of $z_6(0)$ defined as $|z_6(0)|$ has an approximate Rayleigh distribution with a mean of $\left(\sqrt{\frac{\pi}{2}} \cdot \sqrt{\frac{1}{3N}}\right)$ and a variance of $\left[\left(2 - \frac{\pi}{2}\right) \cdot \frac{1}{3N}\right]$.

Using a similar analysis, all the third harmonic response frequencies shown in Figure 5.7 can be shown to have a mean squared value of $1/9$ of the maximum response channel. Likewise, the variance in the fifth harmonic channels is approximately $\frac{1}{25} \cdot \frac{1}{3N}$ and, in general, for the K^{th} harmonic response the variance is approximately given by $\frac{1}{K^2} \cdot \frac{1}{3N}$.

Although the statistical analysis in this section is not rigorous in the sense that the correlation functions it represents are actually deterministic, it has utility in that, for long signals

with $M \gg 1$, it gives an approximate but useful model of the average correlation and its variation for all Worst Case frequencies. For signals whose time duration T is not long relative to a block interval T_p , the effects of the finite T often dominate the higher order harmonic effects as will be shown by some examples in Section 5.5.

5.5 Example Using Pseudorandom Block Sampling

In Section 4.7, a method for generating a repetitive set of non-uniform sampling times using pseudorandom number generators (PRNG's) was described. Although this sampling scheme was shown to be non minimum variance in general, it does possess a high degree of randomness, has a unique spectral amplitude suppression characteristic for small k and has a good deal of flexibility in the selection of the number of sampling times per block N , and the number of possible sampling instants per block K . A digital computer simulation of a quadrature correlation function for clipped sinusoids with pseudorandom block sampling was made in order to experimentally verify the theoretical model of Figure 5.8. A summary of the results of that simulation are presented in this section.

The block sampling parameters chosen for the simulation are summarized in the following table:

Parameter	<u>Simulation Value</u>	
	Example 1	Example 2
Sample Pairs Per Block, N	96	24
Possible Sampling Instants Per Block, K	12, 192	3048
Blocks Per Signal Duration, M	3	3
PRNG Codes	Several	Several

As previously mentioned, a typical correlation function for clipped sinusoids and pseudo-random sampling has a noiselike characteristic because of the presence of odd harmonic components and tends to lose the narrowband appearance of a linear correlation function with uniform sampling. This fact is illustrated in Figure 5.9 where one period of a typical correlation function from the simulation program for Example 1 is shown. The two quadrature phases of the correlation function, shown by the solid curves are seen to be $\pi/2$ phase shifted translations of each other. Although the fundamental 2π "carrier" periodicity is still evident in these functions, their "noisy" shapes vary considerably from the conventional sinusoidal carriers found in linear correlation functions. The dashed curve in Figure 5.9 shows that the narrow band definition of envelope, as the square root of the sum of the squares of the two quadrature components, does not have the usual geometrical interpretation here of a slowly varying function passing through the peaks of the carrier.

Some examples of correlator output functions are shown in Figure 5.10 for Example 2 ($N = 24$), where $\phi_6(\tau)$ is plotted for

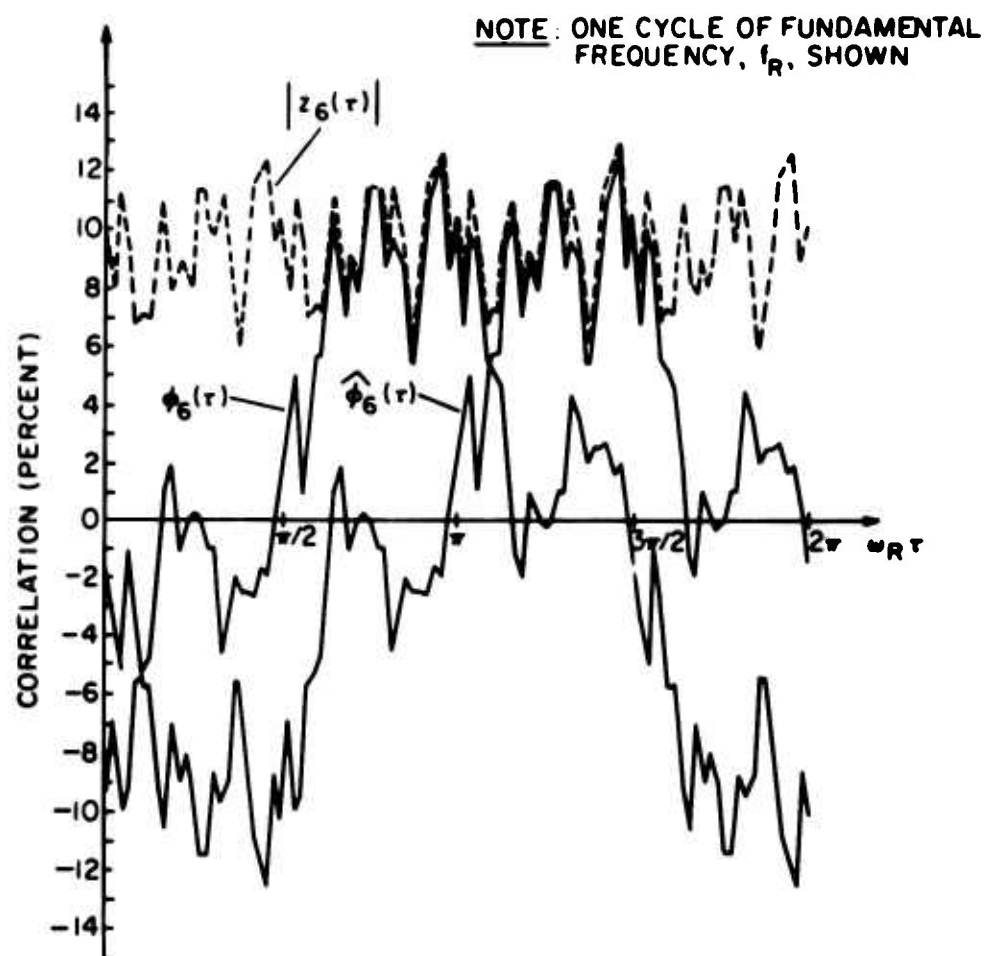
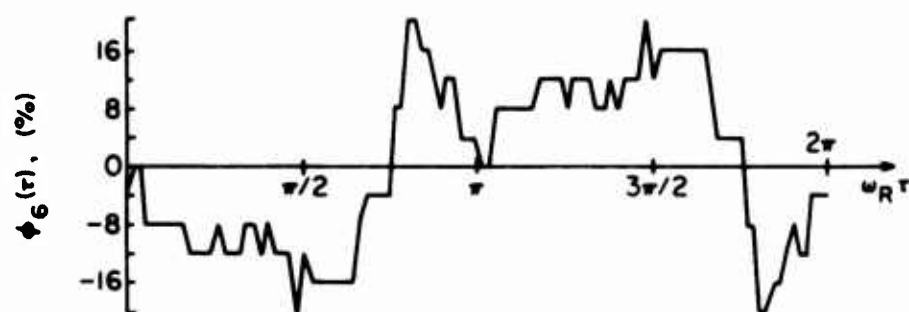


Figure 5.9 Correlation Function Example Using Pseudo-Random Block Sampling ($N = 96$)



(a) TYPICAL WORST CASE REFERENCE OUTPUT

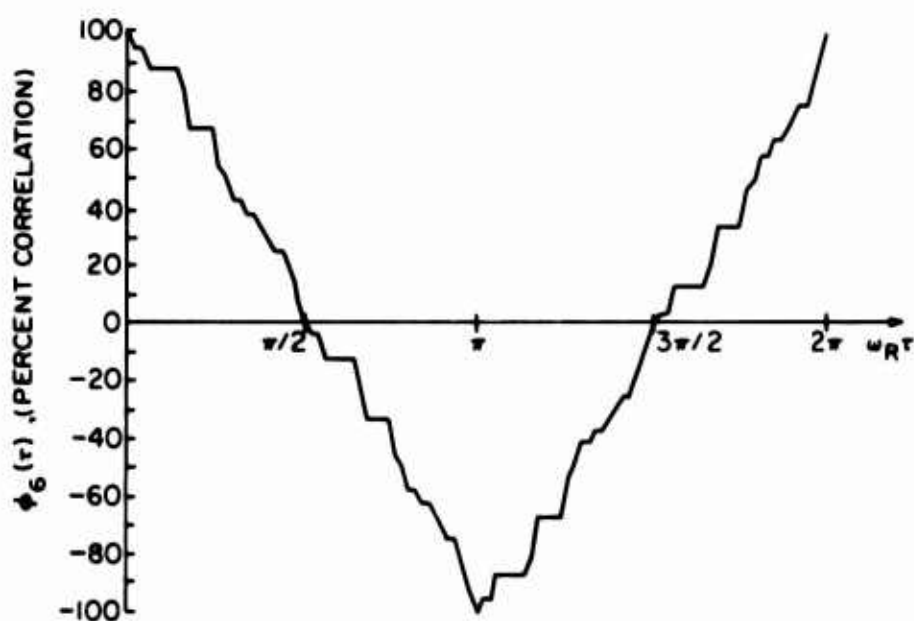
(b) MATCHED CHANNEL ($f_I = f_R$) OUTPUT

Figure 5.10 Correlation Function Examples Using
Pseudo-Random Block Sampling ($N = 24$)

one output repetition period. The typical Worst Case correlation function of Part (a) shows a high degree of randomness in the waveform similar to that of Figure 5.9. The correlation function shown in Part (b) is for a perfectly matched frequency case in which the reference frequency f_R is equal to the input frequency f_I . For a correlation function with uniform sampling, the plot of Part (b) would have a linear sawtooth characteristic of period 2π . The deviation from linearity (i.e., the granularity) of the correlation function of Figure 5.10(b) as well as the stepwise character of Figure 5.10(a) is due both to the nonuniformity of the sampling function and to the relatively small number of samples per block N .

The computer simulation consisted of computing the exact correlation function by simulating two square waves with frequencies f_R and f_I , time shifting the reference square wave, sampling both signals at the pseudo-random sampling times, and correlating the sampled signals. The curves of Figures 5.9 and 5.10 were generated in this way using 100 increments of $\omega_R \tau$ in a 2π output interval. In addition, a second computer program, useful for studying the effects of specific harmonics, was written to compute the correlation function term by term from Equation (5.16). Figure 5.11, which shows a typical Worst Case output correlation function from the small k suppression region for Example 1 ($N = 96$), shows a four-step comparison of the simulation model with the Equation (5.16) expansion. The dashed curve, which is identical in all three plots, represents the exact output correlation function while the four solid curves represent

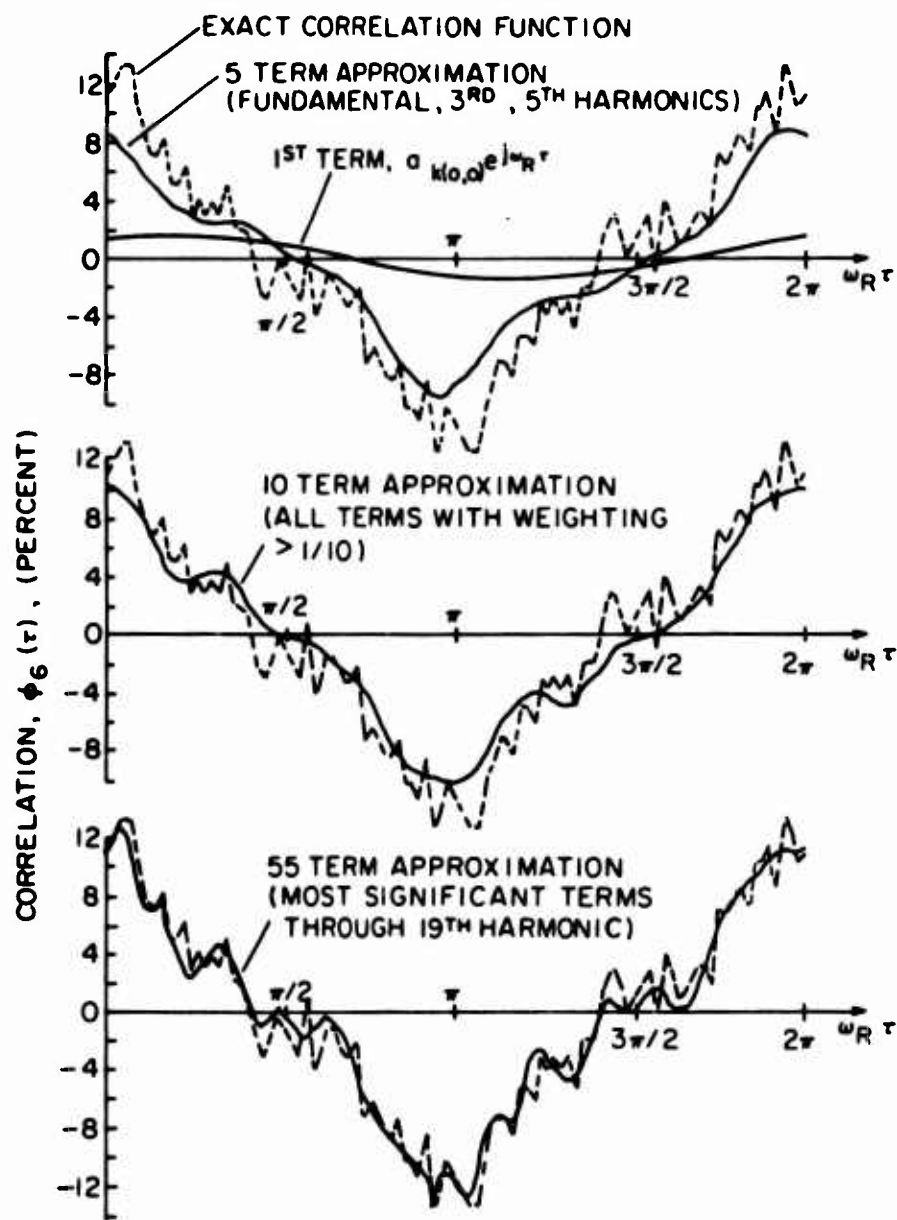


Figure 5.11 Comparisons of Typical Correlation Function with Output Approximations Using 1, 5, 10, and 55 Odd Harmonic Terms

approximations using Equation (5.16) with 1, 5, 10, and 55 terms.

The $a_{k(0,0)}$ term shown in the top plot is not a major contributor since its peak amplitude is only about 1.6 percent. This is characteristic of all Worst Case correlation functions in the small k region. The five-term approximation which contains the fundamental, third, and fifth harmonic terms is seen to follow the general shape of the dashed curve, but the approximate correlation is inaccurate by as much as 6 percent and the high frequency variations are not present. The 10-term approximation, which has reduced the maximum error to about 4 percent, is starting to conform a little more closely to the exact wave shape. The 55-term approximation shows the approximation slowly converging to the true correlation function. This relatively slow convergence shows that a significant number of the a_k terms in Equation (5.16) are important and emphasizes the importance of maintaining a low variance of $|a_k|^2$ over the entire spectral period while keeping the $a_{k(0,0)}$ term low by small k suppression as discussed in Sections 4.6 and 4.7.

The significance of the small k spectral suppression effect, a characteristic of all PRNG generated sequences, is seen by an examination of Figure 5.12 which shows three plots of peak output correlation (over a $\omega_R T = 2\pi$ interval) versus reference frequency for fixed input frequency. Figure 5.12(a) shows a typical example for reference frequencies with $a_{k(0,0)}$ terms in the high k region and a Worst Case input frequency satisfying $4f_I = m_I f_p$. The reference frequencies marked (W_1) are the computed Worst Case

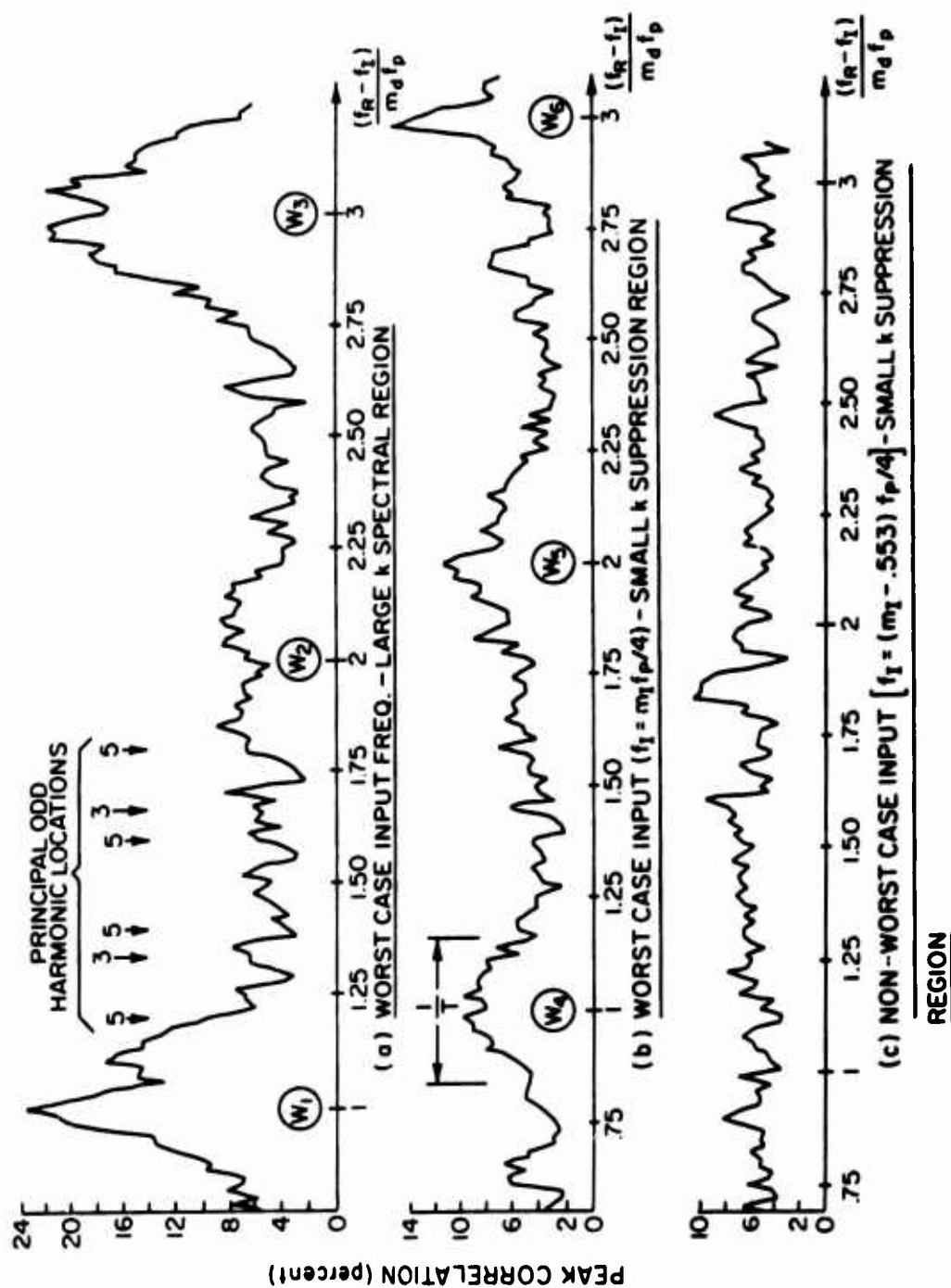


Figure 5.12 Typical Experimental Plots of Peak Correlation Vs. Reference Frequency for Pseudo-Random Block Sampling ($N = 96, M = 3$)

frequencies satisfying $lf_R = m_R f_p$. Because of the finite signal duration of T seconds, the typically large peak correlations associated with the Worst Case reference frequencies extend over approximately a reference frequency region of width $1/T$. Although the maximum of the jagged peak correlation versus reference frequency curve occurs near the (W) points, they do not always fall exactly on the Worst Case frequencies (e.g., see (W_3)). Although the (W) frequencies tend to have the largest correlations, sometimes, as shown at (W_2) , the odd harmonic terms add in such a way that the peak correlation never achieves a significant value. As shown in Figure 5.12(a), the higher order odd harmonic effects occurring between the (W) frequencies are essentially dominated by the $1/T$ spreading effects for the particular parameters (high N , low M) of this example. The example shown in Figure 5.12(b), which covers reference frequencies in the small k suppression region, shows typical reductions in the Worst Case frequency peak correlation of about 33 percent relative to those for Figure 5.12(a). This is attributable to the absence of significant $a_{k(0,0)}$ terms in this region. The average correlation level in the odd harmonic response region between Worst Case references, as expected, did not change from Figure 5.12(a) to Figure 5.12(b) because the a_k terms for these harmonics are generally found in the high k spectral region in both cases. The example of Figure 5.12(c) for a non-Worst Case input frequency shows much less fluctuation of peak correlation versus reference frequency because the Worst Case frequencies are substantially reduced and the

odd harmonics are more randomly spaced in the reference frequency. The odd harmonic effects predicted in Section 5.4 would be more prominent for examples with longer T and larger M .

Section 5.4 discussed the possibility of assuming the $i = 0$ samples of all Worst Case correlation functions $\phi_G(0)$ have a Gaussian probability distribution with a variance of $1/2N$. This assumption was verified experimentally as shown in Figure 5.13 using the computer simulation program. Figure 5.13(a) shows the results of 300 measurements for Example 1 ($N = 96$) taken over a wide range of Worst Case reference frequencies, all with $a_{k(0,0)}$ terms in the high k region. The experimental histogram shown by the solid curve had a measured standard deviation of $\sigma = 7.5$ percent or equivalently a variance of $\sigma^2 = 0.005625 = \frac{1.08}{2N}$ which deviates from the theoretical value of $\frac{1}{2N}$ by only 8 percent. The histogram is seen to match the dashed Gaussian distribution with a theoretical standard deviation of 7.21 percent very closely except for very low correlations around zero, a problem which is believed to be due to the fact that the granularity of the correlation function is roughly equal to the cell size used for plotting the histogram. The absolute value of the correlation was used instead of its full positive and negative range in order to double the sample size in each cell. Figure 5.13(b) shows a plot of the histogram of the "envelope" function $|z_G(0)|$ for the same reference frequencies used in Figure 5.13(a) with a sample size of 150. The measured square value was $|z_G(0)|^2 = 0.0116 = \frac{1.11}{N}$

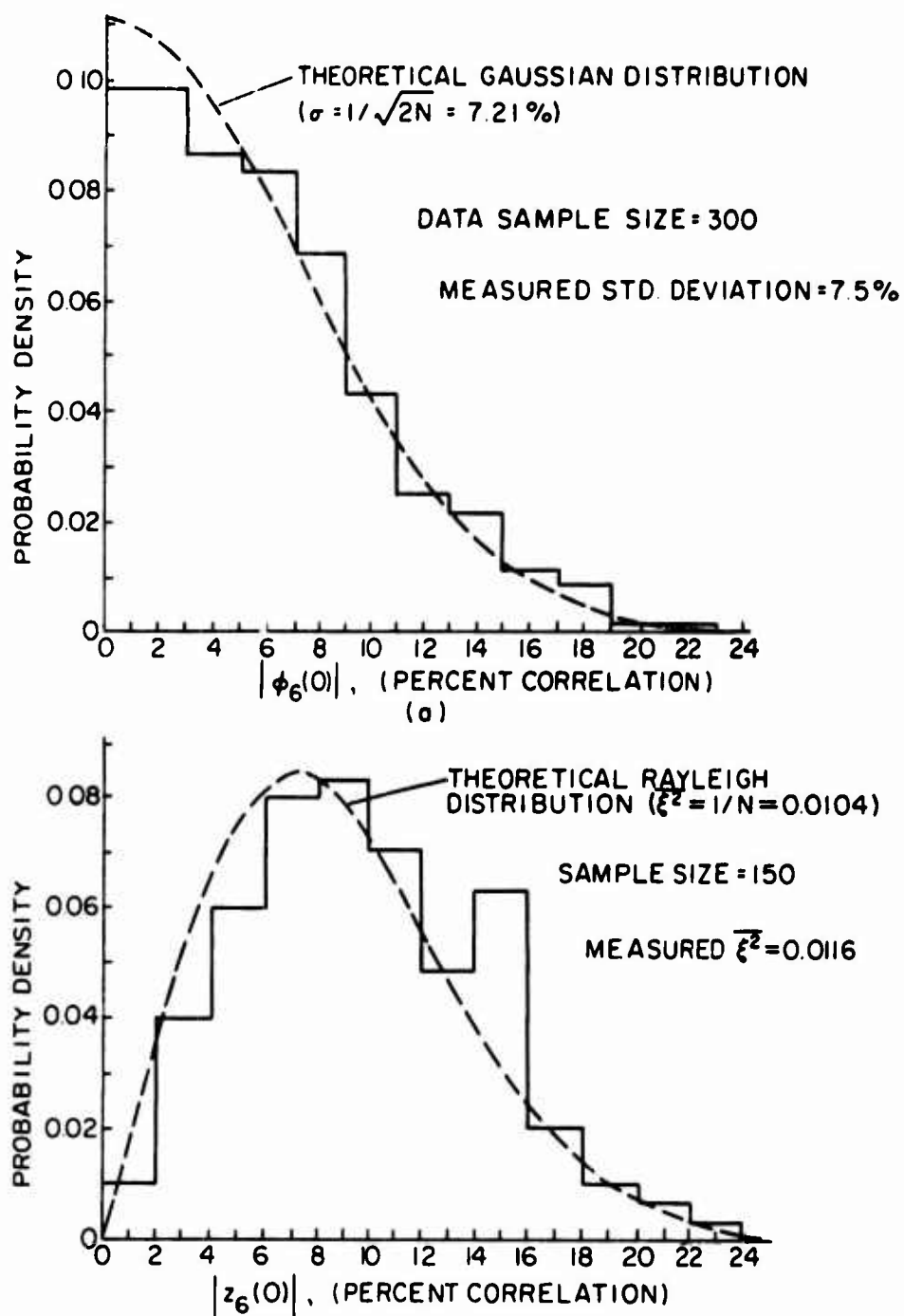


Figure 5.13 Measured Correlation Histograms for Worst Case Frequencies in Large k Region - PRNG Sampling ($N = 96$)

compared with a theoretical value of $1/N = 0.0104$. The data is seen to fit fairly well to the theoretical Rayleigh distribution with $\overline{\xi^2} = 1/N = 0.0104$.

Figure 5.14 contains experimentally measured histograms for Worst Case reference frequencies from the small k spectral suppression region. Since, for the high k region, Equation (5.28) shows that the $a_{k(0,0)}$ terms contributed about $\frac{64}{\pi} = 65.5$ percent of the total variance measurement, Figure 5.14 shows that the $a_{k(0,0)}$ contribution has been reduced by about 90 percent in the low k region.

Because of the noisy nature of the envelope function $|z_6(\tau)|$, the addition statistic $\text{MAX} \{ \phi_6(\tau) \}$, the maximum value of the output correlation function over one 2π period was measured and plotted for 571 Worst Case channels in the small k region as shown in Figure 5.15 for samples of data from Example 1 ($N = 96$). A comparison of the peak statistic histogram of Figure 5.15 with the histogram of $|z_6(0)|$ in Figure 5.14 shows that the mean of the peak distribution is about twice as large as the mean of the $|z_6(0)|$ distribution.

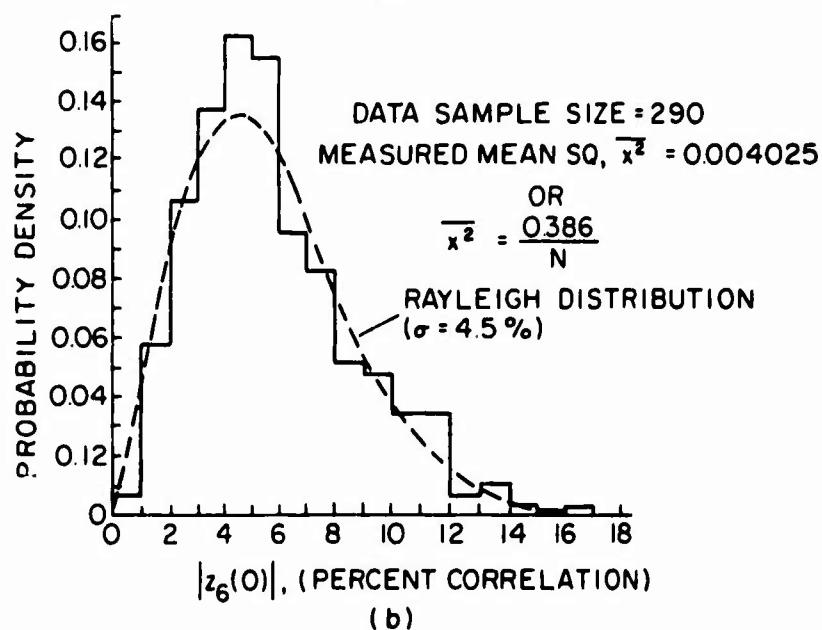
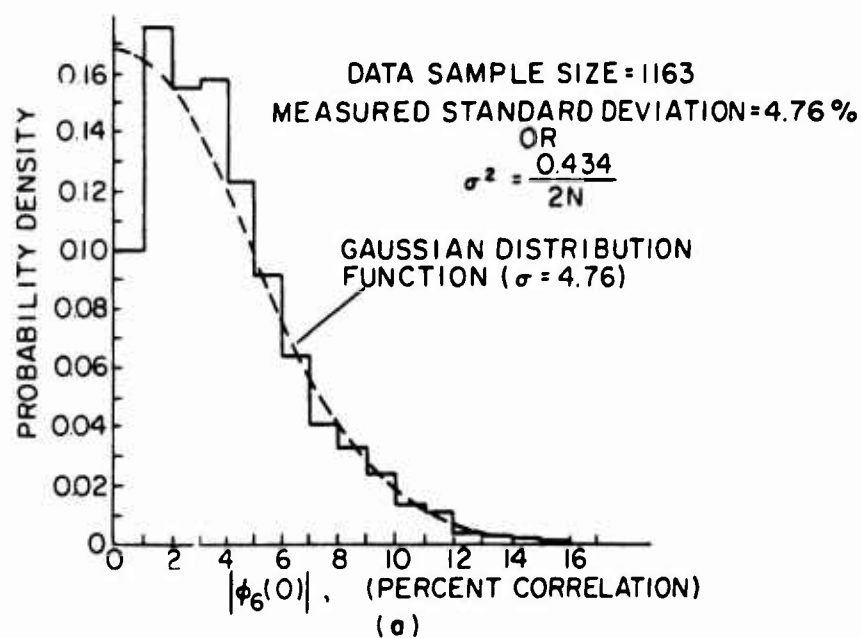


Figure 5.14 Measured Correlation Histograms for Worst Case Preferences in Small k Suppression Region - PRNG Sampling ($N = 96$)

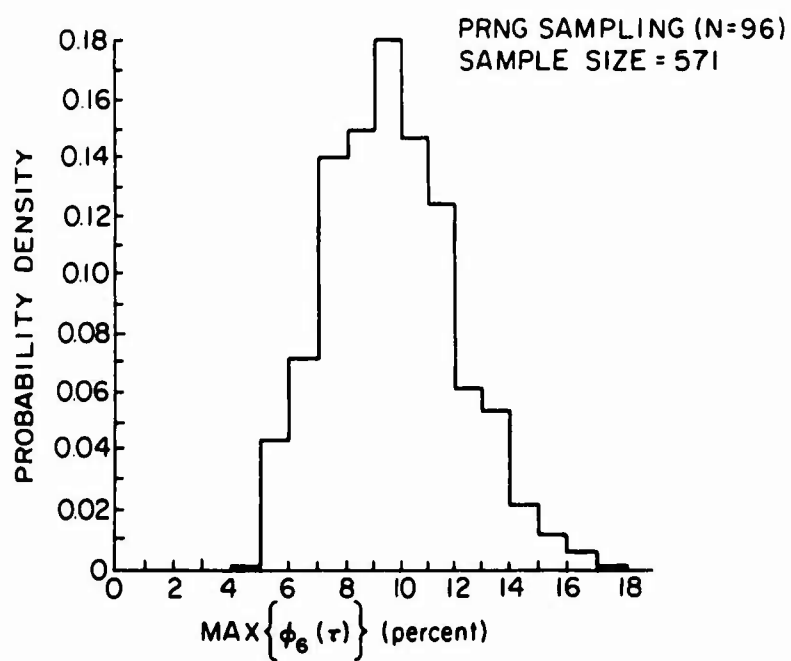


Figure 5.15 Correlation Peak Histograms for Worst Case References in Small k Suppression Region

CHAPTER VI

SUMMARY AND CONCLUSIONS

6.1 Statement of the Problem

The general topic of the research reported in this thesis is the study of nonuniform block sampling theory and its application to the study of correlation functions of sampled signals that are limited to a frequency band. The research evolved from the specific problem of trying to reduce the odd harmonic terms which appear in the correlation function of hard limited and uniformly sampled sinusoidal signals. These odd harmonic terms arise because of the synchronism between the periodicity of the uniform samples and the periodicity of the odd signal harmonics produced by hard limiting.

6.2 Approach

The general approach to the problem was the use of nonuniform sampling to reduce the undesirable periodicity effects and thus to reduce the correlation function odd harmonic terms. A particularly useful class of nonuniform sampling functions for this application was found to be "block sampling functions;" i.e., short sequences (or blocks) of nonuniform samples which are repeated periodically.

As a preliminary to a study of block sampling functions and their application to the odd harmonic problem, a detailed study of the

general properties of correlation functions for large TW signals with uniform sampling was made. These results were then extended to the case of sinusoidal signals with uniform sampling to illustrate the role of both clipping and sampling in the generation of the undesirable odd harmonic terms in the correlation function. The uniform sampling correlation function results along with the results of the block sampling spectrum analysis then formed the basis for analysis of correlation functions of sinusoidal signals with nonuniform block sampling.

6.3 Discussion of Results

In the study of correlation functions, two alternative definitions of sampled correlation functions were compared, the regular correlation function given by:

$$z(MT_s) = \frac{1}{M} \sum_{m=1}^M x(mT_s) y(mT_s)$$

and the quadrature correlation function given by:

$$z_q(MT_s) = \frac{1}{M} \sum_{m=1}^{M/2} [x(2mT_s) y(2mT_s) + \hat{x}(2mT_s) \hat{y}(2mT_s)],$$

where $x(t)$ and $y(t)$ are the signals of duration T to be correlated and $\hat{x}(t)$ and $\hat{y}(t)$ are their Hilbert transforms. The regular correlation function requires M uniform signal samples taken at T_s second intervals in T seconds to compute each point of $z(MT_s)$,

whereas the quadrature correlation function requires $M/2$ sample pairs of the signal and its Hilbert transform taken at $2T_s$ second intervals to compute $z_q(MT_s)$. It was shown that the basic difference between the two correlation function definitions is that quadrature correlation eliminates the second harmonic in the spectrum of the product $x(t) \cdot y(t)$. One implication of the second harmonic elimination for unclipped signals was that (for sampling faster than the Shannon rate) the quadrature correlation function eliminates second harmonic sampling errors that occur in the regular correlation function. Another implication is that the sampled quadrature correlation function variance for narrowband stationary random signals is independent of sampling rate, whereas the regular correlation function variance versus sampling rate response contains large peaks at some values of f_s due to the presence of the second harmonic. Thus, for no increase in the number of computations per correlation function point, quadrature correlation, in general, achieves more accurate correlation for deterministic signals and lower variance at all sampling rates for narrowband random process signals.

A comparison of the sampled quadrature correlation function variance for clipped and unclipped narrowband random processes showed that, although some second harmonic effects appeared for the clipped signal case, the variance could be reduced by as much as 3 dB by sampling faster than the Shannon rate.

In extending the study of quadrature correlation function properties to sinusoidal signals, the effects of linear sampling and

clipping were derived separately and the combined effects of both sampling and clipping were examined. Uniform sampling was shown to make the correlation function periodic (as a function of frequency) with a repetition period equal to the sampling rate, while clipping was shown to introduce extraneous correlations for input signals with frequencies which are odd multiples of the reference signal frequency. When both clipping and sampling are employed, each odd harmonic correlation response is repeated at periodic intervals which are related to the sampling rate, thus giving rise to the odd harmonic problem. When a sinusoid is correlated with a narrowband random function, the quadrature correlation function variance versus sampling rate curve approaches its high sampling rate asymptote more slowly than in the large TW signal case, and the second harmonic ripple is more pronounced.

After proposing nonuniform block sampling as a possible solution to the odd harmonic problem in the correlation function of clipped and sampled sinusoids, the spectral properties of block sampling were analyzed. Although other studies have considered block sampling from the points of view of signal reconstruction from sampled values [41, 24], sampling interval statistics [7], and sampled-data control system analysis [36], they did not analyze the basic properties of the sampling function or its frequency spectrum which are necessary for a study of correlation functions of nonuniformly sampled signals. Accordingly, this thesis examined in detail the complex frequency spectrum properties of ideal (zero sampling pulse width) block sampling

functions including amplitude and phase characteristics of each spectral component, spectral periodicity conditions, conservation of spectral energy properties, and conditions for minimum variance of the sampling power spectrum. The significant sampling spectrum parameter was shown to be the complex sampling coefficient a_k , given by

$$a_k = \frac{1}{N} \sum_{n=1}^N e^{-j2\pi k \frac{t_n}{T_p}},$$

where k is an integer designating the k^{th} spectral component, t_n are the nonuniform sampling times, T_p is the block repetition period in seconds, and N is the number of samples per block. Conditions on t_n/T_p for all values of n were derived such that a_k will be periodic; i.e., such that $a_k = a_{k+K}$ for some K and all k . A power spectrum conservation property was established stating that the average value of $|a_k|^2$ taken over one spectral period K was equal to $1/N$ independent of the specific sampling times t_n . Thus, each block sampling function with N samples per block (of which uniform sampling is a special case) merely redistributes a fixed amount of spectral energy as a function of frequency. Although the average value of $|a_k|^2$ was shown to be a constant equal to $1/N$ independent of the sampling times t_n , the variance of $|a_k|^2$ was found to be very dependent on the specific sampling times t_n . Accordingly, a set of conditions on t_n were derived which would minimize the variance of $|a_k|^2$. If σ_K^2 denotes the variance of $|a_k|^2$ over one spectral period K , it was shown that

$$\frac{1}{N^2} \left(1 - \frac{1}{N}\right) \leq \sigma_K^2 \leq \frac{1}{N} \left(1 - \frac{1}{N}\right),$$

where the lower limit is determined by the minimum variance conditions and the upper limit is set by uniform sampling. As an example of sampling spectrum shaping; i.e., of controlling the values of $|a_k|$ in specific spectral regions, by choice of t_n , a block sampling function example was introduced which used a pseudo-random number generator (PRNG) for sampling time selection. Although this sampling scheme does not yield a minimum variance sampling spectrum, it achieves a unique spectrum shaping by suppressing the values of $|a_k|$ for small k , a property that is important in the reduction of odd harmonic responses in correlation functions of clipped sinusoidal signals.

Finally, having derived the fundamental properties of quadrature correlation functions and of nonuniform block sampling, the application of block sampling to the reduction of odd harmonics in correlation functions of clipped sinusoids was studied. Considering the quadrature correlation function $z(\tau, f_I, f_R)$ between two clipped sinusoidal signals with block sampling as a function of the two sinusoidal frequencies f_I and f_R , it was shown that, although the odd harmonic responses are greatly reduced, certain combinations of input frequency f_I and reference frequency f_R result in correlations whose average value is greater than those for other values of f_I and f_R . These significant combinations of f_I and f_R , which are called Worst Case combinations, are given by the equations

$$4f_I = m_I/T_p,$$

$$4f_R = m_R/T_p$$

and

$$(f_I - f_R) = m_d/T_p,$$

where m_I , m_R , and m_d are integers. Based on an analytical model similar to one used by Tou [36], an expression relating the correlation function at these Worst Case frequencies to the sampling function coefficients a_k and the signal odd harmonics was obtained. This expression was useful for studying the effect of each odd harmonic on the correlation function as well as for demonstrating the effectiveness of the small k suppression property of PRNG sampling functions in reducing the correlation function amplitude for the Worst Case conditions. This model was also useful for obtaining some average correlation characteristics taken over all Worst Case frequency combinations. Some experimental results, based on a digital computer simulation, were obtained to verify the theoretical correlation function model. Both the analysis and the experimental results confirmed that, by proper choice of sampling parameters, block sampling could reduce the undesirable odd harmonic correlation function responses due to clipping and sampling by any desired degree.

6.4 Suggestions for Further Research

The quadrature correlation function properties obtained in Chapters II and III were derived for single input and reference signals. In many applications, it is important to consider sums of signals [23] or signals plus random noise processes [30] instead of single signals. In the possible extension of the results of Chapters II and III to these cases, of particular interest would be the effects of hard limiting and uniform sampling on the quadrature correlation functions of narrowband signals--especially sinusoids.

Throughout this thesis, only extreme signal quantization (i.e., hard limiting) was considered. However, because of the wide spread use of digital computers and other digital devices to calculate correlation functions, it is also important to study other levels of quantization. For example, since all computers have finite word length, some degree of round-off (i.e., quantization) is always present.

In the analysis of the sampling function spectrum of Chapter IV, the sampling spectrum variance σ_K^2 was minimized over a complete spectral period. Many times, however, an entire spectral period need not be considered. In these cases, it would be more meaningful to minimize the spectrum variance over an arbitrary spectral range at the expense of spectral amplitudes out of the range of interest. In addition to optimizing the spectrum variance by choice of sampling times, it might also be possible to fix the nonuniform sampling times and minimize the sampling spectrum variance by the choice of amplitude

weighting coefficients for each sample. Another more difficult related problem is the synthesis problem of specifying the exact desired shape of the sampling spectrum and finding a set of sample times which yields this spectrum (or a closest fit to it).

In Chapters IV and V, out of many possible specific nonuniform block sampling schemes, only PRNG sampling was studied in detail. Many other interesting sampling schemes for further study suggest themselves, such as using a probability law (Gaussian, Poisson, etc.) to select the nonuniform sampling times or restricting the freedom of each sample within the sampling block. For the PRNG sampling scheme studied, additional comparative analysis of the effects of specific pseudo-random codes are suggested.

APPENDIX

CORRELATION FUNCTION VARIANCE FOR RANDOM PROCESS
INPUT SIGNALS WITH RECTANGULAR POWER SPECTRUM

We wish to compute the correlation function variance for a typical example where the input and reference signals are assumed to be random variables with Gaussian distributions and to be represented by

$$x(t) = \sigma_n n(t) = \sigma_n (N_1 \cos \omega_0 t - N_2 \sin \omega_0 t) \quad (\text{A.1})$$

and

$$y(t) = s(t) = E_1 \cos \omega_0 t - E_2 \sin \omega_0 t. \quad (\text{A.2})$$

Assume that the power spectrum of both $s(t)$ and $n(t)$ are equal and given by

$$P_s(\omega) = P_n(\omega) = \begin{cases} \frac{1}{2W}, & \text{for } (-\omega_0 - \frac{2\pi W}{2}) \leq \omega \leq (-\omega_0 + \frac{2\pi W}{2}), \\ \frac{1}{2W}, & \text{for } (\omega_0 - \frac{2\pi W}{2}) \leq \omega \leq (\omega_0 + \frac{2\pi W}{2}), \\ 0 & \text{elsewhere.} \end{cases} \quad (\text{A.3})$$

The correlation functions of both $s(t)$ and $n(t)$ are, therefore,

$$\begin{aligned}\phi_{ss}(\tau) &= \phi_{nn}(\tau) = \frac{1}{2\pi} \int_{-\infty}^{\infty} P_s(\omega) e^{j\omega\tau} d\omega \\ &= \frac{\sin \pi W\tau}{\pi W\tau} \cos \omega_o \tau.\end{aligned}\quad (A.4)$$

Also,

$$\phi_{s\Delta}(\tau) = \phi_{n\Delta}(\tau) = \frac{\sin \pi W\tau}{\pi W\tau} \sin \omega_o \tau, \quad (A.5)$$

$$\phi_{N_1 N_1}(\tau) = \phi_{N_2 N_2}(\tau) = \phi_{E_1 E_1}(\tau) = \phi_{E_2 E_2}(\tau) = \frac{\sin \pi W\tau}{\pi W\tau}, \quad (A.6)$$

$$\phi_{N_1 N_2}(\tau) = \phi_{E_1 E_2}(\tau) = 0, \quad (A.7)$$

$$\phi_{xx}(\tau) = \sigma_n^2 \phi_{nn}(\tau) \quad (A.8)$$

and

$$\phi_{yy}(\tau) = \phi_{ss}(\tau). \quad (A.9)$$

For the regular correlation function, σ_R^2 from Equation (2.40) is

$$\frac{\sigma_R^2}{\left(\frac{\sigma_n}{2TW}\right)^2} = \frac{2TW}{M} + \frac{4TW}{M} \sum_{m=1}^M \left(1 - \frac{m}{M}\right) \left(\frac{\sin \pi WmT_s}{\pi WmT_s}\right)^2 \cos^2 \omega_o mT_s \quad (A.10)$$

$$= \frac{1}{R} \left[1 + 2 \sum_{m=1}^M \left(\frac{\sin \frac{m\pi}{2R}}{\frac{m\pi}{2R}}\right)^2 \cos^2 \frac{m\pi \frac{f_o}{W}}{R} \left(1 - \frac{m}{M}\right) \right], \quad (A.11)$$

where $R = f_s/2W =$ ratio of sampling rate to Shannon rate,

$T =$ signal duration,

$M =$ total samples in T seconds

and

$f_s = 1/T_s =$ sampling rate.

Equation (A.11) is plotted in Figure 2.6 for $f_o/W = 9$ and

$2TW = 50$.

For the quadrature correlation, σ_Q^2 from Equation (2.46) is given by

$$\frac{\sigma_Q^2}{\left(\frac{\sigma_n^2}{2TW}\right)} = \frac{1}{R} \left[1 + 2 \sum_{m=1}^{M/2} \left(\frac{\sin \frac{m\pi}{R}}{\frac{m\pi}{R}} \right)^2 \left(1 - \frac{2m}{M} \right) \right], \quad (\text{A.12})$$

where $R = \hat{f}_s/W$ and $\hat{f}_s = 1/2T_s$. Equation (A.12) is plotted in Figure 2.7 for $f_o/W = 9$ and $2TW = 50$.

For the clipped signal case, from Equation (2.59), $\overset{\sim}{\sigma}_Q^2$ for quadrature correlation is

$$\begin{aligned} \frac{\overset{\sim}{\sigma}_Q^2}{(1/2TW)} = \frac{1}{R} \left\{ 1 + \frac{8}{\pi^2} \sum_{m=1}^{M/2} \left\{ \left[\sin^{-1} \left(\frac{\sin \frac{m\pi}{R}}{\frac{m\pi}{R}} \cos \frac{2\pi f_o m}{WR} \right) \right]^2 \right. \right. \\ \left. \left. + \left[\sin^{-1} \left(\frac{\sin \frac{m\pi}{R}}{\frac{m\pi}{R}} \sin \frac{2\pi f_o m}{WR} \right) \right]^2 \right\} \left(1 - \frac{2m}{M} \right) \right\} \quad (\text{A.13}) \end{aligned}$$

as shown in Figure 2.9. The corresponding regular correlation function variance

$$\frac{\overline{\sigma_R^2}}{(1/2TW)} = \frac{1}{R} \left\{ 1 + \frac{8}{\pi^2} \sum_{m=1}^M \left[\sin^{-1} \left(\frac{\sin \frac{m\pi}{2R}}{\frac{m\pi}{2R}} \cos \frac{\pi f_o m}{WR} \right) \right]^2 \left(1 - \frac{m}{M} \right) \right\} \quad (\text{A.14})$$

is plotted in Figure 2.10.

BIBLIOGRAPHY

1. Andeen, R. E., "Staggered Sampling to Improve Stability of Multiple Sampler Feedback Systems," Trans. AIEE, Vol. 77, Pt. II, 1958, pp. 399-403.
2. Balakrishnan, A. V., "On the Problem of Time Jitter in Sampling," IRE Trans. on Info. Theory, Vol. IT-8, 1962, pp. 226-236.
3. Bedrosian, E., "The Analytic Signal Representation of Modulated Waveforms," Proc. IRE, Vol. 50, 1962, pp. 2071-2076.
4. Beutler, F. J., "Sampling Theorems and Bases in a Hilbert Space," Info. and Control, Vol. 4, 1961, pp. 97-117.
5. Beutler, F. J., "Error-Free Recovery of Signals from Irregularly Spaced Samples," SIAM Review, Vol. 8, 1966, pp. 328-335.
6. Beutler, F. J. and Leneman, O. A. Z., "Random Sampling of Random Processes: Stationary Point Processes," Info. and Control, Vol. 9, 1966, pp. 325-346.
7. Beutler, F. J. and Leneman, O. A. Z., "The Theory of Stationary Point Processes," Acta Mathematica, Vol. 116, Oct. 1966, pp. 159-197.
8. Blackman, N. B., "The Output Signal-to-Noise Ratio of a Power Law Device," J. of Appl. Physics, Vol. 24, June 1953, pp. 783-785.
9. Brown, W. M., "Sampling with Random Jitter," J. Soc. Indust. Appl. Math., Vol. 11, June 1963, pp. 460-473.
10. Cahn, C. R., "A Note on Signal-to-Noise Ratio in Band-Pass Limiters," IRE Trans. on Info. Theory, Vol. IT-7, January 1961, pp. 39-43.
11. Cook, C. E. and Bernfeld, M., Radar Signals: An Introduction to Theory and Application, Academic Press, New York, 1967.
12. Davenport, W. B., Jr., "Signal-to-Noise Ratios in Band-Pass Limiters," J. of Appl. Phys., Vol. 24, No. 6, June 1953, pp. 720-727.

13. Davenport, W. B. and Root, W. L., An Introduction to the Theory of Random Signals and Noise, McGraw-Hill, New York, 1958.
14. Deutsch, R., Nonlinear Transformations of Random Processes, Prentice-Hall, Inc., 1962.
15. Downing, J. J., Modulation Systems and Noise, Prentice-Hall, Inc., 1964.
16. Doyle, W., et. al., "Approximate Band-Pass Limiter Envelope Distributions," IEEE Trans. IT, Vol. IT-10, No. 3, July 1964, pp. 180-185.
17. Dugundji, J., "Envelopes and Pre-Envelopes of Real Waveforms," IRE Trans. on Info. Theory, Vol. IT-4, No. 1, March 1958, pp. 53-57.
18. Goldman, S., Information Theory, Prentice-Hall, Inc., 1953.
19. Goulomb, S. W., Editor, Digital Communications with Space Applications, Prentice-Hall, Inc., 1964.
20. Grace, O. D. and Pitt, S. P., "Quadrature Sampling of High Frequency Waveforms," J. Acoust. Soc. Am., Vol. 44, No. 5, 1968, pp. 1453-1454.
21. Haddad, A. H. and Thomas J. B., "Integral Representations for Non-Uniform Sampling Expansions," Proc. of the Fourth Annual Allerton Conf. on Circuit and System Theory, Oct. 5-7, 1966.
22. Hufnagel, R. E., "Analysis of Cyclic Rate Sampled-Date Feedback Control Systems," Trans. AIEE, Vol. 77, pt. II, 1958, pp. 421-423.
23. Jones, J. J., "Hard Limiting of Two Signals in Random Noise," IEEE Trans. on Info. Theory, Vol. IT-9, No. 1, January 1963, pp. 34-42.
24. Kohlenberg, A., "Exact Interpolation of Band-Limited Functions," J. of Appl. Phys., Vol. 24, No. 12, December 1953, pp. 1432-1436.
25. Lampard, D. G., "A New Method of Determining Correlation Functions of Stationary Time Series," IEE Monograph, No. 4, August 1954.
26. Lee, Y. W., Statistical Theory of Communication, John Wiley and Sons, Inc., New York, 1960.

27. Leneman, O. A. Z., "Random Sampling of Random Processes: Impulse Processes," *Info. and Control*, No. 9, 1966, pp. 347-363.
28. Leneman, O. A. Z. and Lewis, J. B., "Mean-Square Error of Step-Wise Interpolation for Various Sampling Schemes," *J. of the Franklin Institute*, Vol. 282, No. 2, August 1966, pp. 108-120.
29. Lieberman, G., "Quantization in Coherent and Quadrature Reception of Orthogonal Signals," *RCA Review*, Vol. 22, No. 3, September 1961, pp. 461-486.
30. McFadden, J. A., "The Correlation Function of a Sine Wave Plus Noise after Extreme Clipping," *IRE Trans. on Info. Theory*, Vol. IT-2, June 1956, pp. 82-83.
31. Middleton, D., An Introduction to Statistical Communication Theory, McGraw-Hill, New York, 1960.
32. Muehldorf, E. I., et. al., "The Auto and Cross Correlation Functions of Elementary Waveforms," 1959 Nat'l. Conf. Proc. Aeron Electronics Conf., May 1959, pp. 232-239.
33. Papoulis, A., Probability, Random Variables, and Stochastic Processes, McGraw-Hill, 1965, pp. 355-357.
34. Redman, S. J., "Stochastic Sampling of a Binary Random Process," *IEEE Trans. Circuit Theory*, Vol. CT-10, No. 1, March 1963, pp. 3-24.
35. Rubin, W. L. and Kamen, S. K., "S/N Ratios in a Two-Channel Band-Pass Limiter," *Proc. IEEE*, Vol. 51, February 1963, pp. 389-390.
36. Tou, J. T., Digital and Sampled-Data Control Systems, McGraw-Hill, New York, 1959, pp. 308-318.
37. Van Vleck, J. H. and Middleton, D., "The Spectrum of Clipped Noise," *Proc. IEEE*, Vol. 54, No. 1, January 1966, pp. 2-19.
38. Watts, D. G., "A General Theory of Amplitude Quantization with Applications to Correlation Determination," *Proc. Instn. Elect. Engrs., London (Pt.C.)*, Vol. 109, No. 15, March 1962, pp. 209-218.

39. Yao, K. and Thomas, J. B., "On a Class of Nonuniform Sampling Representations for Band-Limited Signals," presented at the Symposium on Signal Transmission and Processing at Columbia Univ., May 13-14, 1965.
40. Yao, K. and Thomas, J. B., "On Some Stability and Interpolatory Properties of Nonuniform Sampling Expansions," IEEE Trans. on Circuit Theory, Vol. CT-14, 1967, pp. 404-408.
41. Yen, H. L., "On Nonuniform Sampling of Bandwidth-Limited Signals," IRE Trans on Circuit Theory, Vol. CT-3, No. 4, December 1956, pp. 251-257.

DOCUMENT CONTROL DATA - R & D

(Security classification of title, abstract and indexing annotation when overall report is classified)

1. ORIGINATING ACTIVITY (Corporate author) Ordnance Research Laboratory University Park, Pennsylvania		2a. REPORT SECURITY CLASSIFICATION UNCLASSIFIED	
		2b. GROUP ---	
3. REPORT TITLE EFFECTS OF NON-UNIFORM SAMPLING AND LIMITING ON CORRELATION FUNCTIONS			
4. DESCRIPTIVE NOTES (Type of report and inclusive dates) Thesis, August 13, 1969			
5. AUTHOR(S) (First name, middle initial, last name) C. L. Ackerman			
6. REPORT DATE August 13, 1969		7a. TOTAL NO. OF PAGES 196 pp. and figs.	7b. NO. OF REFS 41
8a. CONTRACT OR GRANT NO. NOW 65-0123-d		9a. ORIGINATOR'S REPORT NUMBER(S) TM 676.2341-02	
b. PROJECT NO.		9b. OTHER REPORT NO(S) (Any other numbers that may be assigned this report)	
c.		None	
d.			
10. DISTRIBUTION STATEMENT Distribution of this document is unlimited			
11. SUPPLEMENTARY NOTES None		12. SPONSORING MILITARY ACTIVITY Naval Ordnance Systems Command Department of the Navy	
13. ABSTRACT <p>This thesis is a study of nonuniform block sampling theory and its application to the study of correlation functions of sampled signals. The research evolved from the specific problem of reducing the odd harmonic terms that appear in the correlation function of hard-limited and uniformly sampled sinusoidal signals. These odd harmonic terms arise because of the synchronism between the periodicity of the uniform samples and the periodicity of the odd signal harmonics produced by hard limiting. Nonuniform sampling is used to reduce the periodicity effects and, thus, to reduce the odd harmonic terms in the correlation function. With block sampling, the odd-harmonic correlation-function responses resulting from clipping and sampling can be reduced by any desired degree by the proper choice of sampling parameters.</p>			

14.	KEY WORDS	LINK A		LINK B		LINK C	
		ROLE	WT	ROLE	WT	ROLE	WT
	Block sampling	8					
	Correlation function	8					
	Harmonics	8					
	Limiting	8					
	Periodicity effects	8					
	Quadrature correlation	8					
	Sampling	8					